UCRL 8230

UNIVERSITY OF CALIFORNIA

Radiation Laboratory

BERKELEY, CALIFORNIA

DISCLAIMER

UCRL-8230

UNIVERSITY OF CALIFORNIA

Radiation Laboratory
Berkeley, California

Contract No. W-7405-eng-48

THERMAL CONDUCTIVITY AND VISCOSITY OF GAS MIXTURES

Henry Cheung

(Thesis)

April 1958

Printed for the U. S. Atomic Energy Commission

THERMAL CONDUCTIVITY AND VISCOSITY OF GAS MIXTURES

Contents

THERMAL CONDUCTIVITY AND VISCOSITY OF GAS MIXTURES

Henry Cheung

Radiation Laboratory and Department of Chemical Engineering
University of California, Berkeley, California

April 1958

ABSTRACT

Correlations based upon empirical modified equations derived from kinetic theory have been developed for the thermal conductivity and viscosity of gas mixtures. The conductivity equation proposed in this work has been compared to 226 binary mixture conductivities in temperatures from 0° to 774°C from the literature and this work. The average deviation is 2.1%. In correlating conductivity data of mixtures of polyatomic molecules, the energy transport is considered in two parts, i.e., one portion transferred by collision and the other by diffusion. The proposed viscosity equation reproduces 103 binary data points with an average deviation of 1.3%. These equations are more consistent with experiment than existing correlations in the literature. The relation of the conductivity or viscosity to composition and temperature are discussed in the light of the proposed equations. It has been demonstrated that, at a given composition, the ratio of the measured conductivity to that calculated on the molar average basis for mixtures of most simple molecules and the ratio of the measured viscosity to that calculated on the molar average basis for mixtures of most gases should be nearly constant over a temperature range of 200° to 300°C.

The thermal conductivity of ten gases and selected binary and ternary mixtures of them were measured in a concentric silver cylinder cell in the temperature range of 100° to 540°C. The gases are He, A, N_2, O_2, CO_2, CH_4, C_2H_4, C_3H_8, methyl ether, and methyl formate.

THERMAL CONDUCTIVITY AND VISCOSITY OF GAS MIXTURES

Henry Cheung

Radiation Laboratory and Department of Chemical Engineering
University of California, Berkeley, California

INTRODUCTION

The transfer of heat, momentum, and mass occurs when gradients in temperature, velocity, and concentration respectively exist within a gas. The transport coefficients of a gas, λ, η, and D, describe the rates of transfer under a given gradient. According to the kinetic theory, these coefficients are related to the mean free path of gas molecules and so are related to one another. Thus, the expression $\lambda = 2.5\ \eta\ C_v$ gives the thermal conductivity of all monatomic gases with an error of less than 4%, and the coefficient of self-diffusion is proportional to kinematic viscosity according to

$$D = C\nu = \frac{C\eta}{\rho}$$

where C depends upon intermolecular forces.

For gas mixtures, no such simple relation exists. While it is possible with a certain amount of mathematical labor to calculate with fair accuracy from the kinetic theory the transport coefficients of simple molecules following a given law of interaction,[24] the work involved in the case of mixtures is beyond practical limits. Further, the rigorous kinetic theory has not yet been fully extended to cover the case of the conductivity of polyatomic molecules, the internal molecular energy of which requires special treatment. Thus, there exists a continuing need for means of predicting the conductivity and viscosity without excessive mathematical labor. As a result, a number of empirical and semi-empirical relations have been proposed.[5,12,23,34,40] They agree with the experimental data in varying degrees of success.

An objective of this work is to develop relatively simple correlations that will be more consistent with the experimental data of thermal conductivity and viscosity of mixtures than those found in the literature. An attempt is also made to deal with the energy of polyatomic molecules by splitting it into two parts, one of which is

transported by a collision process and the other by diffusion. An explanation of the usually observed deviation of conductivity and viscosity from the simple mixing rule and a discussion of the temperature dependence of these properties are presented on the basis of the correlations developed.

With a few exceptions, conductivity data of mixtures found in the literature were measured at or near room temperature. As viscosity measurements are comparatively easier to make, data for a number of mixtures at temperatures up to 1000°C are available. Conductivity data at higher temperatures are needed to test the present theories and correlations; therefore, another objective of this work is the experimental determination of the conductivity of a number of binary and ternary mixtures in the temperature range of 100° to 540°C.

The topics referred to above are discussed in five chapters in this dissertation. Chapter I consists of a brief review of selected literature on the viscosity and conductivity of pure and mixed gases. A new scheme for correlating these transport properties is developed in Chapter II. The experimental method employed for determining conductivity is described in Chapter III. Experimental results and evaluation thereof are presented in Chapter IV. In the final chapter, the correlations developed in Chapter II are compared with experimental data collected from the literature and those presently measured. They are also compared with existing correlations.

CHAPTER I. Review of Theoretical and Empirical Relations for Thermal Conductivity and Viscosity of Gases.

A. Interrelations of the Transport Properties of Pure Gases

The relations between the transport coefficients can be deduced directly from the kinetic theory of dilute gases. In the elementary kinetic theory treatment of the transport phenomena, the following assumptions are made:

(1) molecules are rigid nonattracting spheres.

(2) all molecules travel with the same speed.

(3) one-third of all molecules travel in a direction paralled to any one of the three perpendicular coordinate axes in space.

On the basis of these assumptions, the following relations are obtained:

$$D = \frac{\lambda}{\rho \ C_v} \tag{1}$$

$$\eta = \rho \ D \tag{2}$$

$$\lambda = C_v \eta \tag{3}$$

The rigorous kinetic theory treatment of Chapman[8] and Enskog[13] involves the solution of the Maxwell-Boltzmann integro-differential equation. This procedure takes into account the variation of mean free path with velocity, the persistence of velocity after impact, and the fact that the most rapidly moving molecules also have the greatest translation kinetic energy and momentum. The results thus obtained are:

$$[D]_1 = \frac{12 \ \Omega^{(2,2)^*} [\lambda]_1}{25 \ \Omega^{(1,1)^*} \rho \ C_v} \tag{4}$$

$$[\eta]_1 = \frac{5}{6}\frac{\Omega^{(1,1)^*}}{\Omega^{(2,2)^*}} \rho [D]_1 \qquad (5)$$

$$[\lambda]_1 = 2.5 \; c_v \; [\eta]_1 \qquad (6)$$

where the brackets with the subscript "1" denotes the first approximation to the transport properties and the Ω quantities depend upon the potential function employed to describe molecular interactions. For rigid spheres, these quantities are unity. It is seen that the results of the elementary theory and the rigorous theory differ only by a numerical factor.

Equation 6 has been used widely in correlating conductivity with viscosity. Experimental data show that the numerical factor in Eq. 6 is not 2.5 but lies between 1 and slightly greater than 2.5. For monatomic gases it is found to be within a few percent of the theoretical value of 2.5. That Eq. 6 fails to be applicable to polyatomic molecules is attributable to the existence of modes of molecular motion other than translation, asymmetry of the molecules, and inelastic collisions.

The first attempt to account for the effect of internal degrees of freedom was that of Eucken[14] who separated the ratio λ/η into two terms, one for translational kinetic energy and one for all other forms of molecular energy. He assumed that the transfer of translational kinetic energy follows the equation derived from the rigorous theory, Eq. 6, and that the transfer of internal energy follows the relation obtained on the basis of the elementary treatment, Eq. 3. He wrote

$$\frac{\lambda}{\eta} = \frac{5}{2} \; c_{vt} + 1.0 \; c_i \; . \qquad (7)$$

Comparison with the experimental data indicates that Eq. 7 holds fairly well for most nonpolar gases over a certain limited range of temperature and poorly for polar gases at all temperatures.

Hirschfelder[22] has derived the Eucken type equation in a rigorous way. He showed that the numerical factor in front of c_i, which has been frequently written as f_{int}, should be

$$f_{int} = \frac{15\,R\,n\,D_{11}}{4\,\lambda_{mon}} , \qquad (8)$$

where λ_{mon} is a fictitious conductivity calculated on the assumption that the polyatomic molecule is effectively monatomic. For the Lennard-Jones 6–12 potential and the Buckingham 6–exp. potential, it can be shown that f_{int} has the value of 1.328 to within a few percent.

Schafer[45], Franck,[16] and Bromley[6] have independently refined the Eucken relation by splitting the internal energy contribution to the ratio, λ/η, into its various components and have proceeded to evaluate the f's in Eq. 9,

$$\frac{\lambda}{\eta} = f_t c_{vt} + f_r c_r + f_{ir} c_{ir} + f_v c_v + \cdots . \qquad (9)$$

The most recent and comprehensive work in this direction is that of Bromley,[6] who collected literature data for λ, η, C_v, and $\gamma = C_p/C_v$ and derived therefrom the numerical values for the f's. He showed that, except for H_2, $f_r = 1.0$, and that f_{ir} and f_v decreased from 1.32 to 1.0 with rising temperature. For H_2, f_r was found to be 1.32. These results are in general agreement with the theoretical predictions that $f = 1.0$ if internal energy transfer by collision is rapid, and $f = \rho D/\eta$ if a large number of collisions (100 or more) are required for equalization of internal energy, because in this case the mechanism of energy transfer is one of pure diffusion rather than collision.[6,10a] Thus rotational energy is seen to be readily transferred except in the case of H_2, for which the data of Huber and Kantrowitz showed that several hundred collisions are necessary for rotational equilibrium.[29] Bromley has also pointed out that, except at extreme temperatures, most gases will have $\rho D/\eta$ equal to about 1.32, which supports the fact that vibrational and internal rotational energy at low and moderate temperatures are transferred by diffusion. At high temperatures, as the vibrational heat capacity approaches the classical values, f_v and f_{ir} tend toward unity.

Hirschfelder pointed out that the Eucken expression would not be valid if nonadiabatic collisions distort the molecular distribution function.[22] Uhlenbeck, Wang Chang, and deBoer have extended the formal treatment of the kinetic theory to polyatomic molecules.[61] They also have shown that, in the limit when nonadiabatic collisions are infrequent as compared to adiabatic collisions, the Eucken-type formula is valid. In their treatment, the translational energy is considered classically and the internal energy, quantum mechanically. Each quantum state of the molecule is taken to be a separate chemical specie having its own Boltzmann equation. Except for the special cases of a perfectly smooth sphere and a rigid spheroid, extensive numerical results from this theory are not yet available.

B. Thermal Conductivity and Viscosity of Mixtures

In this section, a brief review of selected literature on conductivity and viscosity of mixtures is presented. On the basis of the elementary kinetic theory, Wassiljewa proposed the following equation for the conductivity of a binary mixture,[65]

$$\lambda_m = \frac{\lambda_1}{1 + A_{12} \frac{x_2}{x_1}} + \frac{\lambda_2}{1 + A_{21} \frac{x_1}{x_2}} , \qquad (10)$$

which is identical in form to Sutherland's equation for the viscosity of a binary mixture.[50] Weber showed that the A's should be the same for both viscosity and conductivity;[66] but, experimentally, different values are found. In contrast to pure gases, no simple relation exists between the conductivity, viscosity, and heat capacity of a mixture. It has been customary in this field to treat the two transport properties separately. They will be discussed here also under two headings.

1. Thermal Conductivity

The rigorous kinetic-theory treatment of conductivity leads to expressions that are complicated even for very simple molecular models.

Numerical results have been obtained only for mixtures of spherical molecules that interact according to the Lennard-Jones 6–12 potential and the modified Buckingham 6–exp potential. For monatomic mixtures, Hirschfelder et al. demonstrated that calculations based on the Lennard-Jones model yielded values of conductivity that are within a few percent of experimental.[24]

For polyatomic gases, Hirschfelder et al. recommended an empirical procedure that involves the calculation of a fictitious conductivity on the assumption that the polyatomic molecules are effectively monatomic.[23] The result so obtained is then multiplied by a correction factor which is a function of composition and ratios of the experimental conductivity of a pure component to the conductivity calculated by assuming that the component is monatomic. The empirical expression is:

$$\lambda_m = \lambda_{mix\ mon} \left(x_1 E_1 + x_2 E_2 \right) \tag{11}$$

where

$$E_i = \frac{\lambda_{i\ expt}}{\lambda_{i\ mon}} \tag{12}$$

This procedure corresponds to correcting the calculated monatomic mixture condictivity by a linearly averaged Eucken-type factor of the pure components. Further refinement in the Eucken-type correction has been developed by Hirschfelder in the following relation:[22]

$$\lambda_m = \lambda_{mix\ mon} + \frac{\lambda_1 - \lambda_{1\ mon}}{1 + \frac{D_{11}}{D_{12}} \frac{x_2}{x_1}} + \frac{\lambda_2 - \lambda_{2\ mon}}{1 + \frac{D_{22}}{D_{21}} \frac{x_1}{x_2}} \tag{13}$$

Equations 11 and 13 have been tested for several systems.[22] In most instances, the deviation from experiment is under 10%. The calculations are quite laborious even for the simplest binary mixtures. Because these equations are of the same order of accuracy as other simpler, though empirical, expressions, extensive computation based on them do not appear very profitable practically.

A number of authors have attempted to correlate the conductivity of mixtures on a strictly empirical basis. Kennard and others recommended

an equation of the following form:

$$\lambda_m = \lambda_1 x_1^2 + K x_1 x_2 + \lambda_2 x_2^2 \qquad (14)$$

where K is an empirical constant.[34] Lindsay and Bromley pointed out that the agreement of this equation with experiment is poor even if the constant, K, is determined by least squares from the data.[40] Davidson and Music represented their data for several mixtures at 0°C by

$$\lambda_m = e^{a+bx}, \qquad (15)$$

wherein a and b are constants characteristic of each pair, and x is the mole fraction of the light component.[12] More recently Brokaw proposed

$$\lambda_m = \alpha' \lambda_{sm} + (1-\alpha') \lambda_{rm}, \qquad (16)$$

in which λ_{sm} and λ_{rm} are the conductivities of the gas mixture calculated according to the simple mixing rule and the reciprocal mixing rule, respectively, and α' is an empirical function of the mole fraction of light constituent of a binary pair.[5] For a mixture of more than two compenents, he arbitrarily takes $\alpha' = 0.5$. Lacking in sound theoretical foundation, these equations conform to experimental facts only under certain limited conditions, and their general application cannot be taken too seriously.

Bromley and Lindsay chose to work with relations of the form of Eq. 10.[40] They have expressed the A values as functions of the properties of the pure components. Two alternate equations are proposed. Following the method of Buddenberg and Wilke for the viscosity of gas mixtures,[7] they found that

$$\lambda_m = \frac{\lambda_1}{1 + \frac{1.114\,\lambda_1}{\rho_1 C_{p_1} D_{12}} \frac{x_2}{x_1}} + \frac{\lambda_2}{1 + \frac{1.114\,\lambda_2}{\rho_2 C_{p_2} D_{21}} \frac{x_1}{x_2}} \qquad (17)$$

correlates data near room temperature with an average deviation of 3.5% and a maximum deviation of 11.7%. Because of the difficulty of obtaining accurate diffusion coefficients, they empirically modified Sutherland's equation for the viscosity of a mixture[50] (see Eq. 19 below) and arrived at the following expression for the A's in Eq. 10:

$$A_{12} = \frac{1}{4}\left\{1 + \left[\frac{\eta_1}{\eta_2}\left(\frac{M_2}{M_1}\right)^{3/4}\frac{1 + \frac{S_1}{T}}{1 + \frac{S_2}{T}}\right]^{\frac{1}{2}}\right\}^2 \frac{1 + \frac{S_{12}}{T}}{1 + \frac{S_1}{T}} \quad . \qquad (18)$$

For other A values, the subscripts are interchanged. By making suitable adjustments in the evaluation of the Sutherland constant for the collision of unlike molecules, they succeeded in making Eqs. 10 and 18 applicable to polar as well as nonpolar molecules. Other authors have been content to consider polar mixtures as exceptions in their attempts to correlate conductivity of mixtures. Equations 10 and 18 are in good agreement with data near room temperature. For the 16 gas pairs and 85 different compositions considered by these authors, the average deviation between calculated and experimental values is 1.9% and the maximum deviation, 10%.

2. Viscosity

From the simple kinetic theory and Sutherland's model, Sutherland[50] showed that the constants in Eq. 10 should be

$$A_{12} = \frac{1}{4}\left\{1 + \left[\frac{\eta_1}{\eta_2}\left(\frac{M_2}{M_1}\right)^{\frac{1}{2}}\frac{1 + \frac{S_1}{T}}{1 + \frac{S_2}{T}}\right]^{\frac{1}{2}}\right\}^2 \left(\frac{M_1 + M_2}{2M_2}\right)^{1/2} \frac{1 + \frac{S_{12}}{T}}{1 + \frac{S_1}{T}} \quad . \qquad (19)$$

The subscripts are interchanged in the case of A_{21}. However, it was found that agreement between theory and experiment is improved if the right-hand member of Eq. 19 is multiplied by $[2M_2/(M_1 + M_2)]^{3/4}$. Lindsay and Bromley developed their formula for conductivity by a similar empirical modification of this expression.[40]

Taking a more rigorous theoretical approach, Thiesen also developed a formula for viscosity of binary mixtures in the form of Eq. 10.[52]

Schudel showed that A_{12} and A_{21} are related as follows:[47]

$$\frac{A_{12}\,\rho_1}{\eta_1} = \frac{A_{21}\,\rho_2}{\eta_2} = G \,. \tag{20}$$

From a careful analysis of the data, Buddenburg and Wilke found that G may be expressed in terms of the diffusion coefficient:[7]

$$G = \frac{1.385}{D_{12}} \,. \tag{21}$$

Furthermore, they have expanded Eq. 10 to a more general form to include multicomponent mixtures. They proposed the following expression:

$$\eta_m = \sum_{i=1}^{n} \frac{\eta_i}{1 + \dfrac{1.385\,\eta_i}{x_i\,\rho_i} \displaystyle\sum_{\substack{j=1 \\ j\neq i}}^{j=n} \frac{x_i}{D_{ij}}} \,. \tag{22}$$

By application of the kinetic theory, Wilke eliminated the empirical coefficient and D_{ij} from Eq. 22, and obtained a relation that gives mixture viscosity as a function of the viscosities of the constituents and their molecular weights:[67]

$$\eta_m = \sum_{i=1}^{n} \frac{\eta_i}{1 + \dfrac{1}{x_i} \displaystyle\sum_{\substack{j=1 \\ i\neq j}}^{j=n} x_j\,\phi_{ij}} \tag{23}$$

The value of ϕ_{ij} in Eq. 23 is

$$\phi_{ij} = \frac{\left[1 + \left(\dfrac{\eta_i}{\eta_j}\right)^{1/2} \left(\dfrac{M_j}{M_i}\right)^{1/4}\right]^2}{\dfrac{4}{\sqrt{2}} \left[1 + \dfrac{M_i}{M_j}\right]^{1/2}} \,. \tag{24}$$

A method for estimating mixture viscosity from the principle of corresponding states was developed by Uyehara and Watson.[61a] Kuenen derived an equation by a corrected mean-free-path method.[39]

From the rigorous kinetic theory, Chapman and Cowling derived an equation for the first approximation to the viscosity of binary mixtures.[9] This equation expresses the viscosity as a function of the viscosities and molecular weights of the components and two constants that depend upon the interactions of molecules of different kinds. Hirschfelder et al. also developed from the rigorous theory an expression for binary mixtures in terms of the viscosities and molecular weights of the constituents and a quantity that may be regarded as the viscosity of a hypothetical pure substance having a molecular weight of $(2M_1M_2)/(M_1 + M_2)$ and following the law of interaction governing collision of molecules of different kinds.[25] For multicomponent mixtures, Hirschfelder et al. put forth a rather complex expression based on the rigorous theory. After making certain approximations, they reduced their equation to the form identical with the Buddenburg-Wilke equation, with the constant 1.385 replaced by 2. They thus established the theoretical basis of Eq. 22.

CHAPTER II. Alternate Correlations of Thermal Conductivity and Viscosity of Gas Mixtures.

A. Relations Between the Transport Properties of Gas Mixtures

According to the kinetic theory, the thermal diffusivity, diffusion coefficient, and the kinematic viscosity for an ideal gas are of the order of the product of the mean free path and the root-mean-square velocity of the molecules:

$$\frac{\lambda}{\rho\ C_v} \approx D \approx \frac{\eta}{\rho} \approx \Lambda\ v\ . \tag{25}$$

For a single component system, we have

$$\lambda_1 \approx D_{11}\ \rho_1\ C_{v_1}\ . \tag{26}$$

Thus, thermal conductivity is proportional to the rate of movement of the individual molecules within the gas and the heat capacity per unit volume of the molecules. Analogously, for the same gas in a mixture we have

$$\lambda_{1m} \approx D_{1m}\ \rho_{1m}\ C_{v_1}\ . \tag{27}$$

Dividing 27 by 26 and assuming the proportionality constant to be the same in both expressions, we find

$$\frac{\lambda_{1m}}{\lambda_1} = \frac{D_{1m}\ \rho_{1m}}{D_{11}\ \rho_1} = x_1\ \frac{D_{1m}}{D_{11}}\ . \tag{28}$$

The diffusion coefficient, D_{1m}, is a measure of the rate of movement of a molecule of type 1 within a mixture of other molecules of type 1 with molecules of other types. Following Wilke's treatment of the diffusion of a gas into a multicomponent mixture, we may write D_{1m} as[68]

$$\frac{1}{D_{1m}} = \frac{x_1}{D_{11}} + \frac{x_2}{D_{12}} + \cdots\ . \tag{29}$$

After Eq. 29 is multiplied through by D_{11} and inverted, the ratio $\frac{D_{1m}}{D_{11}}$ required in Eq. 28 is obtained:

$$\frac{D_{1m}}{D_{11}} = \frac{1}{x_1 + \frac{D_{11}}{D_{12}} x_2 + \frac{D_{11}}{D_{13}} x_3 + \cdots} \quad . \tag{30}$$

The thermal conductivity of a mixture is the sum of the conductivities of the individual components, i.e.,

$$\lambda_m = \lambda_{1m} + \lambda_{2m} + \cdots \quad . \tag{31}$$

Combining Eqs. 28, 30, and 31, we have

$$\lambda_m = \frac{\lambda_1}{1 + \frac{D_{11}}{D_{12}} \frac{x_2}{x_1} + \frac{D_{11}}{D_{13}} \frac{x_3}{x_1} + \cdots} + \frac{\lambda_2}{1 + \frac{D_{22}}{D_{21}} \frac{x_1}{x_2} + \frac{D_{22}}{D_{23}} \frac{x_3}{x_2} + \cdots} + \cdots$$

$$= \sum_{i=1}^{n} \frac{\lambda_i}{1 + \sum_{\substack{i=1 \\ i \neq j}}^{n} \frac{D_{ii}}{D_{ij}} \frac{x_j}{x_i}} \quad . \tag{32}$$

B. Thermal Conductivity of Nonpolar Mixtures

In order to calculate the conductivity of a mixture from Eq. 32, it is necessary to have the data for the pure components and the ratios of the diffusion coefficients. Experimental values for the latter quantities are presently scarce. However, they may be calculated with fair accuracy by either the method of Hirschfelder et al.,[27] which is based on the Lennard-Jones 6–12 model, or the method of Arnold.[4] With the former method, Eq. 32 was applied to several binary systems. In all cases, the calculated conductivity was found to be higher than the

experimental values. The maximum deviation appears to be about 15%. A comparison of Eq. 32 with the experimental data for He-A mixtures is shown in Fig. 1. The trend of the deviations is such that the largest discrepancies occur in systems having components whose molecular weights differ most widely. It appeared possible to improve Eq. 32 by taking A_{ij} as the product of a power of D_{ii}/D_{ij} and an empirical function of the molecular weight in the form of $(M_{ij}/M_i)^n$. Hence, we obtain

$$\lambda_c = \sum_{i=1}^{n} \frac{\lambda_i}{1 + \sum_{\substack{i=1 \\ i\neq j}}^{n} \left(\frac{D_{ii}}{D_{ij}}\right)^m \left(\frac{M_{ij}}{M_i}\right)^n \frac{x_j}{x_i}} , \qquad (33)$$

where M_{ij} is the arithmetic average of M_i and M_j. When energy transfer occurs by collision, the exponent m and the factor $(M_{ij}/M_i)^n$ may be considered as corrections for the difference in the mean free paths appropriate to diffusion and to heat conduction and for the difference of the effects of persistence of velocity upon conductivity and upon diffusion. In the case of energy transfer by diffusion, the use of a value of m other than unity and n different from zero cannot be justified on similar grounds. It seems reasonable to assume that Eq. 33 would apply only to the collisional contribution of conductivity, and that Eq. 32 would apply only to the diffusional contribution. Therefore, we have

$$\lambda_m = \sum_{i=1}^{n} \frac{\lambda_{ci}}{1 + \sum_{\substack{i=1 \\ i\neq j}}^{n} \left(\frac{D_{ii}}{D_{ij}}\right)^m \left(\frac{M_{ij}}{M_i}\right)^n \frac{x_j}{x_i}} + \sum_{i=1}^{n} \frac{\lambda_{di}}{1 + \sum_{\substack{i=1 \\ i\neq j}}^{n} \frac{D_{ii}}{D_{ij}} \frac{x_j}{x_i}} , \qquad (34)$$

where $$\lambda_{ci} = \frac{2.5\, c_{vt} + 1.0\, c_r}{2.5\, c_{vt} + 1.0\, c_r + 1.32\,(c_v + c_{ir} + \cdots)} \lambda_i \qquad (35)$$

and $$\lambda_{di} = \lambda_i - \lambda_{ci} , \qquad (36)$$

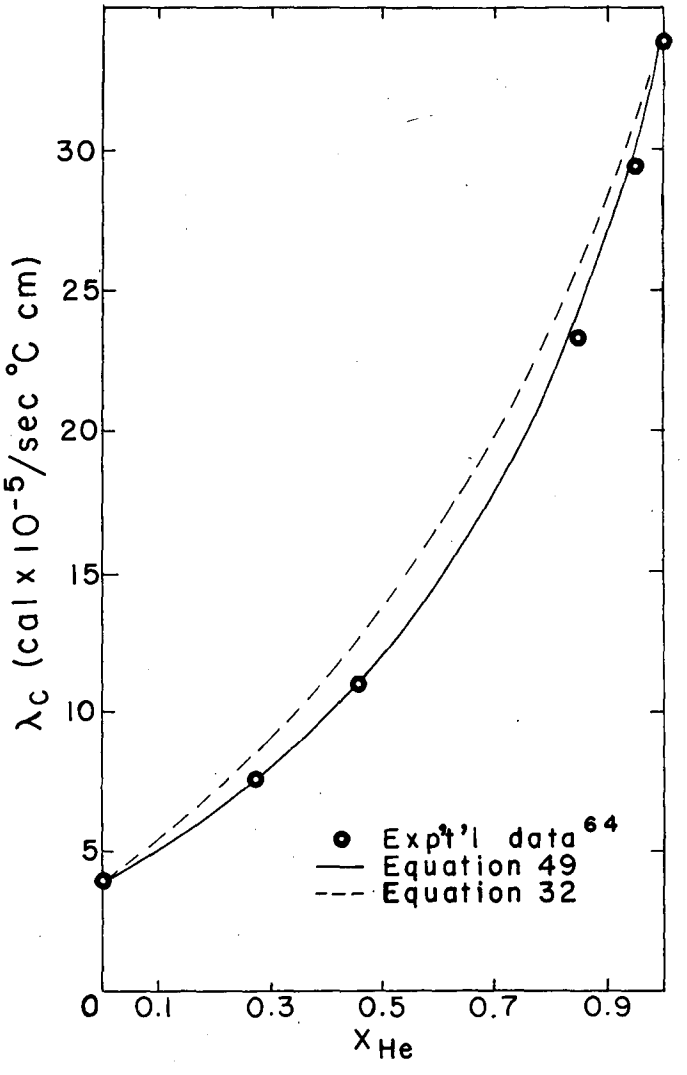

Fig. 1. Experimental and calculated conductivity of He–A mixtures at 0°C.

except in the case of hydrogen, for which the c_r term does not appear in the numerator and the numerical factor in front of c_r in the denominator is about 1.32 (as pointed out in Chapter I). The evaluation of the empirical constants m and n and comparison of the resulting correlation with experimental data are presented in Chapter V.

C. Thermal Conductivity of Polar-Nonpolar Mixtures

It is reasonable to believe that Eq. 34 should also be applicable to mixtures containing polar molecules, provided the ratios of the diffusivities are known either from experiment or calculation. As in the case of nonpolar mixtures, the paucity of experimental data requires that a good method be found for predicting these ratios. The method of Hirschfelder et al. for averaging the force constants for the Lennard-Jones 6–12 potential cannot be applied to polar-nonpolar mixtures.[27] Moreover, in many instances, it is impossible to determine these force constants for the polar components. Arnold's method of calculation yields binary diffusion coefficients that are too high in nearly all cases.[4] Theoretically, it should be possible to determine from experimental data the molecular volume and the Sutherland's constant that would be appropriate for a polar molecule in a mixture containing nonpolar molecules. An experimentally determined diffusion coefficient for the diffusion of a polar gas into a nonpolar gas provides a relation between the molecular volume and the Sutherland's constant of the polar gas; therefore, two such measurements would be sufficient for the calculation of these parameters. Once these parameters are obtained, the diffusion coefficient for the diffusion of the polar gas into any other nonpolar gas may be readily calculated. However, calculations based on data for the diffusion of water into CO_2 and water into H_2 indicate that it is impossible to obtain a set of values for the molecular volume and the Sutherland's constant for water that would fit both cases. Apparently, Arnold's equation is not sufficiently rigorous to withstand such a test. Another difficulty may be that the molecular volume and/or the

Sutherland's constant are not truly constants. Even if it were possible to determine the constants, the scarcity of data would still impose a serious limitation.

An alternate approach would be to modify Arnold's equation by taking the mean Sutherland's constant to be $0.733\sqrt{S_1 S_2}$, according to Gruss and Schmick.[20] Lindsay and Bromley recommended this procedure in their correlation of mixture conductivities,[40] but Vine and Bennett found that all of their data did not fit the Lindsay-Bromley relation using the value of 0.733.[62] They showed that in order to make the Bromley-Lindsay relation agree with the data, it was necessary to replace 0.733 by a number ranging from 0.60 to 0.93. Apparently the constant 0.733 is only a rather rough approximation to the experimental facts. However, until the interaction between polar and nonpolar molecules is better understood, the use of 0.733 or a number based on experimental data, if such is available, seems to be the simplest method at hand for correlating the data of polar-nonpolar mixtures.

D. Viscosity

The analog of Eq. 32 for viscosity is

$$\eta_m = \sum_{i=1}^{n} \frac{\eta_i}{1 + \sum_{\substack{i=1 \\ i \neq j}}^{n} \frac{D_{ii}}{D_{ij}} \frac{x_j}{x_i}} \,. \tag{37}$$

Equation 37 yields calculated viscosities that are a few percent higher than experimental values. A comparison of this equation with the data of H_2–Ne mixtures is shown in Fig. 2. For the same reasons as in the case of thermal conductivity, it appears desirable to modify this equation in the manner as in Eq. 32 above; hence, one assumes

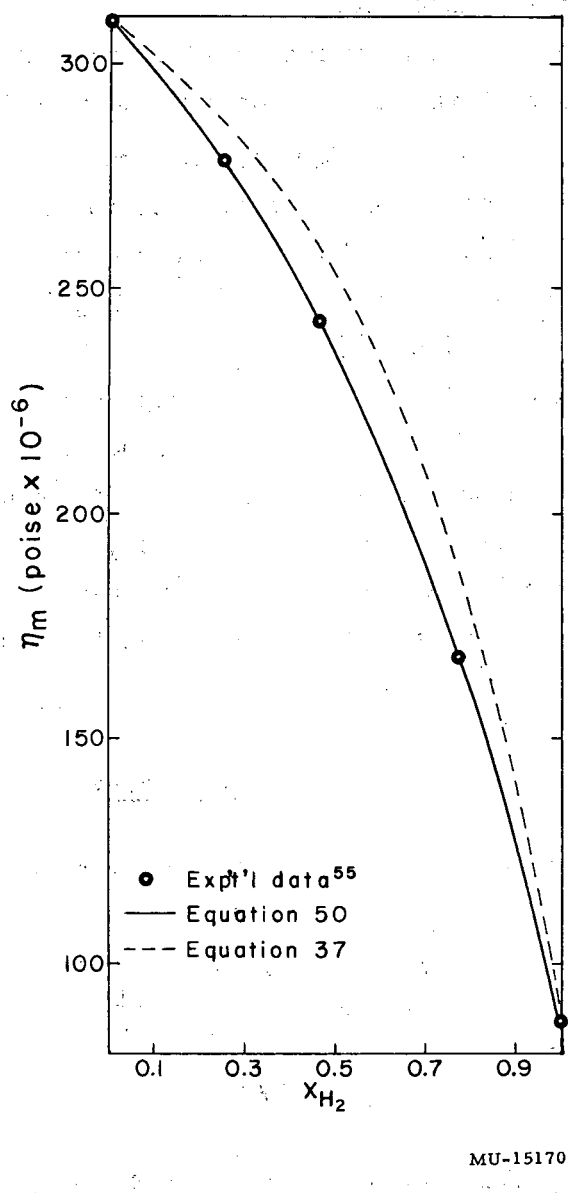

Fig. 2. Experimental and calculated viscosity of H_2–Ne mixtures at 20°C.

$$\eta_m = \sum_{i=1}^{n} \frac{\eta_i}{1 + \sum_{\substack{i=1 \\ i \neq j}}^{n} \left(\frac{D_{ii}}{D_{ij}}\right)^p \left(\frac{M_{ij}}{M_i}\right)^q \frac{x_j}{x_i}} \quad . \tag{38}$$

The determination of the empirical constants p and q and comparison with experimental data are discussed in Chapter V.

Equation 38 may also be applied to polar-nonpolar mixtures. The diffusivity ratios for such mixtures may be calculated from the modified form of Arnold's equation as discussed in Section C above.

With certain appropriate assumptions, Eq. 37 can be shown to be identical with that proposed by Wilke, although he had approached the problem from quite a different direction.[67] The identity of the Ratio D_{ii}/D_{ij} with Wilke's ϕ_{ij} is proved in Appendix I. This result also yielded a method for estimating self-diffusion coefficients as discussed in Appendix II.

CHAPTER III. Experimental Method

A. Introduction

The thermal conductivities of pure and mixed gases in the temperature range of 100° to 540°C were obtained by means of a thermal-conductivity cell of the concentric cylinder type.[44] A schematic diagram of the cell used in this work is shown in Fig. 3. The principle components of the cell are the two concentric silver cylinders and the heat guard. The inner cylinder is supported within the outer hollow cylinder by means of Lava* tips. An electrical heater is placed inside the inner cylinder to supply the energy to be transported across the gas filled annular space between the inner and outer cylinders as well as the space at the bottom end of the cylinders. The heat guard is a silver cylinder containing an electrical heater. The purpose of the heat guard is to prevent heat flow from the upper end of the inner cylinder. Thermocouples measure the temperature of the inner cylinder, the outer cylinder, and the heat guard. Auxiliary equipment described below maintains the cell at steady-state conditions of temperature, pressure, and electrical-energy input to the inner cylinder. From the temperature measurements, the electrical energy input, and the dimensions of the cell, the conductivity of the gas within the space between the inner and outer cylinders may be computed as discussed in Section E. below.

The details of the experimental equipment, the gases used, the experimental procedure, and the method of calculation are described in this chapter.

---

* Lava is a product of American Lava Corporation, Chattanooga, Tennessee. It is a natural stone which may be machined and then fire-hardened to a refractory.

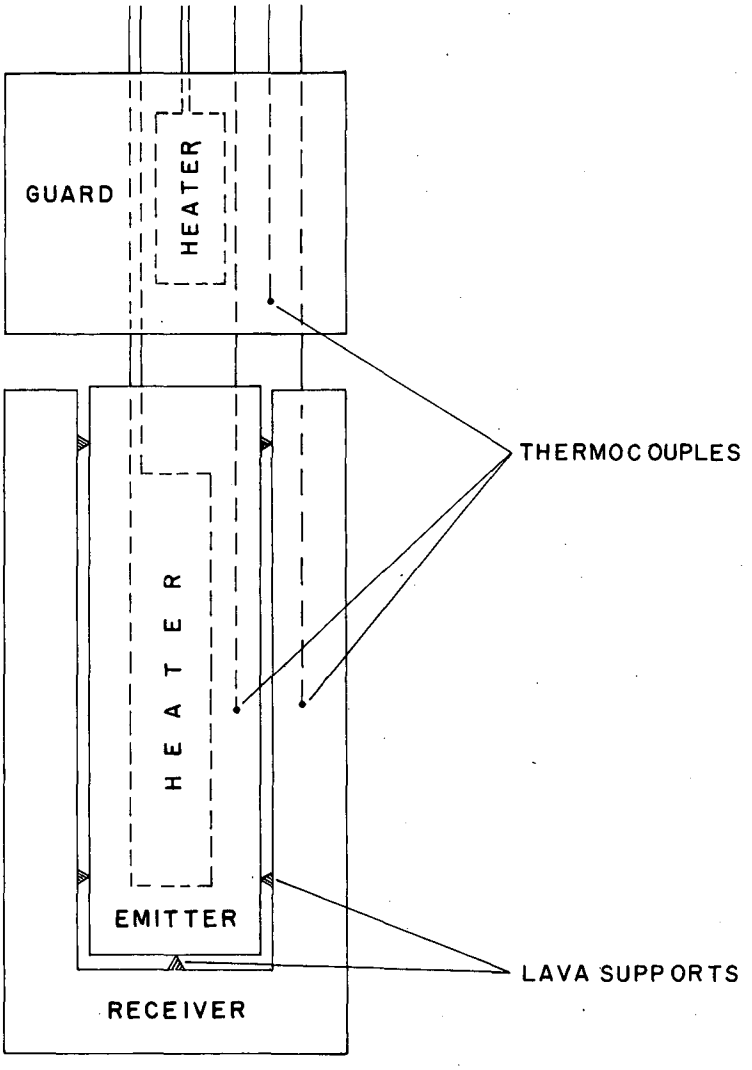

Fig. 3. Schematic diagram of thermal-conductivity cell.

B. Equipment

1. Conductivity Cell and Associated Components.

With the exception of certain modifications and additions, the equipment used in this work is essentially that described by Rothman[44] unless otherwise noted. The thermal-conductivity cell consists of two concentric silver cylinders 7 inches long (Fig. 4). The inner cylinder, the emitter, has a 0.7197-inch radius. The hollow outer cylinder, the receiver, has radii of 0.7530-in. and 1.25-in. The width of the annalus between the emitter and the receiver is 0.0333-in. Concentricity between the two cylinders is maintained by six Lava supporting tips. The bottom of the receiver is closed by a silver disk, and the emitter is supported 0.053-in. above it by a Lava tip.

The emitter contains a heater, the electrical energy input into which can be accurately regulated and measured. It consists of a spirally wound 0.016-in.-diam. nichrome coil encased in a shell of 0.015-in. stainless steel. Nine-inch lengths of 0.015-in. platinum are fused to the ends of the nichrome wires in order to reduce energy loss by heat conduction along the two wires leading from the emitter. The other ends of the platinum wires are fused to 24 in. of 0.015-in. gold wires which serve to minimize the voltage drop between the emitter and the external measuring circuit.

In order that the energy input to the emitter be totally transferred to the receiver, energy flow from the top of the emitter is prevented by the heat guard, located 0.5 in. above the emitter. This is a silver cylinder 3 in. in length and 2.5 in. in diameter, containing a heater similar to that inside the emitter. Through regulation of energy input, the temperature of the heat guard may be maintained equal to that of the emitter.

Thermocouple wells are drilled into each of the three silver cylinders. Temperature measurements are made with three Pt-PtRh thermocouples encased in ceramic protection tubes and inserted into thin-walled stainless steel casings which fit tightly in the wells drilled in the

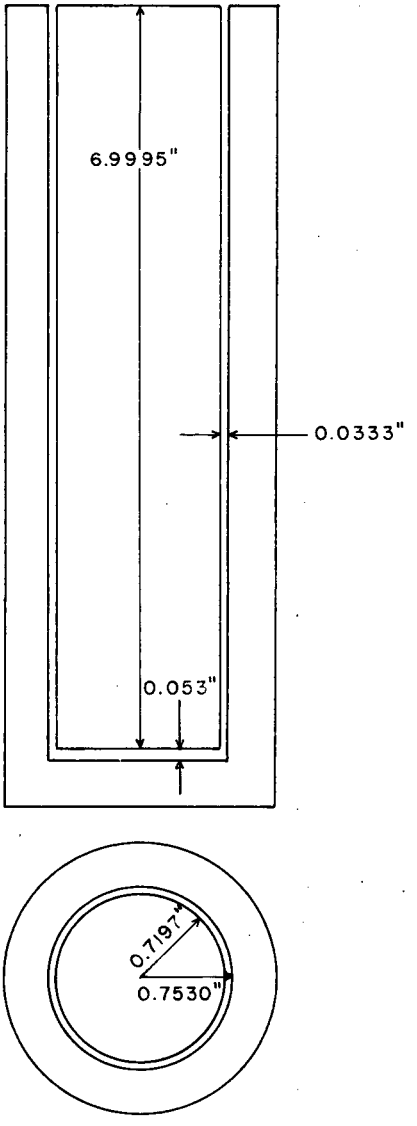

MU-15172

Fig. 4. Conductivity-cell dimensions.

silver. The couples may be raised or lowered inside the steel casing to allow temperature exploration along the axis of the cell.

The cell is enclosed in a stainless steel casing made in three parts: the top flange, the gasket, and the body (Fig. 5). The three stainless steel thermocouple wells and conduits for the electrical leads of the heaters are passed through the top flange and welded thereon, so that the thermocouples and the heaters are isolated with respect to pressure from the silver cylinders. A pipe for evacuating the cell and admitting gas is also welded onto the top flange. A bundle of 0.25-in. stainless stell tubes is placed within the vertical section of this pipe in order to prevent convective currents generated by temperature gradients from reaching the annulus space of the cell. Vacuum tightness is effected by proper application of pressure on the steel gasket through tightening the bolts between the top flange and the cell casing body.

The above assembly is placed inside an 800-lb copper cylinder which was cut into three sections and machined to fit snugly over the stainless steel parts (Fig. 6). This copper cylinder takes the place of the tin bath used by Rothman who found corrosion a serious problem.[44] The large heat capacity and the high heat conductivity of the copper cylinder serve to help maintain constant and uniform ambient temperature for the cell. Four chromel-alumel thermocouples and two nichrome-wire heaters are located strategically within the copper cylinder to measure and to regulate its temperature. An electronic controller described below regulates the temperature by varying the electrical energy input to the heaters in response to ambient conditions.

The copper block is surrounded by a 2 in. layer of Superex.* Nichrome-V heating coils are imbedded 0.5 in. into the outer surface of the top, bottom, and side of the Superex. Outside the coils is another 6 in. layer of Superex. The low thermal conductivity and thermal diffusivity of this material help to filter out short-term temperature

---

* Superex is a product of Johns-Manville. It is a high-temperature insulation made of diatomaceous earth.

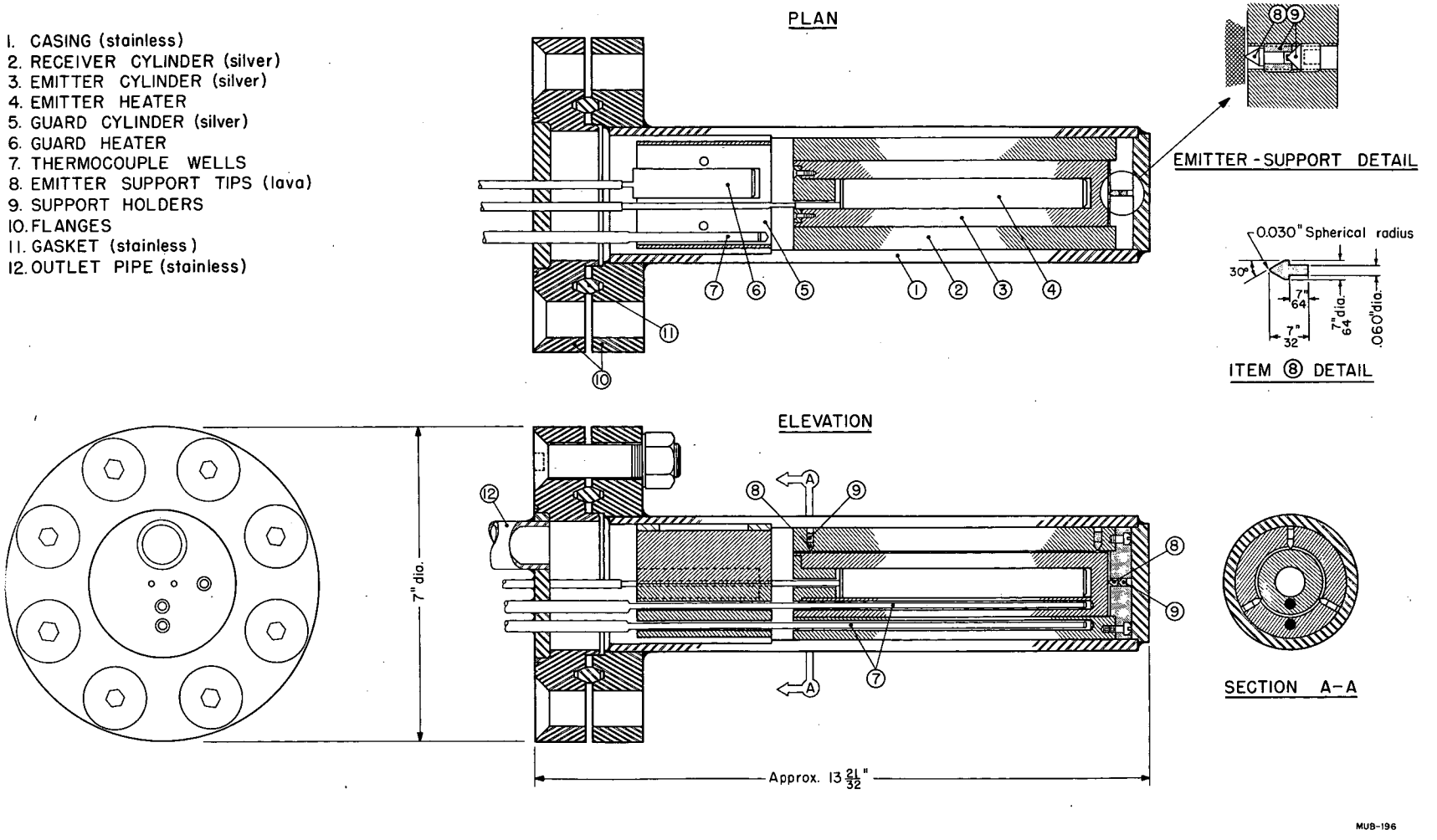

Fig. 5. Conductivity-cell assembly.

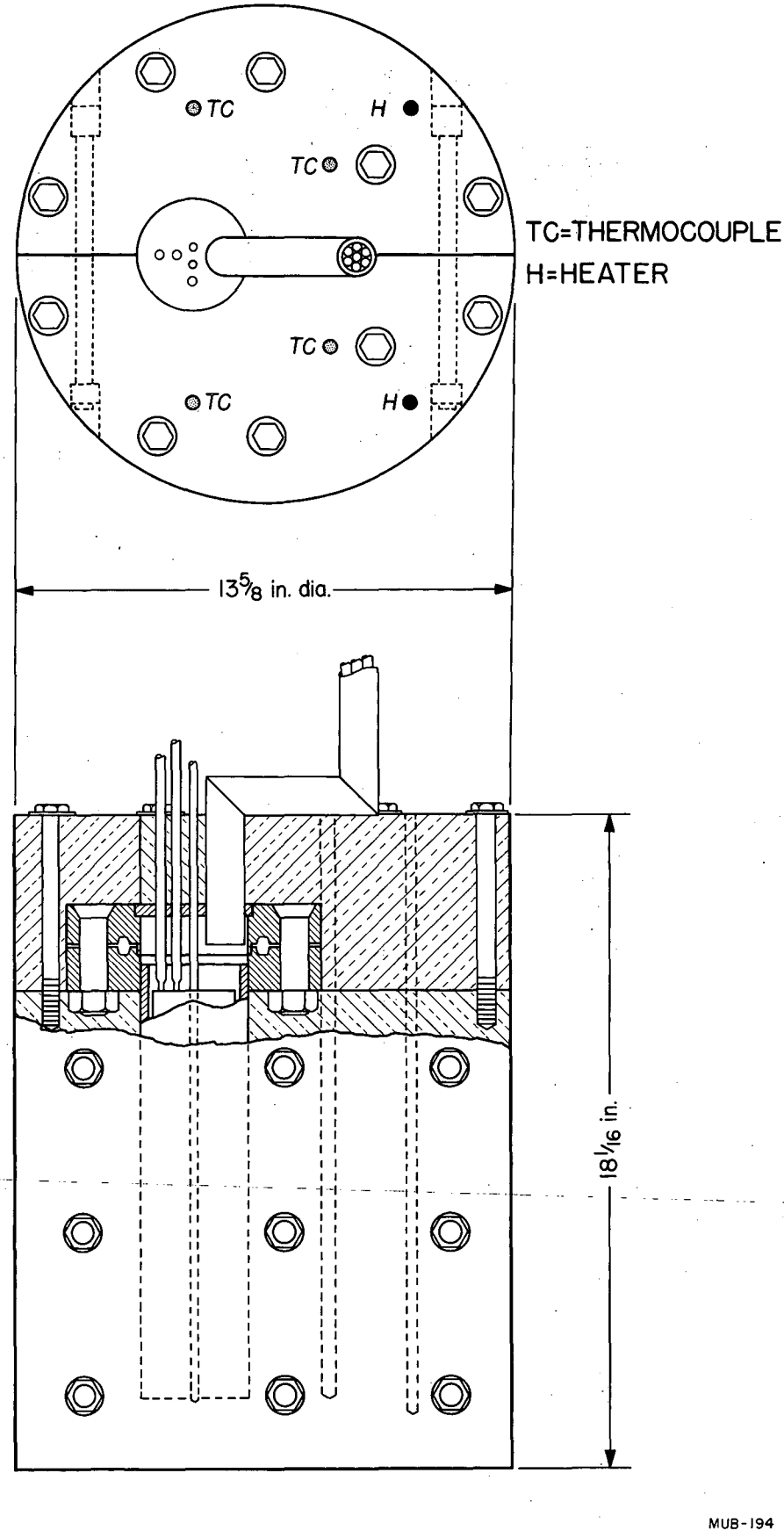

Fig. 6. Constant-temperature block.

fluctuations in the heating coils caused by voltage changes in the line. The outer casing of the equipment is a sheet-iron container onto which are soldered copper coils through which water circulates to maintain a constant and moderate temperature.

2. Gas-Handling System

In order to facilitate the handling of gas mixtures containing components condensable above liquid air temperatures, the piping system as used by Rothman[44] was completely dismantled and a new system was designed and constructed. The cell is evacuated and filled through a 0.75 in. I. P. S. stainless steel pipe (1 in. inside diameter) welded to the top flange of the cell casing. This pipe is connected by a flexible stainless steel tubing to the piping system as shown in Fig. 7. The evacuating equipment consists of a Kinney KC5 vacuum pump connected in series with a Distillation Products VMF-20 oil-diffusion pump. Pressure may be reduced to 0.1 micron of mercury. Gas is introduced into the cell from a cylinder in the case of pure components and from a mixing tank in the case of mixtures.

Six stainless steel tanks, whose volumes have been accurately measured, are used for preparing gas mixtures. Each of the tanks has its own calibrated thermometer and connection to a manometer. A Welch Duo-Seal No. 1405 vacuum pump is connected through a manifold that allows the tanks to be evacuated individually. A seventh tank is used for gas storage and for mixing when needed.

Pressure in the cell is measured with a McLeod gage for pressures down to 0.03 micron, with a thermocouple gage for pressures down to 5 micron, an absolute mercury manometer for pressures to 200mm, and an open-end manometer for pressures up to two atmospheres. Pressures up to 2.5 atmospheres in the gas tanks are determined with open-end manometers. A barometer in the laboratory is used in conjunction with the open-end manometers.

Because the equipment needs to withstand only relatively low pressures and the gases used are noncorrosive, choice of material of consturction is not a serious problem. Steel, brass, and glass are used throughout, depending upon convenience of fabrication.

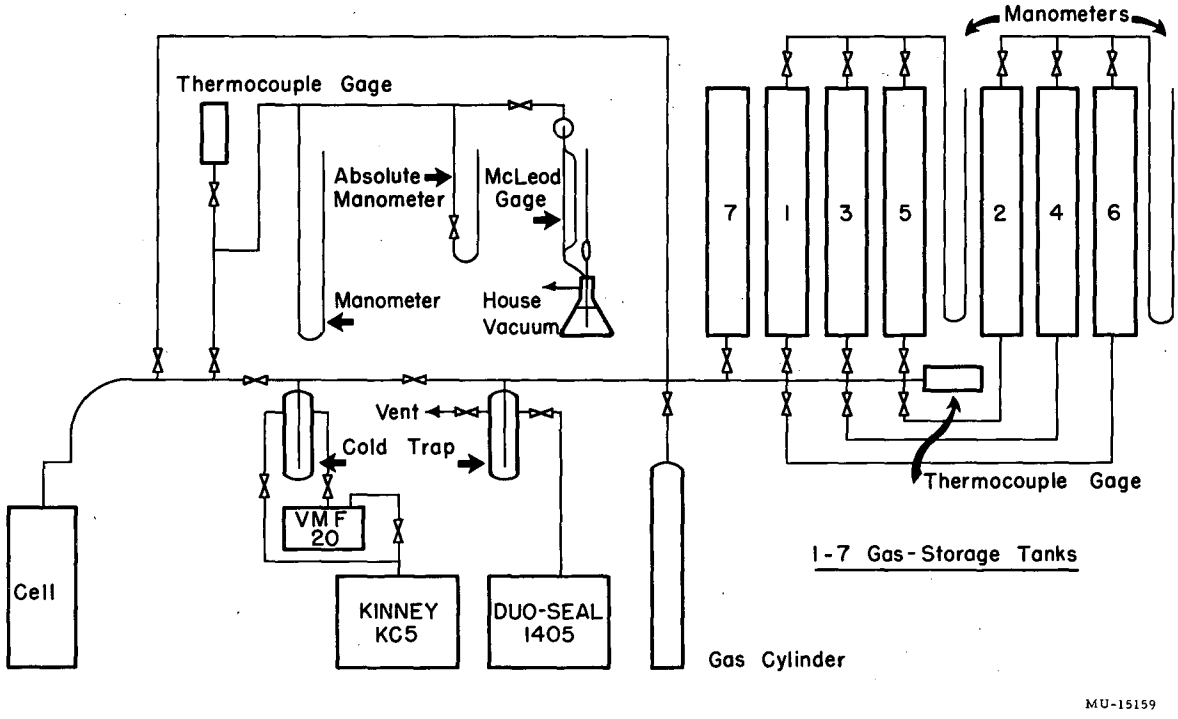

Fig. 7. Gas-handling system.

3. Electrical Circuits

a. Emitter and guard heaters. Constant voltage sources required for the emitter and guard heaters consist of 6-v wet storage batteries connected in parallel with a rectified output from the regulated 115-v A.C. line. A Sorensen Model 250S regulator is used to keep the variation in the A.C. voltage to within 0.1%. The voltage applied to the heaters is varied roughly by changing the number of storage batteries in the circuit and by varying the rectifier voltage output with variable transformers (Variacs). The rectifier output voltage is adjusted in such a manner that the current through the storage batteries is slightly above zero. In this way, the batteries act as a reservoir to help maintain the output of the parallel circuit constant. Fine variation of the currents through the heaters is made by a series of wire-wound rheostats ranging from 1 to 800 ohms. These circuits are shown in Fig. 8.

The guard and emitter circuits are identical except for the size of the heaters and instrumentation. The guard heater is approximately 35 ohms; the heater in the emitter is 90 ohms. Because the guard heater current is adjusted so that the temperature difference between the guard and the emitter is zero, accurate determination of the power through it is not required. An ordinary milliammeter is the only instrument used in this circuit. The energy input to the emitter is determined accurately from voltage and current measurements made with either a Leeds and Northrop No. 8662 or a Rubicon portable precision potentiometer (catalog No. 2745). Current is measured by the voltage drop across a standard 0.1-ohm resistor, and the voltage across the heater and standard resistor in series is measured with the usual voltage-divider–potentiometer circuit as shown in Fig. 8. The high resistance box in this curcuit was calibrated with standard resistors and found to be correct to better than 0.1%.

b. External heaters. These heaters are not associated with the cell proper but are required to maintain the cell at an elevated temperature. Two of them are located in the copper cylinder and three are imbedded in

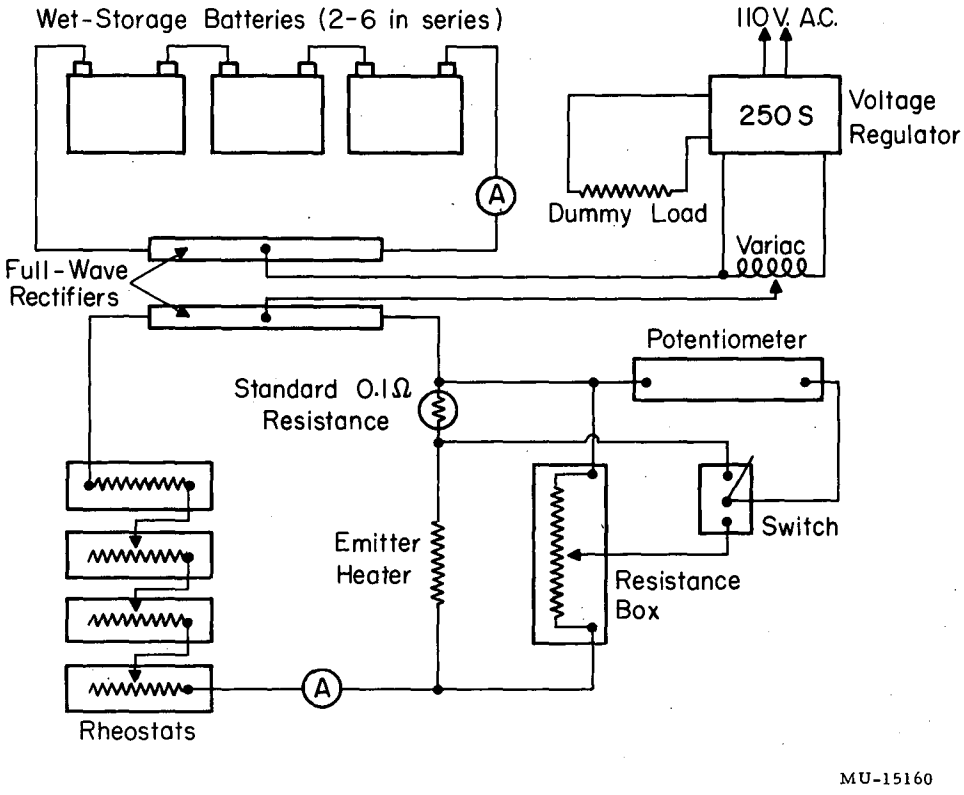

Fig. 8. Emitter heating and measuring circuit.

the Superex. The wiring diagram for these heaters is shown in Fig. 9. Nearly all of the heat required to maintain high temperatures is supplied through the latter heaters. Two input circuits are provided for these heaters as shown in Fig. 9. One is an 8-kw circuit taken directly from the 230-v house line. This is used for rapid warming up of the equipment. The other is a 3-kw circuit supplied from the 115-v line through Solex transformers, which control voltage fluctuation to ± 1%. This circuit is used during steady-state operation.

The two heaters in the copper cylinder are connected to a power supply actuated by the temperature controller which in turn receives its signal from a thermocouple located inside the copper cylinder and near the middle of the cell. These heaters are the counterparts of the tin-bath heaters used by Rothman.[44] Input to these heaters may be varied between 3 and 30 watts in response to the signal generated by the sensing thermocouple. In operation, the temperature controller is set by trial so that at the desired temperature the power input to the two heaters is about 17 w. In this manner, the cell is isolated from ambient temperature fluctuations, and cell temperature can be maintained at ± 0.1°C for periods of several hours. A block diagram of the temperature control loop is shown in Fig. 10.*

4. Temperature Measurement

Temperature is measured with Pt-10% PtRh thermocouples. These consist of 20-mil wires fused together and annealed in air at 1450°C for 1 hr, as recommended by the U.S. Bureau of Standards. They are threaded in 2-hole refractory porcelain insulators, which in turn are encased in a porcelain protection tube to prevent contamination of the platinum.

---

*Detailed drawings of the temperature controller and associated equipment are found in Figs. 5, 6, and 7 of Ref. 44. However only portions of the circuit shown thereon are used in this work. The "winding" preamplifier which receives a signal from a thermocouple is used in conjunction with the amplifier and power circuits marked "bath".

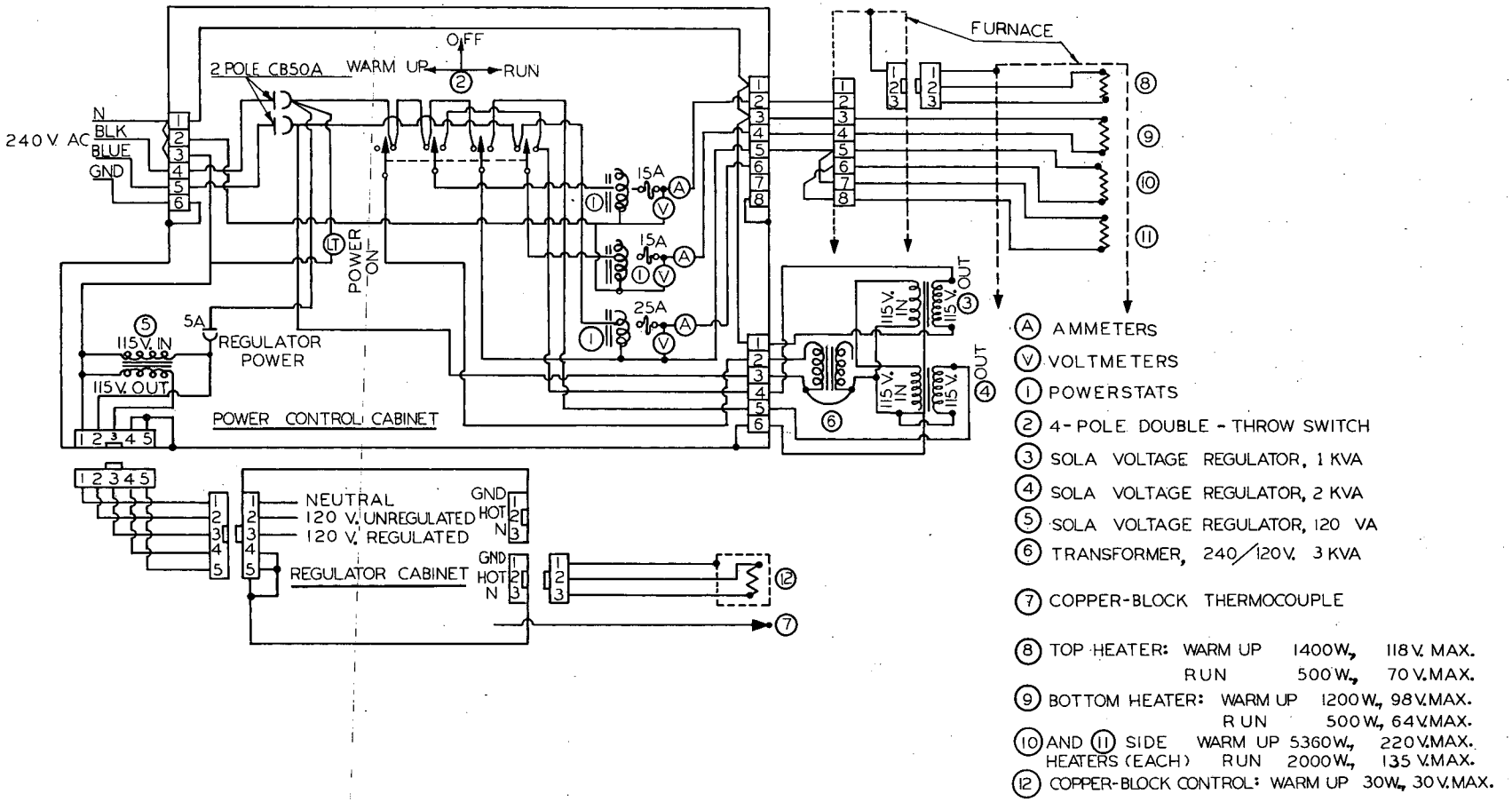

Fig. 9. Circuit of external heaters.

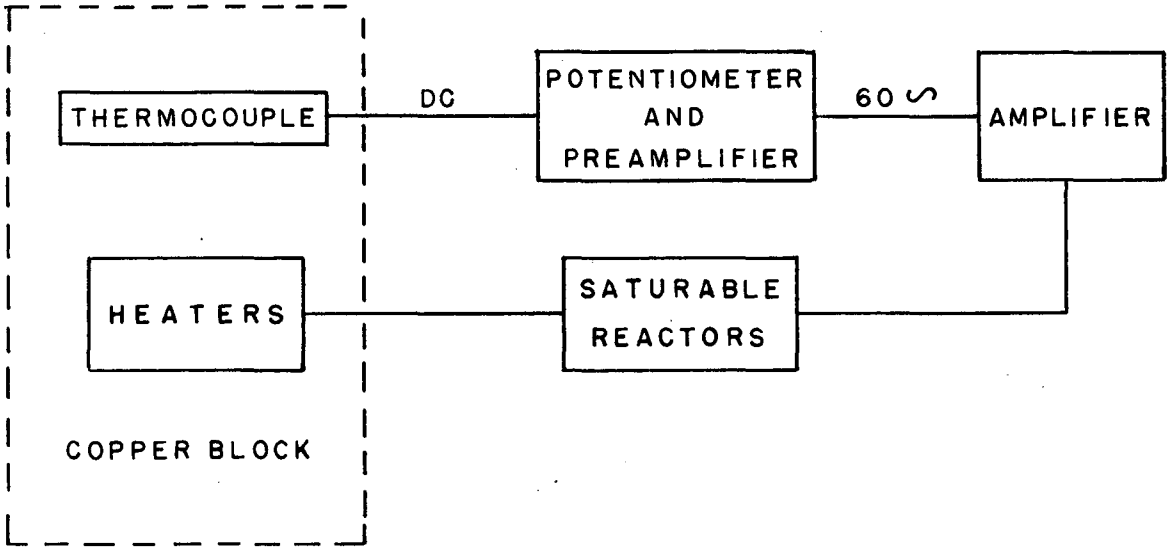

MU-15173

Fig. 10. Block diagram of temperature control loop.

This assembly is inserted into the stainless steel thermocouple wells in the emitter, receiver, and guard. The cold junction is a thermos bottle containing well-packed crushed ice and distilled water. Copper leads run from this cold junction to the emf measuring circuit.

A White double potentiometer is used in conjunction with a Leeds and Northrop No. 2285b high-sensitivity galvanometer for determination of thermal emf. The range of the potentiometer is 1 to 10,000 μv, and the sensitivity of the galvanometer is about 0.05 μv/mm of scale deflection. In the temperature range of this investigation, the rate of change of thermal emf of Pt-PtRh thermocouples with temperature is 6 to 10 μv/°C. In terms of temperature, 1 mm of galvanometer deflection corresponds to 0.005 to 0.008°C. Interconnected shields are used to keep the entire measuring system at the same potential so as to reduce errors caused by stray emf's. By means of a set of copper knife switches between the thermocouple leads and the potentiometer terminals, the absolute thermal emf of any one of the three thermocouples as well as the difference between any two of them may be read rapidly in any desired sequence.

C. Gases Used

The gases and vapors used in this investigation were taken directly from the manufacturer's cylinder or bottle without further purification. The sources and purities of the different materials are listed in Table I.

D. Procedure

The furnace was heated to the desired temperature by trial setting of the main heaters. Equilibrium temperature was usually attained in 24 to 48 hrs after switching on. Then the heaters in the copper block and cell were turned on, and the temperature controller set by trial. The guard temperature was made equal to that of the emitter by trial setting of the guard heater input.*

---

* Except for runs under vacuum, there is no detectable difference in the measured conductivity whether the guard is maintained at the emitter temperature or at the receiver temperature.

Table I

Gas	Source and Grade	Specified Purity(%)	Chief Impurities
N_2	Linde Air Products Co. "water pumped"	99.9	A, Ne
CO_2	Pure Carbonic, Inc.	99.5	Air
A	Linde Air Products Co. Standard grade	99.97	N_2
CH_4	Phillips Petroleum Co.	99	C_2H_6
Methyl formate	Eastman Kodak Co. S 1227 Spectro grade	--	--
C_2H_4	The Mathieson Co., Inc. C.P. grade	99.5	--
$(CH_3)_2O$	The Mathieson Co., Inc.	99.9	--
C_3H_8	The Mathieson Co., Inc. Instrument grade	99.9	--
O_2	Liquid Carbonic Co. Commercial grade	99.5	A
He	U. S. Navy Research grade	99.99	H_2, H_2O

At the beginning of a series of measurements at a particular temperature level, the cell was evacuated to a pressure of 1 μ of mercury or less in order to determine the rate of heat transfer by radiation across the annular space and by conduction across the Lava supports. After steady state was reached, the emf's of the thermocouple in the receiver and that in the emitter, and the difference in voltage between the two thermocouples were measured at regular intervals. These measurements were made with the thermocouples at the bottom of the wells because axial temperature exploration showed that conduction along the wells might cause the measured temperature to differ considerably from the actual temperature, especially for runs under vacuum. The experimental and theoretical justifications for positioning the thermocouples in this manner are given in Appendix III. The voltage across the 0.1-ohm standard resistor in the emitter circuit and that across the terminals to the emitter were also recorded periodically. The same procedure was followed when the cell was filled with gas. In most of the runs, the measurements were continued for at least half an hour at 5 to 10-min intervals.

In order to account for the difference of emf of the different couples, they were compared against the standard couple at each temperature level. Because the size of the thermocouples and of the wells are such that only one couple may be inserted in each well at a time, comparison had to be made under steady state condition by replacing each one of the couples in turn with the standard couple. Values of T_e, T_r, and ΔT were measured as described above. The positions of the standard couple and the couple under comparison were then quickly interchanged and again readings of T_e, T_r, and ΔT obtained. This procedure yielded three independent values of the difference between the ordinary and the standard couple at two different temperatures. Because the change with temperature of the emf difference between two couples is small with the usual ΔT of $10^{\circ}C$ or less, the average of the three values was taken as the proper correction. This procedure was repeated for each couple, and the two couples ordinarily used in the receiver and the emitter were also similarly compared as a check.

Measurements were made at several pressures in order to make correction for temperature discontinuity at the gas-solid interface. Usually three pressures were chosen in the range of 30 to 150 mm of mercury. In a number of cases more than three pressures were taken, while in a few others, only two were taken. At each different pressure, the following procedure was used. The cell was filled with the gas to a pressure between 0.5 and 1 atmos and then evacuated to 5mm of Hg or less. The filling and evacuating were repeated at least three times. The cell was then filled to the desired pressure, which was determined with an absolute manometer as well as with an open-end manometer.

Binary mixtures were prepared by allowing the streams from tanks containing the components to impinge against each other and flow simultaneously into an evacuated tank. The number of moles of each component was determined from the measured temperature, pressure, and volume of the gases in the tanks before and after mixing. The ideal gas law was used, since all pressures were under 2 atmos. The number of moles of mixtures was used as a check. Ternary mixtures were prepared in the same manner by mixing a binary with a pure gas.

E. Method of Computation

Experimental conductivity was calculated from the measured values of heat input to the emitter, the corresponding temperature difference between the emitter and receiver, and the geometry of the cell. It has been shown that the cell may be considered as a combination of infinite concentric cylinders and a pair of parallel plates.[44] An expression for the heat conducted by the gas from the emitter to the receiver may, therefore, be written in three parts as

$$q = \frac{2 \pi L \lambda_a \Delta T}{\ln \frac{r_2}{r_1}} + \frac{\pi r^2 \lambda_a \Delta T}{x} + q_{corner} . \qquad (39)$$

The corner effect may be accounted for with a maximum error of about 0.3% by taking an average for L in the first term as $L + \frac{x}{2}$ and for r^2 in the

second term as $(r_1^2 + r_2^2)/2$.[44] Thus we have

$$q = \frac{2\pi\left(L + \frac{x}{2}\right)\lambda_a \Delta T}{\ln \frac{r_2}{r_1}} + \frac{\pi\left(\frac{r_1^2 + r_2^2}{2}\right)\lambda_a \Delta T}{x} \qquad (40)$$

or $$Q = C' \lambda_a \Delta T, \qquad (41)$$

where

$$C' = \frac{2\pi\left(L + \frac{x}{2}\right)}{\ln \frac{r_2}{r_1}} + \frac{\pi\left(r_1^2 + r_2^2\right)}{2x} . \qquad (42)$$

The cell constant, C', at a particular temperature was calculated from the coefficients of thermal expansion of silver and Lava and the dimensions of the cell measured at room temperature. The average linear coefficient of silver was taken as 20×10^{-6} per $^{\circ}C$ and that for Lava as 3×10^{-6} per $^{\circ}C$. Figure 11 shows C' as a function of temperature.

The total rate of energy transfer from the emitter was determined by the current and the voltage drop across the emitter heater, which was obtained by subtracting the voltage drop across the leads and the standard resistor used for current measurement. When the cell is filled with gas, this rate represents heat transfer by three different avenues: gaseous conduction, radiation, and conduction across the supports. The sum of the heat transferred by the last two mechanisms was taken as that measured at high vacuum. Heat transfer by gaseous conduction was thus taken as the total heat transfer minus that measured under high vacuum. This procedure is based on the assumption that support conduction is independent of the presence of gas in the cell. Although this is an obvious oversimplification, it can be shown that the error involved should be less than 0.1%, because support conduction was a very minor contribution to the total heat transfer.[44]

Temperature difference was computed from the rate of change of thermal emf with temperature, dE/dT, and the difference in emf between the

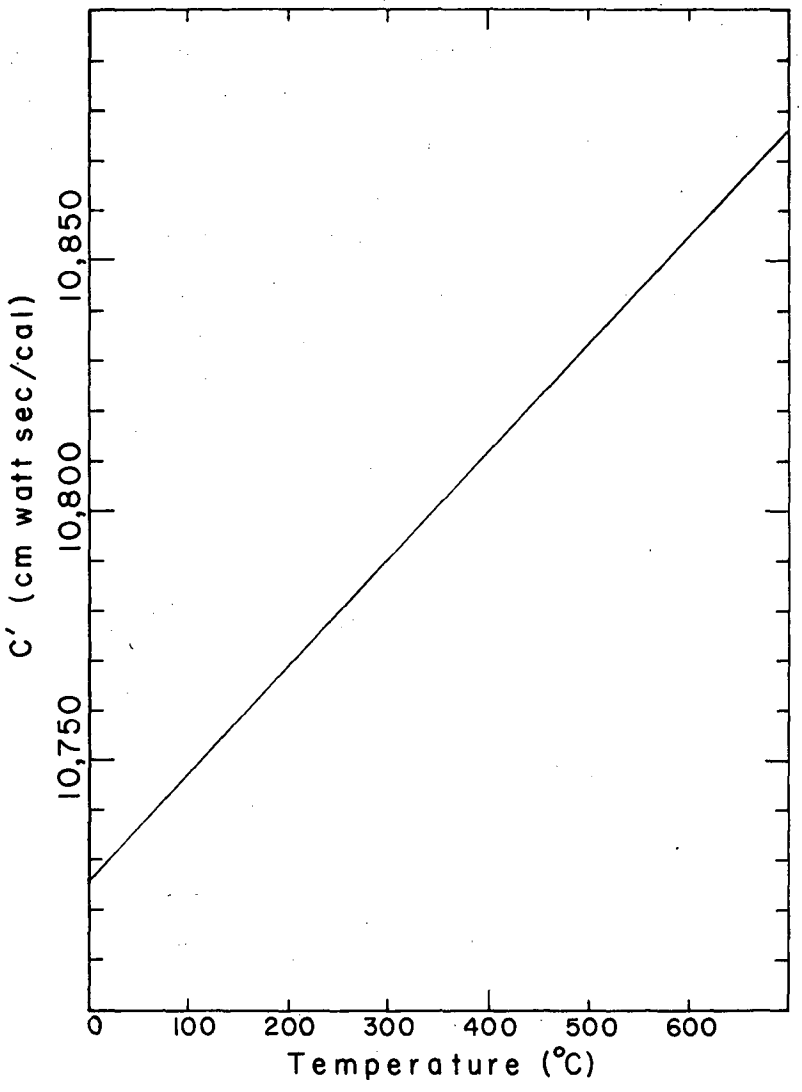

Fig. 11. Cell constant.

thermocouples in the emitter and receiver. Proper correction was applied for the difference in emf from the thermocouples themselves as described in a previous section. The temperature difference calculated this way, however, could not be used directly in Eq. 41 to compute conductivity because of temperature discontinuity at the walls of the cell. An approximate theoretical relation from the kinetic theory shows that the discontinuity at the walls as measured by the so-called temperature-jump distance, g', is related to the accomodation coefficient, a, the pressure, and the properties of the gas in the following manner,[35]

$$g' = \frac{2-a}{a} (2 \pi R T)^{1/2} \frac{\lambda_a}{(\gamma + 1) C_{vp}} . \qquad (43)$$

At infinite or large pressures the discontinuity disappears. The heat conducted per unit area per degree temperature difference between concentric cylinders may be expressed in terms of the conductivity of the medium in the annulus, the radii of the cylinders, and the temperature-jump distances at the two surfaces:[35]

$$\frac{q}{A \Delta T} = \frac{\lambda_a}{r \left(\ln \frac{r_2}{r_1} + \frac{g_1'}{r_1} + \frac{g_2'}{r_2} \right)} . \qquad (44)$$

Combining Eqs. 43 and 44 yields

$$\frac{\Delta T}{q} = \frac{\ln \frac{r_2}{r_1}}{2\pi \lambda_a L} + \frac{B}{p} \left(\frac{\sqrt{T_1}}{r_1} + \frac{\sqrt{T_2}}{r_2} \right) , \qquad (45)$$

where

$$B = \sqrt{\frac{2 \pi M}{R}} \cdot \frac{1}{2 \pi L} \cdot \frac{2 - a}{2 a (C_v/R + 1/2)} . \qquad (46)$$

Equation 45 shows that the plot of $\Delta T/q$ vs $1/p$ should be a straight line whose y intercept gives the value of λ_a and whose slope gives the accomodation coefficient. An expression of the same form as Eq. 45 may be derived for the bottom of the cell. However, this second expression need not be considered in this case because the ratio of the lateral area of the cell to the area of the end is about 20, and the effect of accomodation was at most 12% at 0.03 atmosphere. In a majority of the cases investigated, it was under 3%. Finally, linear relations between $\Delta T/q$ and $1/p$ were found in all cases. This showed that the effect of the end of the cell upon accomodation correction was indeed small.

The values of $q/\Delta T$ at infinite pressure and the slope of the $\Delta T/q$ vs $1/p$ curve were derived from the measurements by the method of least squares. In the case of pure gases, the value of $q/\Delta T$ so determined gives directly the conductivity through Eq. 41. For mixtures, however, Eq. 41 does not yield the true conductivity, since the thermal flux consisted of two terms, namely, that due to conduction and that caused by thermal diffision, as discussed in Section A, Chapter V. The value of λ calculated from Eq. 41 is, therefore, the difference of two terms

$$\lambda_m = \lambda_c - \lambda_{td} \quad , \tag{47}$$

where

$$\lambda_{td} = \alpha^2 DnRx_1x_2 \quad . \tag{48}$$

The thermal flux from diffusion accounts for, at most, 3% of the total flux even in mixtures with high thermal-diffusion factors. In all cases where thermal diffusion was appreciable, the conductivity was taken as the sum of the measured apparent conductivity and a value of λ_{td} estimated from the thermal-diffusion data.

CHAPTER IV. Experimental Results.

A. Data

The pressure-independent thermal conductivity of He, A, CO_2, N_2, O_2, CH_4, C_2H_4, C_3H_8, CH_3OCH_3, $CH_3CO_2CH_3$, forty-nine binary mixtures, and five ternary mixtures of these gases were measured at temperatures ranging from 94 to 538°C. The experimental results are tabulated in Tables II and III. The values of $q/\Delta T$ given therein have been corrected for heat transfer by radiation between the emitter and receiver as explained in Chapter III. The thermal conductivities given have been calculated from values of $\Delta T/q$ extrapolated to infinite pressure, i.e., to $1/p = 0$, by the method of least squares. Figures 12 a and 12 b show some of the typical plots of $\Delta T/q$ vs $1/p$. The slope of the line in such a plot is related to the accommodation coefficient as indicated in Eq. 45. Accommodation coefficients have been calculated from values of the slopes determined by the method of least squares in connection with the computation of conductivity and are tabulated in Table IV. Also given therein for comparison are values found in the literature for both silver and platinum.

Figure 13 shows the relation between conductivity and composition for several binary systems. Similar data are also presented in Figs. 14 and 15. The temperatures shown in these plots are those to which the experimental conductivities have been extrapolated to obtain an isothermal curve. In no case did this extrapolation exceed 4°C, and in most cases it was 1 or 2°C. For a mixture, the molal average value of $d\lambda/dT$ was used. Because the temperature extension was small, the error involved should be negligible in comparison to experimental errors.

The thermal conductivity of several of the pure gases used in this work have been investigated previously in the same temperature range by others. The values shown in Table II for these gases are retabulated in Table V together with the literature data for comparison. The latter values have been obtained in most instances from interpolation of the original data. The measurements of this work are quite consistent with those already reported, except the value for He at 315°C. The high conductivity in this case was probably caused by an error in the small ΔT measured as discussed in Section B.

Table II

Experimental data for pure gases

Date (day-mo.)	Gas	T_{av} (°C)	ΔT (°C)	$q/\Delta T$ (watt/°C)	p (mm Hg)	$\lambda \times 10^5$ cal / sec °C cm
17 V	N_2	104.5	7.826	0.78543	17.0	
			7.700	0.79860	102.0	7.459
			7.802	0.78790	24.5	
			7.678	0.80094	218	
			7.955	0.77239	10	
19 V	A	106.0	10.022	0.55100	154.5	5.125
			10.060	0.54884	38	
			10.111	0.54598	20.5	
20 V			9.951	0.54782	54.5	
21 V			9.940	0.54868	54.5	
22 V	He	100	1.258	4.5087	757.	41.94
			1.278	4.4330	144.5	
			1.338	4.2494	50.5	
			1.423	4.0003	25	
10 VI			1.256	4.4445	459.5	
			1.315	4.2443	61.5	
			1.397	3.9940	27.5	
20 VI	O_2	101	6.617	0.82564	94.5	7.732
			6.746	0.81216	23	
			6.668	0.82188	38	
22 VI	CO_2	103	9.107	0.57126	152	5.331
			9.176	0.56682	45.3	
			9.264	0.56126	23	
26 VI	CH_4	98	4.730	1.1355	153.5	10.60
			4.755	1.1294	51	
			4.798	1.1191	26	
27 VI	C_3H_8	100	7.540	0.69744	155.5	6.500
			7.571	0.69451	48.5	
			7.612	0.69067	24.5	
29 VI	$(CH_3)_2O$	101	8.060	0.64579	130	6.015
			8.087	0.64357	51.5	
			8.128	0.64023	20.5	
29 VII	Methyl formate	99	11.432	0.45250	102	4.217
			11.457	0.45147	50	
			11.477	0.45065	32	

Table II (cont'd.)

Experimental data for pure gases

Date (day-mo.)	Gas	T_{av} (°C)	ΔT (°C)	$q/\Delta T$ (watt/°C)	p (mm Hg)	$\lambda \times 10^5$ cal / sec °C cm
16 VIII	N_2	317	5.906	1.1430	112	10.67
			5.964	1.1316	50	
			6.083	1.1087	22	
17 VIII	He	315	1.180	5.8752	133	58.73
			1.333	5.1965	52.5	
			1.539	4.4957	27	
18 VIII	CO_2	320	6.498	1.0354	126	9.655
			6.559	1.0254	51	
			6.668	1.0080	24.5	
19 VIII	A	321	8.476	0.78479	120.5	7.299
			8.530	0.77958	52.5	
			8.591	0.77377	28	
20 VIII	C_2H_4	318	4.162	1.6381	131.5	15.30
			4.197	1.6242	52.5	
			4.285	1.5900	26.5	
21 VIII	CH_4	317	3.179	2.1566	111.5	20.34
			3.261	2.1014	46	
			3.359	2.0390	26.5	
22 VIII	O_2	319	5.470	1.2372	114.5	11.62
			5.645	1.1977	47.5	
			5.849	1.1546	22.5	
23 VIII	C_3H_8	318	4.335	1.5712	144	14.65
			4.393	1.5500	49.5	
			4.470	1.5226	25	
27 VIII	$(CH_3)_2O$	318	4.866	1.3956	132	12.96
			4.868	1.3950	53	
			4.890	1.3885	25	
			4.859	1.3976	127	
12 IX	C_3H_8	537	2.535	2.6653	118.5	25.08
			2.591	2.6059	55	
13 IX	CH_4	537	2.570	2.677	130	25.25

Table III

Experimental data of mixtures

A. Binary mixtures

Date (day-mo.)	System	x_1	T_{av} (°C)	ΔT (°C)	$q/\Delta T$ (watt/°C)	p (mm Hg)	$\lambda_m \times 10^5$ cal / sec °C cm
15 V	$He-N_2$	0.409	107.5	7.015	1.5588	208	14.59
				7.094	1.5423	27.5	
				7.085	1.5382	27.5	
				7.383	1.4663	9.5	
16 V				7.345	1.4856	16	
				7.383	1.4851	16	
22 V	$He-N_2$	0.837	100	1.782	3.1765	522.	30.33
				1.770	3.1995	119	
				1.797	3.1519	50.5	
				1.846	3.0698	25.5	
23 V				1.773	3.1928	497	
				1.858	3.0492	30.5	
30 V	$He-N_2$	0.219	104	4.848	1.1451	158	10.71
				4.899	1.1455	158	
				4.846	1.1452	158	
				4.895	1.1465	158	
				4.845	1.1455	158	
31V				4.906	1.1439	158	
				4.928	1.1387	158	
				4.929	1.1384	158	
				4.893	1.1398	158	
1 VI				4.902	1.1496	158	
				4.895	1.1512	158	
				4.951	1.1498	158	
2 VI				4.980	1.1528	158	
3 VI				4.928	1.1508	158	
				4.959	1.1516	158	
4 VI				4.927	1.1492	158	
				4.969	1.1492	158	
				4.959	1.1516	158	
				4.973	1.1523	158	
				4.985	1.1497	158	
				4.963	1.1488	158	
7 VI				4.910	1.1498	93	
				4.913	1.1491	93	
				4.916	1.1484	93	
				4.899	1.1480	93	
8 VI				4.857	1.1463	93	
				4.872	1.1427	93	
				4.891	1.1382	34	

Table III (cont'd.)

Date (day-mo.)	System	x_1	T_{av} (°C)	ΔT (°C)	$q/\Delta T$ (watt/°C)	p (mm Hg)	$\lambda_m \times 10^5$ $\frac{cal}{sec\ ^\circ C\ cm}$
				4.939	1.1270	21	
				4.956	1.1266	21	
				4.924	1.1232	21	
11 VI	He-A	0.525	100.5	3.269	1.6868	66.5	15.90
				3.269	1.6868	66.5	
				3.257	1.6931	66.5	
				3.232	1.6926	66.5	
				3.231	1.6931	66.5	
				3.274	1.6815	40.5	
				3.317	1.6594	24.5	
14 VI	He-A	0.780	99	2.141	2.5612	27.5	25.18
				2.075	2.6433	53.5	
				2.040	2.6890	151	
15 VI				2.034	2.7182	151	
				2.049	2.6981	55	
				2.137	2.5862	22	
16 VI				2.112	2.5918	22	
				2.011	2.7229	142	
				2.063	2.6606	50.5	
12 VI	He-A	0.276	102.5	5.390	1.0139	80	9.509
				5.395	1.0130	80	
				5.383	1.0152	171.5	
				5.369	1.0180	38	
				5.312	1.0146	38	
				5.302	1.0159	38	
				5.304	1.0156	38	
				5.370	1.0097	22.5	
				5.474	0.9902	14.5	
2 VII	CH_4-C_3H_8	0.4855	95	6.354	0.81957	147	7.636
				6.376	0.82173	50.5	
				6.398	0.81848	26	
				6.545	0.81808	94	
				6.506	0.81761	94	
				6.559	0.81085	14	
				6.527	0.81492	25	
2 VII	CH_4-C_3H_8	0.3130	94	7.007	0.75526	50.9	7.050
				6.990	0.75715	163.8	
				7.021	0.75372	29.5	

Table III (cont'd.)

Date (day-mo.)	System	x_1	T_{av} (°C)	ΔT (°C)	$q/\Delta T$ (watt/°C)	p (mm Hg)	$\lambda_m \times 10^5$ $\frac{cal}{sec\ °C\ cm}$
2 VII	CH_4-C_3H_8	0.7792	93	5.646	0.95346	54.3	8.841
				5.600	0.95134	174	
				5.625	0.94706	30.7	
5 VII	$(CH_3)_2O$-C_3H_8	0.4983	95	7.981	0.65638	56.5	6.180
				8.066	0.46926	26.5	
				7.920	0.66158	133.2	
6 VII	$(CH_3)_2O$-C_3H_8	0.3149	95	7.944	0.65528	23.9	6.125
				7.959	0.65824	187.2	
				7.982	0.65629	51.9	
8 VII	A-$(CH_3)_2O$	0.4877	96	9.047	0.57680	188	5.372
				9.083	0.57444	37.8	
				9.050	0.57660	118	
8 VII	A-$(CH_3)_2O$	0.6705	96	9.370	0.55626	73	5.183
				9.377	0.55583	30	
				9.359	0.55694	74.5	
8 VII	A-$(CH_3)_2O$	0.3166	95	8.911	0.58589	192.3	5.455
				8.934	0.58434	52.5	
				8.956	0.58285	27.3	
9 VII	CO_2-C_3H_8	0.4490	95	8.277	0.63223	173.5	5.884
				8.290	0.63120	72.7	
				8.299	0.63050	49.9	
				8.304	0.63011	30.7	
11 VII	CO_2-C_3H_8	0.6354	96	8.503	0.61492	107.2	5.738
				8.536	0.61247	51.8	
				8.566	0.61026	31.8	
11 VII	CO_2-C_3H_8	0.2912	95	8.094	0.64695	133.7	6.083
				8.104	0.64613	108.5	
				8.104	0.64613	113.5	
13 VII	O_2-CO_2	0.5356	96	7.685	0.68239	108.8	6.365
				7.767	0.67499	23.5	
				7.702	0.68084	85.1	
				7.704	0.68066	51.5	
				7.698	0.68121	63.3	
15 VII	O_2-CO_2	0.3153	96	8.269	0.63286	186	5.865
				8.304	0.63011	72.5	
				8.329	0.62816	46	
				8.412	0.62178	17.8	
				8.443	0.61942	27	
				8.363	0.62553	115.3	
				8.385	0.62384	53.5	

Table III (cont'd.)

Date (day-mo.)	System	x_1	T_{av} (°C)	ΔT (°C)	$q/\Delta T$ (watt/°C)	p (mm Hg)	$\lambda_m \times 10^5$ cal / sec °C cm
16 VII	O_2-CO_2	0.2699	97	8.511	0.61432	38.5	5.777
				8.452	0.61874	113	
				8.530	0.61291	35.4	
				8.523	0.61343	35.4	
				8.507	0.61462	54.2	
23 VII	O_2-CO_2	0.7776	97	7.106	0.73954	33	7.027
				7.054	0.74513	52.5	
				7.053	0.74742	52.5	
				6.999	0.75114	90.2	
				7.063	0.74416	32.7	
30 VII	C_3H_8-methyl formate	0.530	96	8.948	0.58339	79	5.435
				8.934	0.58434	52	
				8.954	0.58299	27	
				8.941	0.58386	100	
31 VII	$(CH_3)_2O$-methyl formate	0.4841	97	9.843	0.52862	96.5	4.928
				9.877	0.52673	51	
				9.920	0.52437	24.5	
				9.894	0.52579	37	
4 VIII	$(CH_3)_2O$-methyl formate	0.7248	100	9.089	0.57405	99.5	5.361
5 VIII				9.118	0.57216	42	
				9.137	0.57093	24.5	
				9.160	0.56945	24.5	
				9.056	0.57621	158	
7 VIII	$(CH_3)_2O$-methyl formate	0.3059	101	10.288	0.50493	151	4.707
				10.388	0.49987	28	
				10.342	0.50220	52	
13 VIII	He-A	0.573	316	2.819	2.4369	149	23.00
				2.878	2.3862	52	
				3.025	2.2683	25.5	
18 VIII	$(CH_3)_2O$-methyl formate	0.4841	318	4.445	1.5314	98	14.25
				4.465	1.5244	51	
				4.499	15.126	25.5	
19 VIII	A-CO_2	0.4935	320	7.192	0.93177	130.5	8.670
				7.265	0.92202	50	
				7.390	0.90578	20.5	

Table III (cont'd.)

Date (day-mo.)	System	x_1	T_{av} (°C)	ΔT (°C)	$q/\Delta T$ (watt/°C)	p (mm Hg)	$\lambda_m \times 10^5$ cal/sec °C cm
19 VIII	N_2-A	0.4966	320	7.107	0.94338	102	8.788
				7.170	0.93475	49.5	
				7.229	0.92681	27.5	
20 VIII	He-CO_2	0.610	317	2.710	2.5365	50	23.65
				2.685	2.5605	130.5	
				2.717	2.5298	26	
20 VIII	He-N_2	0.637	317	2.306	2.9876	124.5	28.28
				2.334	2.9513	48.5	
				2.454	2.8051	24	
21 VIII	N_2-C_2H_4	0.4980	318	4.799	1.4156	117	13.22
				4.879	1.3918	41	
				4.953	1.3704	23.5	
21 VIII	C_2H_4-CO_2	0.5118	318	4.996	1.3583	104	12.69
				5.029	1.3491	52	
				5.129	1.3220	23.5	
22 VIII	N_2-C_2H_4	0.7558	319	5.261	1.2879	142	12.05
				5.373	1.2603	48.5	
				5.492	1.2321	27	
23 VIII	N_2-O_2	0.3902	319	5.651	1.1964	138	11.19
				5.811	1.1624	48.5	
				5.913	1.1416	28	
23 VIII	CH_4-C_2H_4	0.4894	317	3.799	1.7983	125.5	16.73
				3.824	1.7863	55.5	
				3.863	1.7679	27	
24 VIII	He-CH_4	0.746	316	1.686	4.1004	117	40.63
				1.794	3.8512	53.3	
				2.017	3.4212	27.5	
24 VIII	He-CH_4	0.550	316	2.251	3.0615	54	30.54
				2.149	3.2087	134	
				2.393	2.8776	27	
27 VIII	He-CH_4	0.299	317	2.664	2.5809	131	24.58
				2.770	2.4807	55	
				2.975	2.3071	25	
28 VIII	He-N_2	0.305	318	3.928	1.7380	136.5	16.27
				3.948	1.7290	53	
				4.067	1.6773	27	
				4.090	1.6677	40	

Table III (cont'd.)

Date (day-mo.)	System	x_1	T_{av} (°C)	ΔT (°C)	$q/\Delta T$ (watt/°C)	p (mm Hg)	$\lambda_m \times 10^5$ cal / sec °C cm
30 VIII	$He-N_2$	0.739	316	2.017	3.4212	126	33.47
				2.157	3.1960	48	
				2.412	2.8546	25	
				2.365	2.9121	33	
31 VIII	He-A	0.306	318	4.720	1.4399	130	13.36
				4.885	1.3900	53	
				5.023	1.3507	25.5	
				4.727	1.4377	127	
				4.829	1.4066	24.5	
				4.926	1.3781	40	
31 VIII	He-A	0.774	316	2.041	3.3805	118	33.23
				2.176	3.1684	55	
				2.417	2.8486	28.	
2 IX	C_3H_8-$(CH_3)_2O$	0.4966	317	4.590	1.4818	98	13.78
				4.617	1.4729	53	
				4.646	1.4635	28.5	
1 IX	$N_2-C_3H_8$	0.5253	318	4.866	1.3956	133.5	13.06
				4.896	1.3868	53	
				5.012	1.3538	26	
2 IX	$A-C_3H_8$	0.4712	318	5.317	1.2739	132	11.86
				5.350	1.2658	54.5	
				5.413	1.2507	28	
11 IX	$N_2-C_3H_8$	0.4761	538	3.061	2.1928	53.5	20.99
				3.149	2.1291	30	
				2.996	2.2422	138.5	
10 IX	$A-C_3H_8$	0.4712	538	3.181	2.1069	136.5	19.80
				3.274	2.0446	55	
				3.403	1.9639	28.5	
13 IX	CH_4-A	0.4767	538	3.682	1.8087	137.5	17.03
				3.774	1.7625	58.5	
				3.803	1.7485	52.5	

Table III (cont'd.)

B. Ternary mixtures

Date (day-mo.)	System	x_1	x_2	T_{av} (°C)	ΔT (°C)	$q/\Delta T$ (watt/°C)	p (mm Hg)	$\lambda_m \times 10^5$ cal / sec °C cm
18 VI	$He-N_2-A$	0.415	0.468	99.5	3.590	1.4860	128.5	13.95
					3.634	1.4800	48.5	
					3.708	1.4401	23	
					3.710	1.4479	26	
					3.585	1.4807	67.5	
24 VII	$N_2-O_2-CO_2$	0.3231	0.3729	97	7.291	0.72030	110.8	6.729
					7.379	0.72148	30.6	
					7.337	0.72556	53.5	
					7.346	0.71476	38.8	
26 VII	$A-(CH_3)_2O-C_3H_8$	0.3660	0.3260	98	8.428	0.62056	111.8	5.767
					8.495	0.61551	51	
					8.509	0.61447	30	
					8.483	0.61641	103.5	
29 VIII	$He-CH_4-N_2$	0.159	0.365	317	3.992	1.7095	45	16.74
					4.066	1.6777	33	
					3.871	1.7642	105.5	
					4.183	1.6297	23.5	
3 IX	$A-C_3H_8-(CH_3)_2O$	0.5348	0.2310	318	5.707	1.1842	136	11.01
					5.778	1.1692	53.5	
					5.841	1.1562	26	
					5.824	1.1597	36	

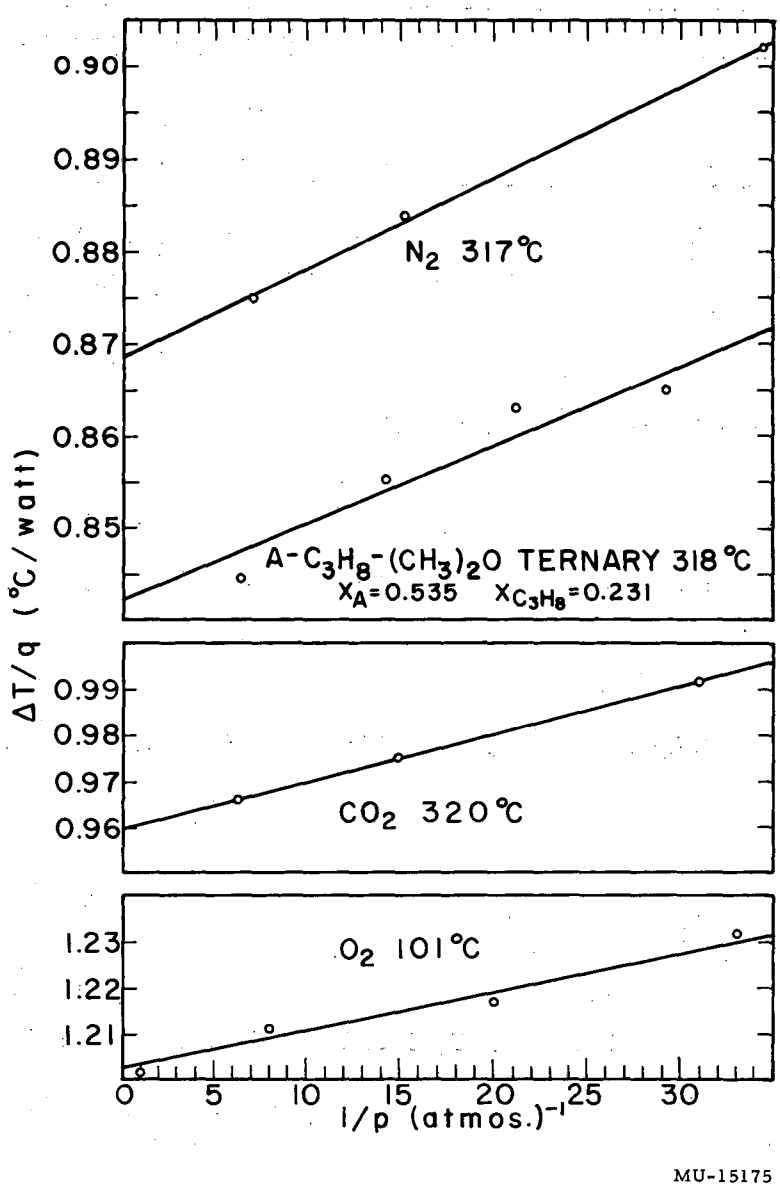

Fig. 12a. Accommodation effect.

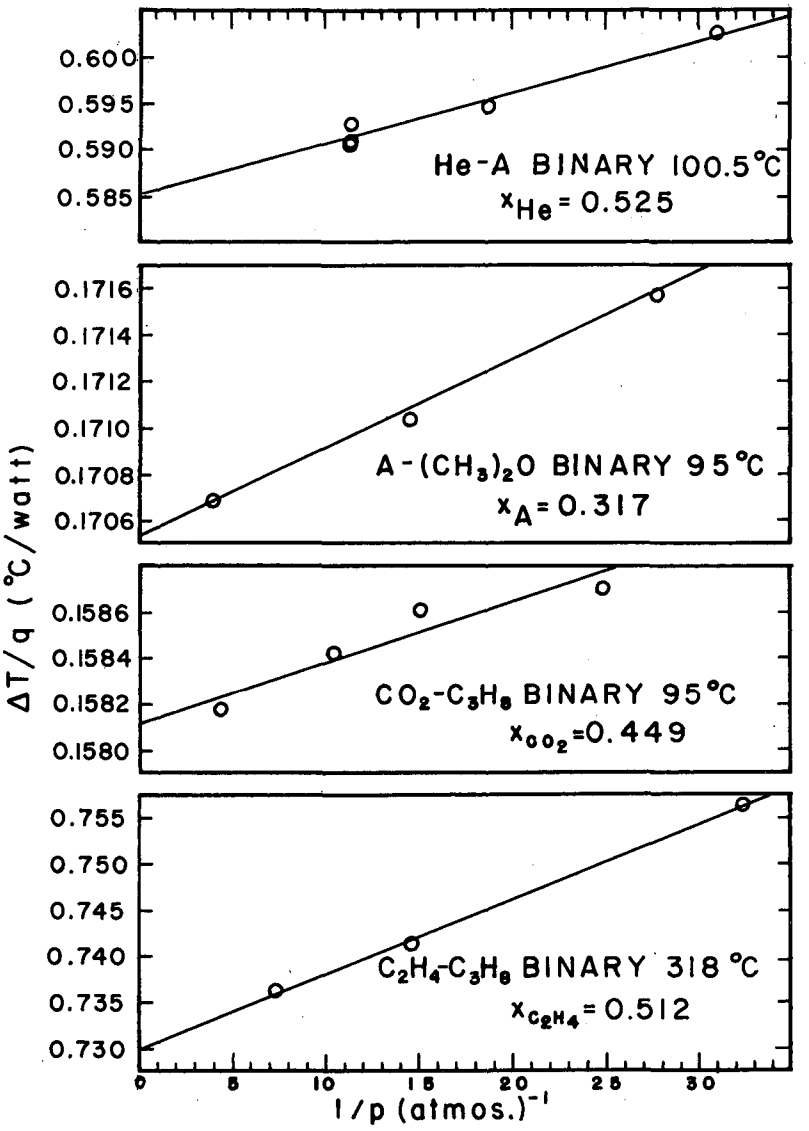

Fig. 12b. Accommodation effect.

Table IV

Accomodation coefficients

Gas	Temp. (°C)	a	Literature value and source for Ag and Pt
N_2	104.5	0.364	
	317	0.343	0.4(Ag^{44})
A	106	0.702	
	321	0.528	0.65(Ag^{44}, 680°C); 0.57(Pt^{53}, 350°C)
He	100	0.148	
	315	0.081	0.13(Ag^{44}, 680°C); 0.17(Pt^{53}, 400°C)
O_2	101	0.299	
	319	0.148	
CO_2	103	0.193	
	320	0.212	0.3(Ag^{44}); 0.3(Pt^{2}); 0.6(Pt^{53})
CH_4	98	0.242	
	317	0.106	
C_3H_8	100	0.175	
	318	0.103	
	537	0.070	
C_2H_4	318	0.153	

Binary mixtures

System	Temp. (°C)	x_1	a	System	Temp. (°C)	x_1	a
He-N_2	104	0.219	0.407	He-CH_4	317	0.299	0.076
	107.5	0.409	0.352		316	0.550	0.097
	100	0.837	0.335		316	0.746	0.072
He-A	102.5	0.276	0.622	He-CO_2	317	0.610	0.226
	100.5	0.525	0.496				
	99	0.780	0.424	A-C_3H_8	318	0.471	0.192
CH_4-C_3H_8	94	0.313	0.537	N_2-C_3H_8	318	0.525	0.131
	95	0.486	0.625				
	93	0.779	0.691	N_2-A	320	0.497	0.394
CO_2-C_3H_8	95	0.291	0.073	A-CO_2	320	0.494	0.309
	95	0.449	0.255				
	96	0.635	0.568	C_2H_4-CO_2	318	0.512	0.195

Table IV (cont'd.)

System	Temp. (°C)	x_1	a	System	Temp. (°C)	x_1	a
O_2-CO_2	97	0.270	0.227	N_2-C_2H_4	318	0.498	0.187
	96	0.315	0.321		319	0.756	0.145
	96	0.536	0.355				
	97	0.778	0.230	N_2-O_2	319	0.390	0.166
He-A	318	0.306	0.377	CH_4-C_2H_4	317	0.489	0.267
	316	0.573	0.307				
	316	0.774	0.129	N_2-C_3H_8	538	0.476	0.099
He-N_2	318	0.305	0.263	A-C_3H_8	538	0.471	0.083
	317	0.637	0.337				
	316	0.739	0.105	CH_4-A	538	0.477	0.149

Ternary mixtures

System	Temp. (°C)	x_1	x_2	a
He-N_2-A	99.5	0.396	0.482	0.366
N_2-O_2-CO_2	97	0.323	0.373	0.254
He-CH_4-N_2	317	0.135	0.374	0.113

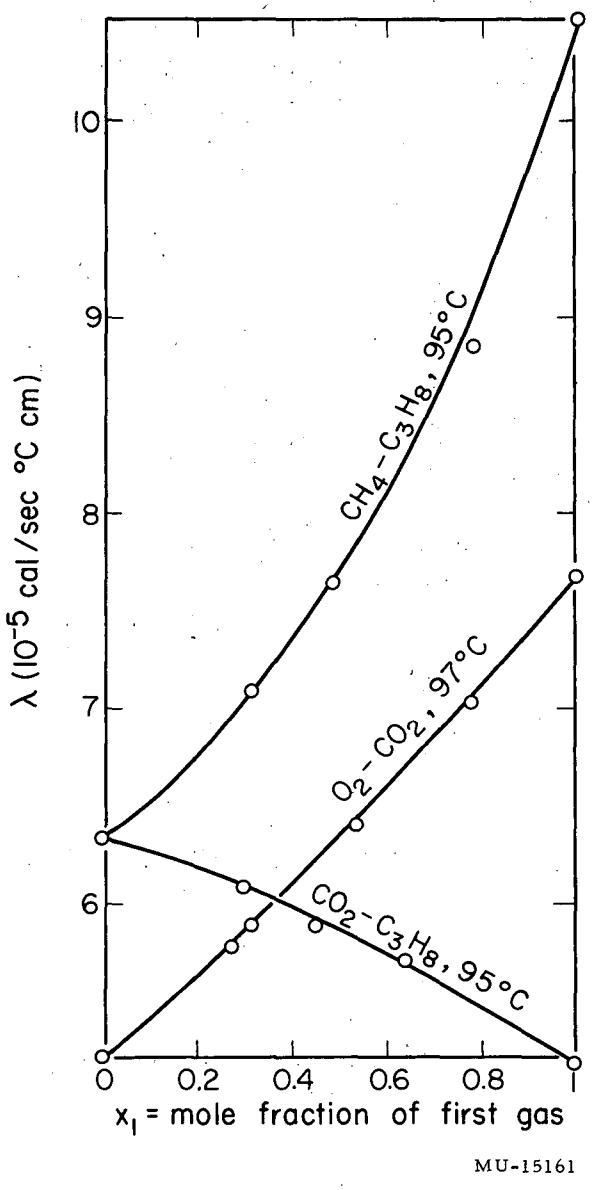

Fig. 13. Conductivity of some binary mixtures.

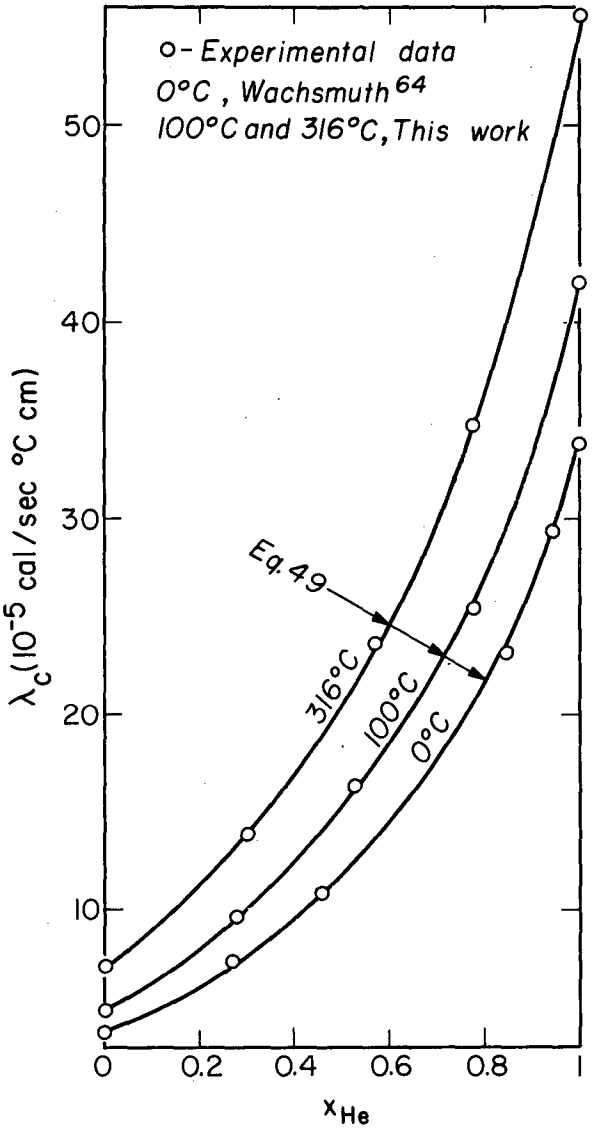

Fig. 14. Comparison of experimental and calculated conductivity of He–A mixtures at various temperatures.

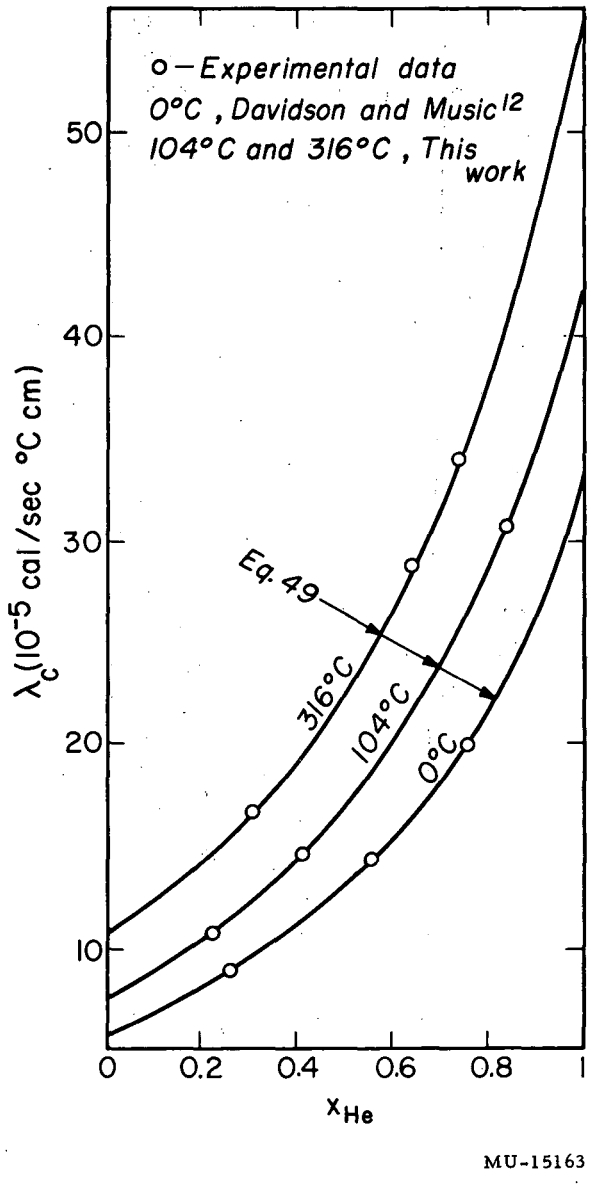

Fig. 15. Comparison of experimental and calculated conductivity of He–N_2 mixtures at various temperatures.

Table V

Gas	Temp. (°C)	$\lambda \times 10^5$ $\frac{cal}{sec\ ^oC\ cm}$	Literature value and source $\lambda \times 10^5$ $\left(\frac{cal}{sec\ ^oC\ cm}\right)$
N_2	104.5	7.459	7.58(Keyes,1952)[37] 7.33(Schottky,1952)[46] 7.25(Rothman,1954)[44] 7.56(Nuttall and Ginnings,1957)[43]
N_2	317	10.77	10.62(Stops,1949)[49] 10.77(Keyes,1952)[37] 10.85(Schottky,1952)[46]
O_2	101	7.732	7.90(Johnston and Grilly,1946)[32] 7.80(Keyes,1952)[37]
O_2	319	11.62	11.73(Franck,1951)[16]
CH_4	98	10.60	10.86(Johnston and Grilly,1946)[32] 10.30(Schottky,1952)[46]
CH_4	317	20.34	21.00(Keyes,1952)[37] 18.87(Schottky,1952)[46]
C_3H_8	100	6.500	6.24(Mann and Dickens,1931)[41]
He	100	41.94	40.75(Johnston and Grilly,1946)[32] 41.65(Kannuluik and Carman,1952)[33] 40.86(Keyes,1952)[37]
He	315	58.73	55.58(Kannuluik and Carman,1952)[33]
A	106	5.125	5.113(Kannuluik and Carman,1952)[33] 5.16(Keyes,1952)[37] 5.155(Schottky,1952)[46]
A	321	7.299	6.962(Kannuluik and Carman,1952)[33] 7.26(Keyes,1952)[37] 7.165(Schottky,1952)[46]
CO_2	103	5.331	5.20(Eucken,1940)[15] 5.56(Johnston and Grilly,1946)[32] 5.35(Keyes,1952)[37]
CO_2	320	9.655	8.89(Eucken,1940)[15] 9.89(Keyes,1952)[37]

B. Error Analysis

In this section, the sources of errors are evaluated and an estimate of the maximum error is made. There are two distinct types of errors, namely that involved in the experimental measurements and that in the assumptions made in deriving from the measurements the results presented in the preceding section. The principal experimental quantities required for the determination of thermal conductivity and accommodation coefficient are (1) temperature difference between the emitter and the receiver, (2) rate of energy input to the emitter, (3) the dimensions of the cell, (4) pressure, and (5) the rate of heat transfer by radiation and conduction in the cell under vacuum. In the case of mixtures, the composition is also required for calculation of accommodation coefficient. The total error is the sum of these errors in measurements and those involved in the assumptions discussed in Paragraph 2 below.

1. Errors in Measurement

a. Δ T measurements. Temperature difference is calculated from the measured difference of the thermal emf of two thermocouples that have been calibrated against a standard couple. The major error in this quantity appears in the stray emf's arrising from various lead connections. It was found that these emf's fluctuated from 0 to 0.6 mv. For a temperature difference of $6^{\circ}C$, this amounts to a maximum error of 1.1%. The average error from this source is estimated to be 0.5%. Intercalibrations of thermocouples were reproducible to within 0.2 mv. A part of this difference was probably caused by fluctuation in stray emf's; hence, it is estimated that error from intercalibration is at most 0.2% at a Δ T value of $6^{\circ}C$. The dE/dT calibration of the standard couple is known to $\pm$ 0.3 to $\pm$ 0.5%. An error in calibration of this magnitude would cause the same degree of error in the final result.

b. Heat input. Negligible errors are involved in current and voltage measurements. Heater-lead corrections amounted to 1% of the total voltage drop, and these are known to within 5%.

c. Cell dimensions. Errors in the measurements of the cell dimensions are negligible. Annulus measurements are reproducible to within 0.1%. This may introduce an error of the same order in the calculated conductivity.

d. Pressure. The maximum error in pressure readings is 3%. These measurements were made in order to correct for the accomodation effect by extrapolating the $\Delta T/q$ vs $1/p$ line to infinite pressure. In the pressure range chosen, the difference between the apparent conductivity at the lowest pressure and that at infinite pressure is less than 3%, except in the case of He and mixtures containing He, for which this difference may be as high as 12%. Because the pressure dependence of the apparent conductivity is small and measurements were made at three different pressures in most instances, the error in the final result caused by errors in pressure measurements should be negligible.

e. Vacuum correction. The maximum vacuum correction occurred in runs made at 540°C. The radiation and support conduction at this temperature amounted to 4% of the gas conduction in the case of gases having low conductivities. Because vacuum correction is known to within 5%, the corresponding error in the conductivity is 0.2%.

f. Composition. The number of moles of each component in a mixture was determined from pressure and temperature measurements of the gases in storage tanks of known volume. Temperature measurements involved errors of 0.05%. Pressure values might be in error by 0.2%. The volume of the tanks were known with an accuracy of 1 part in 20,000. Thus the number of moles of a gas introduced into a previously evacuated tank for mixing should not be in error by more than 0.25%. In the initial runs, the pure gases were let into the mixing tank alternately in small portions. Although the mixtures were usually allowed to stand for 48 to 72 hrs before use, some difficulty of poor mixing was experienced, as indicated by the scattering of data points in the $\Delta T/q$ vs $1/p$ plots. In one case, the scattering was 2.5%, but in most others it was under 1%. In later runs, this difficulty was eliminated by allowing the gases to impinge upon each other before flowing into the mixing tank.

2. Other Possible Errors

a. Axial uniformity of temperature. In order to ascertain that the temperature difference between the emitter and receiver was the same over the entire length of the cell, measurements were made with the thermocouples at different levels from the bottom of the wells. This temperature exploration revealed that the indicated ΔT decreased as the thermocouples were moved toward the top of the cell. By varying the guard temperature, it was found that at least a part of the cause of the change of ΔT with depth of immersion of the thermocouples was heat conduction between the cell and guard by way of the thermocouple assembly. When the guard was maintained at the temperature of the emitter, the indicated temperature of the receiver increased as the thermocouple was raised toward the top of the cell. Similarly, when the guard was kept at the temperature of the receiver, the indicated temperature of the emitter dropped as the thermocouple was raised. The small amount of heat conducted by the thermocouple wells and the high thermal conductivity of silver led one to suspect that the actual temperature gradient was in the well rather than in the silver. If the gradient had been in the wells, then altering the conditions within the cell to improve cooling of the wells should simultaneously extend the constant ΔT zone and increase the ΔT near the top of the cell. This point was proved experimentally. At 100°C and under vacuum, ΔT did not become constant until the thermocouples were placed at a depth of 4 in. from the top of the cell, and the ratio of the ΔT at the top of the cell to that in the constant ΔT region was 0.3. When the cell was filled with air, the corresponding quantities were 2 in. and 0.5. Further experiments showed that the constant-ΔT zone lengthened, and the ratio of the ΔT's increased with the conductivity of the gas in the cell.

Conduction along the parts of the thermocouple assembly within the well was also studied. The dimensions and conductivities of these parts are such that the amount of heat conducted by them is small in comparison to that conducted along the well. The important question here is the effect of conduction upon junction temperature rather than upon the temperature of the silver. The parts within the well are the thermocouple wires,

a two-hole ceramic insulating tube through which the wires were threaded, a ceramic protecting tube surrounding the two-hole tube, and concentric air spaces. Just as in the case of the well above, the persistence of temperature in these parts depends upon their rate of lateral heat transfer. Because the conductivities of the ceramic tubes and air spaces are negligible in comparison to that of the wires, the problem reduced to one of cooling the wires. In order to determine whether the change in the observed ΔT with distance was partly caused by the resistance to lateral heat transfer from the wires, the protection tube was removed and the well filled with dimethylformamide. It was found that both the zone of constant ΔT and the ΔT at the top of the cell again increased. This result shows that the junction does not indicate the exact temperature of the well until a certain depth of immersion is reached.

The experiments described above indicated that persistence of temperature in the thermocouple assembly from axial conduction along the well and along the wires was in part responsible for the apparent change in ΔT with distance. There remains to be shown whether or not this cause alone was sufficient to account entirely for the experimental observations.

From the dimensions and thermal properties of the parts of the thermocouple assembly and certain reasonable assumptions, it is possible to estimate with fair accuracy the temperature at the junction at various axial positions under the condition of constant axial temperature in the silver. A comparison of the temperature distribution so calculated with the experimental data should indicate whether or not a temperature gradient existed in the silver.

Computation of the junction temperature had to be carried out in two steps. First, the temperature distribution of the well was calculated by assuming it to be a semi-infinite hollow cylinder extending from a region of constant temperature in the guard into another region of constant temperature in the receiver or in the emitter. The inside of the well was assumed to be insulated, since the conductivity of the parts within the well is small in comparison to that of the well. The junction temperature was then calculated by treating the thermocouple wires as a finite cylinder extending from the region of constant temperature in the guard into

the well, a region whose temperature depended upon the distance from the guard. Details of the calculations and discussion of the assumptions made are given in Appendix III. Computations were carried out for four distinct cases with two different thermocouple assemblies and three different conditions in the cell. Each case corresponded to an experiment described above. Excellent agreement between calculated and experimental values is found in all cases in which the cell was filled with gas. In the case for the cell under vacuum, the calculated values are lower than the experimental data. The discrepancy was probably due to error in estimating the radiant-heat-transfer coefficient between the well and the silver. Even if the coefficient had been estimated correctly, contact between the well and silver would have caused the higher rate of heat transfer indicated by the data. However, even in this extreme case, the theoretical curve predicts that at the bottom of the well the indicated ΔT should be nearly 95% of the actual ΔT. A comparison of the calculated and measured ΔT values as a function the axial position of the thermocouple junction is shown in Appendix III, (Fig. 5-III). The agreement shown thereon between data and calculation based on the assumption of constant temperature in the cell indicates that the observed nonuniformity of axial temperature should cause practically no error in the conductivity values.

b. Thermal diffusion. In the cases of mixtures, the effects of unmixing because of temperature gradients in the experimental equipment must be considered. The temperature difference between the heated cell and the connecting pipes at room temperature provides a driving force that may be as high as several hundred degrees for thermal diffusion to take place. Within the annular space between the receiver and emitter unmixing of the gas because of the temperature gradient also occurs.

That part of the experimental system consisting of the stainless steel cell casing and the pumping line up to the valve at the end of the flexible tubing may be visualized as an ordinary two-bulb-type apparatus for the determination of thermal-diffusion coefficients. The amount of separation for a given temperature gradient can be readily determined

from data on thermal diffusion. The time required to attain steady-state concentrations in the hot and cold parts of the system may also be estimated. Details of these calculations and a discussion of the necessary approximations are given in Appendix IV.

Of the mixtures investigated in this work, those for which the effect of thermal diffusion is most pronounced are He–A, He–N_2, and He–CH_4. The results in Appendix IV show that, for these cases, the difference in steady state concentration between the cell at 320°C and that part of the connecting pipes at room temperature is of the order of 6% for an initial mixture of 1 : 1. The estimated relaxation time, i.e., time required for the difference in concentration to attain (e - 1)/e of the steady-state value, for these mixtures is about 0.5 min at 20 mm pressure to 20 min at one atmos. Because most of the data were taken at 0.25 atmos or less, and the time between filling the cell and taking the first readings of ΔT and q was half an hour or longer, the measured conductivity of these cases was that for a mixture at the steady-state concentration in the cell, i.e., a mixture that may be as much as 6% richer in the lighter component than was the original composition. For these mixtures, a correction must be applied to the composition as determined in Paragraph 1f above. It is estimated that the calculated separation based on thermal-diffusion data may be in error by as much as 30%. This error would give rise to an uncertainty in the composition correction of 1.8% or an error in the composition of the same magnitude. For the other mixtures investigated, the separation is of the order of 1% or less, and the relaxation time is from 2 to 10 min in the experimental pressure range. The error in composition from correction for thermal diffusion in these cases would be 0.2% or less.

In computing the conductivity for mixtures, it was necessary to make estimates of the contribution to thermal flux across the cap space by thermal diffusion. The error involved in these estimates based upon thermal-diffusion data is considered to be not greater than 30%. As thermal diffusion amounted to less than 3% of the total thermal flux, a 30% error in these estimates corresponds to 0.9% error in thermal conductivity. Because thermal diffusion is important only in the region of composition

near the 1 : 1 ratio, this error becomes smaller for mixtures rich in either component, even for cases of high thermal-diffusion factors. For most of the mixtures investigated in this work, the error involved in ignoring thermal diffusion entirely is negligible.

c. Convection. The plots of $\Delta T/q$ vs $1/p$ indicate that convection is practically negligible at a pressure as high as one atmosphere. The insertion of a tube bundle in the verticle pipe leading from the cell was apparently sufficient to keep the convective currents originating in the cooler section of this pipe from reaching the cell, as observed by Rothman.[44] As a further precaution, all data were taken at 0.25-atmosphere pressure or less; hence, it may be safely assumed that error from convection was completely eliminated.

d. Effect of ΔT. Rothman[44] studied the effect of ΔT on apparent conductivity in the range of ΔT from 2 to 25°C and estimated the error from variation of conductivity with ΔT to be less than 0.2%.[44] In the present work, the data were taken at a ΔT value of 2 to 10°C; therefore no more than 0.2% error would be involved here also.

e. Eccentricity of the cell. When the emitter is not concentric with the receiver, higher values of apparent conductivity are observed. Calculation based on the maximum possible displacement from concentricity indicates an error of less than 0.3% in the temperature range of the data of this work.[44]

3. Summary of Errors

The largest error in measurement appears in ΔT, and the largest error in computation occurs in the estimated correction for thermal diffusion in certain mixtures. The former may cause a maximum error of 4% in the few measurements taken at ΔT of 2°C or less, and the latter, 0.9% in some of the mixtures containing helium. With the addition of errors from other sources, the total maximum error may reach 5.7%. This is the

worst possible case for a mixture. For measurements at higher values of ΔT and most of the mixtures studied, for which thermal diffusion is unimportant, the maximum error is of the order of 2%, and the average error is in the neighborhood of 1.2%.

CHAPTER V. Evaluation of Empirical Constants and Comparison with Experimental Data.

A. Evaluation of Empirical Constants for Proposed Correlations

Empirical relations for the thermal conductivity and viscosity of gas mixtures were proposed in Chapter II. Because these equations are presumably approximately applicable in general, the constants in them may be evaluated from the data on any arbitrarily chosen set of binary mixtures. However, because of the variables appearing in these equations, the data from certain systems are more desirable than others. For the determination of m and n in the thermal conductivity correlation, the most logical data to be used are those of monatomic gas mixtures. Because these gases do not possess any internal degrees of freedom, the second term in Eq. 34 does not exist. Furthermore, the factors D_{ii}/D_{ij} and M_{ij}/M_i indicate that it would be advantageous to choose mixtures whose components have widely different molecular weights.

In order to develop a correlation that will apply to all mixtures on an equal basis, the effect of thermal diffusion must be considered. According to the rigorous kinetic theory, the heat flux in a gas mixture consists of two terms, one from conduction and the other from thermal diffusion.[10] Franck[17] pointed out that the existing correlations of conductivity of mixtures do not take the effect of thermal diffusion into account. To calculate the contribution of thermal diffusion to conductivity, he wrote

$$\lambda_m = \lambda_c - \lambda_{td} \tag{47}$$

where

$$\lambda_{td} = \alpha^2 D n R x_1 x_2 \ . \tag{48}$$

The conductivity because of thermal diffusion, λ_{td}, depends principally upon molecular-weight differences of the constituents. In all cases, λ_{td}, is small compared to λ_m. For example, the maximum value of λ_{td} for He—A mixtures at $0^{\circ}C$ is about 2.5% of λ_m. When the molecular-weight difference.

is small, the effect of thermal diffusion is negligible. A correlation that applies equally to all mixtures should, therefore, be based on λ_c rather than λ_m.

For the empirical determination of m and n in Eq. 34, the data for He–A mixtures were chosen. Proper corrections for the effect of thermal diffusion were made according to Eqs. 47 and 48. Calculations showed that the best values of m and n for this system are approximately 1 and 1/8 respectively. With the introduction of these constants, Eq. 34 becomes

$$\lambda_c = \sum_{i=1}^{n} \frac{\lambda_{ci}}{1 + \sum_{\substack{i=1 \\ i\neq j}}^{n} \frac{D_{ii}}{D_{ij}} \left(\frac{M_{ij}}{M_i} \right)^{1/8} \frac{x_j}{x_i}} + \sum_{i=1}^{n} \frac{\lambda_{di}}{1 + \sum_{\substack{i=1 \\ i\neq j}}^{n} \frac{D_{ii}}{D_{ij}} \frac{x_j}{x_i}} \quad . \tag{49}$$

A comparison of this expression with the existing data of He–A at 0°C is shown in Fig. 1.

Out of considerations similar to that in the case of the conductivity correlation, the viscosity data for binary mixtures of Ne and H_2 was chosen for the determination of p and q in Eq. 38. It was found that Eq. 38 conforms most closely to the data of this system when p and q have the values of 2/3 and zero respectively; thus, the empirically modified expression for viscosity becomes

$$\eta_m = \sum_{i=1}^{n} \frac{\eta_i}{1 + \sum_{\substack{i=1 \\ i\neq j}}^{n} \left(\frac{D_{ii}}{D_{ij}} \right)^{2/3} \frac{x_j}{x_i}} \quad . \tag{50}$$

A comparison of this relation with experimental data of H_2—Ne mixtures at 20°C is shown in Fig. 2.

B. Comparison of Data and Correlations

1. Introduction

The relation between the thermal conductivity or the viscosity and the composition of a mixture depends mainly upon the following factors: (1) temperature, (2) relative mass and size of the component molecules, (3) difference in intermolecular forces, and (4) polar characteristics. In the case of conductivity, the proportion of molecular energy associated with internal degrees of freedom and the ease of transfer of such energy by collision are also important.

The character of a collision between like or unlike molecules in a mixture is temperature-dependent. At high temperatures, the repulsive forces between molecules are the determining factor, i.e., molecules behave as centers of repulsion during a high-energy collision. At low temperatures, the attractive forces play the major role in molecular encounters. Thus the angle of deflection suffered by a molecule during collision is profoundly influenced by temperature. The transport of kinetic energy and momentum are directly related to the angle of deflection,[28] and the conductivity and viscosity vary with temperature.

The conductivity of polyatomic molecules is further influenced by temperature through its effect upon the rate of transfer by collision of energy associated with internal degrees of freedom. With decreasing temperature, inelastic collisions among polyatomic molecules become more numerous. The proportion of energy associated with the internal degrees of freedom also increases with temperature. For example, about one fourth of of the heat capacity of CO_2 at 0°C is due to internal degrees of freedom, but at 1000°C, the proportion rises to nearly three quarters. If the rate of transfer of internal energy by collision is slow, this means that as the temperature rises, the proportion of energy transported by diffusion increases. Furthermore, the conductivity for internal energy depends also upon the effects of temperature on the diffusion coefficient.

The relative mass of the different components in a mixture affects the number of collisions between unlike molecules as well as the persistence of velocity of the molecules involved in these collisions. In a mixture of molecules of unequal masses, the persistence of velocity of the heavier molecule is increased, while that of the lighter molecule is reduced. As a result, the contribution of the heavier molecule to the conductivity and the viscosity of the mixture is enhanced, and the lighter molecule becomes less efficient in transporting kinetic energy and momentum. Mass difference is an important factor causing nonlinear relations between conductivity or viscosity and composition.

The force fields of molecules in a mixture may range from the simple spherical field of monatomic gases to that of highly polar polyatomic molecules. The interactions of molecules having widely different force fields causes in part the deviation from the ideal mixing rule. It has been pointed out that polar molecules in low concentrations may behave simply as nonpolar molecules, because in such mixtures, polar-polar encounters would be negligible in comparison to polar-nonpolar encounters, in which the polar characteristics are much less important.[62] Even in mixtures of nonpolar gases, unsymmetrical force fields may be important in determining the shape of the conductivity or viscosity vs composition curve.

The agreement between the experimental data and a correlation depends, therefore, upon how nearly the correlation accounts for the effects of the factors mentioned.

2. Thermal Conductivity

In a comparison of conductivity data with correlations, it is convenient to classify molecules according to the following scheme:

Type I. Monatomic molecules.

Type II. Rotators without energy of vibration or internal rotation.

Type III. Molecules having energies of vibration and/or internal rotation and H_2.

Hydrogen is classified as Type III because its energy of rotation is known to be transferred by diffusion.[29] With the molecules so classified

the mixtures may then be discussed in groups according to the types of constituents.

a. Monatomic mixtures. It is with this type of mixture that the effects of relative molecular masses and temperature can be best assessed, because these gases possess only translational kinetic energy, and their intermolecular forces should be quite similar. The factors A_{ij} in Eq. 49 indicate that these mixtures should have a conductivity-vs-composition curve lying below the linear relation. Both D_{ii}/D_{ij} and M_{ij}/M_i (where i refers to the lighter component) are larger than unity; hence, the contribution of the lighter component to mixture conductivity is reduced. The reduction usually cannot be balanced by the increase in the contribution of the heavier molecule. The net result is negative deviation from the linear relation.

Temperature may influence the conductivity of monatomic mixtures through its effect upon A_{ij} and upon the conductivities of the pure gases. A_{ij} should be nearly independent of temperature. The conductivity of the gases can be represented quite well over extended temperature ranges by aT^n with a value of n between 0.5 and 1. If A_{ij} were constants, and the n values for all components of a mixture are equal, then the ratio of the actual conductivity of the mixture to that calculated from the ideal mixing rule λ_c/λ_ℓ would be independent of temperature. Actually, λ_c/λ_ℓ would be a function of $T^{n'-n''}$ if it were assumed that temperature has no effect upon A_{ij} (see Appendix V).

A comparison of the conductivity of the binary system of He–A with Eq. 49 was made in the light of the foregoing points. For this system, the ratio of the molecular weights is ten; hence, the conductivity of the mixtures should be well below that calculated by the simple mixing rule. Over the temperature range of 200 to 800°K, the conductivities of He and A are proportional to the 0.63 and 0.78 power of the absolute temperature, respectively. Thus, the ratio λ_c/λ_ℓ should be a function of $T^{0.15}$. Because the variation of λ_c/λ_ℓ with temperature is much less than proportional to $T^{n'-n''}$, and $n'-n''$ is small compared to unity in this case, λ_c/λ_ℓ should vary only very slowly with temperature.

As a first approximation, λ_c/λ_ℓ may be assumed independent of temperatute. In order to demonstrate the validity of this assumption, the experimental and calculated data for this system are shown in Fig. 16. It is seen that a single curve represents the data in this manner quite well for various temperatures. There is some scattering of the experimental points about the curve; however, the deviations are not greater than expected. It appears that Eq. 49 predicts quite accurately for this system the variation of mixture conductivity with temperature and with composition.

The experimental data and values calculated by means of Eq. 49 for 35 mixtures of 5 binary systems of monatomic gases are tabulated in Table VI. The temperatures at which the measurements were made ranged from 0 to 316°C. For these data, the average deviation of Eq. 49 from experiment is 1.9%. Experimental and calculated conductivities for He—A mixtures and various temperatures are shown in Fig. 14.

b. Mixtures of molecules of Types I and II. Molecules of Type II have rotational energy in addition to translational kinetic energy. Both rotational and translational energies are transferred rapidly by collision;[6,63] therefore, when Eq. 49 is applied to mixtures of this group, the second sum does not appear, i.e., the expression for the conductivity of mixtures in this instance is identical to that for monatomic gas mixtures. The effects of molecular weight difference and temperature upon the conductivity of these mixtures should be similar to their effects upon the conductivity of monatomic mixtures discussed above. Binaries of He and N_2 are typical representatives of this group. The molecular weight ratio of 7 : 1 between He and N_2 should cause considerable negative deviation from the linear λ-vs-x relation. Over the temperature range of 170 to 670°K, the conductivity of N_2 is proportional to the 0.85 power of the absolute temperature. For the same reasons as in the case of the He—A system, λ_c/λ_ℓ for this system should also be essentially independent of temperature. The data for this system in the form of λ_c/λ_ℓ vs x is plotted in Fig. 17. The agreement between experiment and correlation again appears to be quite good. Equation 49 was compared with 23 data

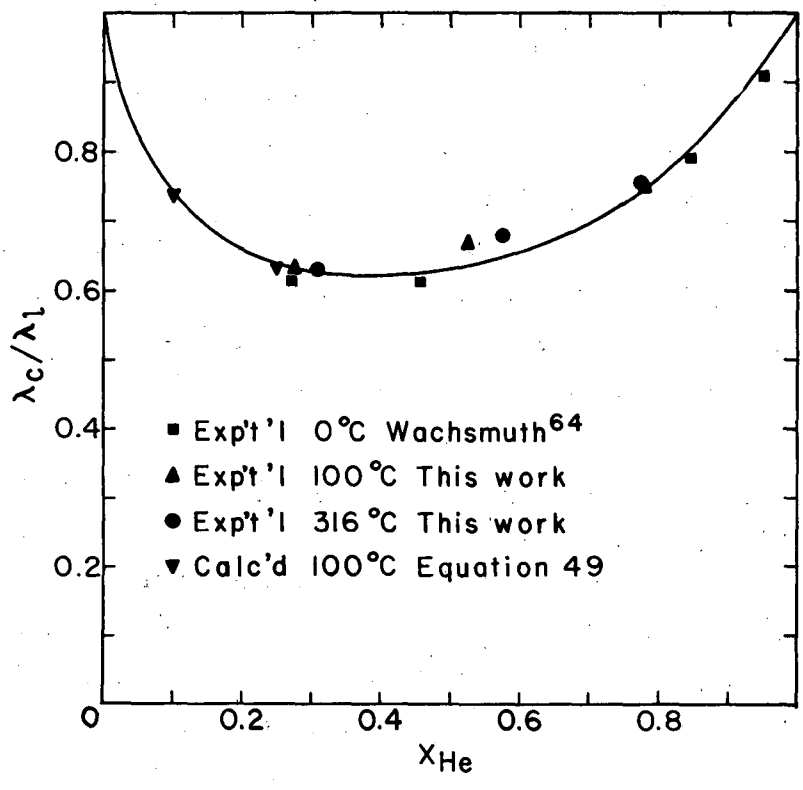

Fig. 16. Temperature effect on λ_c/λ_l of He–A mixtures.

Table VI

Comparison of experimental and calculated conductivities of nonpolar binary mixtures

System and ref.	Temp. (°C)	x_1	$\lambda_m \times 10^5$ $\frac{cal}{sec\ ^oC\ cm}$	$\lambda_c \times 10^5$ $\frac{cal}{sec\ ^oC\ cm}$	$\lambda_{calc'd.}$ (Eq. 49)	Deviation (%)	$\lambda_{calc'd.}$ (Lindsay-Bromley)	Deviation (%)
H_2-CO_2 (30)	0	1	3.60	--	--	--	--	--
		0.100	5.10	5.13	5.16	+0.56	5.04	-0.97
		0.142	5.70	5.75	5.83	+1.51	5.70	-0.07
		0.250	7.70	7.77	7.83	+0.80	7.60	-1.18
		0.355	10.00	10.09	10.12	+0.16	9.76	-2.40
		0.500	13.50	13.60	13.87	+2.10	13.43	-0.34
		0.750	22.70	22.77	23.35	+2.60	22.85	+0.78
		0.901	31.50	31.53	32.53	+3.16	31.90	+1.30
		1.000	40.40	--	--	--	--	--
H_2N_2 (30)	0	0	5.50	--	--	--	--	--
		0.159	8.0	8.05	8.26	+2.46	8.18	+2.27
		0.390	12.7	12.80	13.33	+4.46	13.18	+3.87
		0.652	19.4	19.49	21.50	+10.47	21.33	+10.28
		0.803	25.7	25.76	28.20	+9.40	27.97	+8.90
		1.000	40.4	--	--	--	--	--
H_2-N_2O (30)	0	0	3.8	--	--	--	--	--
		0.209	7.1	7.18	7.11	-1.09	7.06	-0.52
		0.386	10.7	10.83	10.83	0	10.71	+0.07
		0.599	17.0	17.12	16.76	-2.08	16.86	-0.80
		0.812	27.2	27.28	26.68	-2.33	26.32	-3.19
		1.000	40.4	--	--	--	--	--
He-A (64)	0	0	3.894	--	--	--	--	--
		0.2704	7.415	7.589	7.53	-0.65	7.60	+2.56
		0.4537	10.77	10.99	11.07	+0.73	11.12	+1.85
		0.8486	23.20	23.31	24.00	+2.96	24.28	+4.76
		0.9461	29.39	29.43	29.93	+1.78	29.97	+2.04
		1.000	33.86	--	--	--	--	--
H_2CO (30)	0	0	5.3	--	--	--	--	--
		0.163	8.0	8.05	8.12	+0.92	8.03	+0.46
		0.272	10.3	10.38	10.39	+0.32	10.18	-1.00
		0.560	18.0	18.10	18.20	+0.59	17.98	-0.11
		0.634	20.9	20.99	20.83	-0.81	20.35	-2.58
		0.794	27.0	27.06	27.75	-2.70	27.27	+1.10
		1.000	40.4	--	--	--	--	--
H_2-A (30)	0	0	3.9	--	--	--	--	--
		0.180	7.3	7.37	7.21	-2.17	7.14	-2.07
		0.400	12.6	12.71	12.62	-0.71	12.24	-3.12

Table VI (cont'd.)

System and ref.	Temp. (°C)	x_1	$\lambda_m \times 10^5$ cal/sec °C cm	$\lambda_c \times 10^5$ cal/sec °C cm	$\lambda_{calc'd.}$ (Eq. 49)	Deviation (%)	$\lambda_{calc'd.}$ (Lindsay-Bromley)	Deviation (%)
		0.600	18.7	18.81	18.88	+0.37	18.52	-0.99
		0.802	27.0	27.07	27.80	+2.62	27.37	-1.44
		1.000	40.4	--	--	--	--	--
H_2-C_2H_4 (38)	25	0	5.27	--	--	--	--	--
		0.1698	8.61	8.68	8.05	-7.14	7.99	-7.10
		0.3140	11.48	11.58	10.83	-6.35	10.86	-5.32
		0.5137	16.90	17.02	16.13	-5.18	16.12	-4.82
		0.6110	20.6	20.71	19.28	-6.92	19.46	-4.71
		0.8649	32.9	32.96	32.50	-1.42	32.40	-1.51
		1.000	43.7	--	--	--	--	--
N_2-A (66)	0	0	3.849	--	--	--	--	--
		0.2038	4.173	4.173	4.19	+0.59	4.22	+0.99
		0.3587	4.436	4.436	4.47	+0.84	4.49	+1.30
		0.6108	4.896	4.896	4.92	+0.59	4.96	+1.10
		0.7804	5.235	5.235	5.25	+0.24	5.27	+0.55
		1.000	5.66	--	--	--	--	--
H_2-D_2 (3)	0	0	30.8	--	--	--	--	--
		0.187	32.31	32.31	32.80	+0.62	32.70	+1.30
		0.395	34.1	34.1	35.10	+1.66	34.95	+2.54
		0.496	35.0	35.0	36.20	+2.09	36.05	+2.89
		0.655	36.4	36.4	37.97	+2.97	37.86	+3.78
		0.802	38.2	38.2	39.65	+2.98	39.50	+3.36
		1.000	41.8	--	--	--	--	--
H_2-CO_2 (38)	25	0	4.08	--	--	--	--	--
		0.047	4.43	4.45	4.81	+8.07	4.80	+8.39
		0.193	7.58	7.65	7.37	-3.56	7.32	-8.38
		0.496	15.13	15.24	14.87	-2.25	14.73	-2.40
		0.9059	35.0	35.04	35.35	+1.01	35.07	+0.37
		0.9638	40.2	40.20	40.20	0	40.10	-0.22
		1.000	43.7	--	--	--	--	--
H_2-CO_2 (66)	0	0	3.393	--	--	--	--	--
		0.1701	6.073	6.127	6.21	+1.35	5.91	-2.58
		0.3698	10.34	10.43	10.47	+0.48	9.82	-4.91
		0.6068	17.24	17.33	17.76	+2.53	16.66	-3.18
		0.8314	27.99	28.04	28.80	+2.84	27.25	-2.46
		1.000	41.63	--	--	--	--	--

Table VI (cont'd.)

System and ref.	Temp. (°C)	x_1	$\lambda_m \times 10^5$ $\frac{cal}{sec\ ^oC\ cm}$	$\lambda_c \times 10^5$ $\frac{cal}{sec\ ^oC\ cm}$	$\lambda_{calc'd.}$ (Eq. 49)	Deviation (%)	$\lambda_{calc'd.}$ (Lindsay-Bromley)	Deviation (%)
$He-CO_2$ (12)	0	0	3.39		--	--	--	--
		0.25	6.35	6.49	6.27	-3.39	6.01	-5.35
		0.52	11.20	11.38	11.11	-2.37	10.50	-6.25
		0.74	17.83	17.97	17.77	-1.11	17.28	-3.08
		1.000	33.21	--	--	--	--	--
He-Ne (12)	0	0	10.82	--	--	--	--	--
		0.25	14.09	14.28	14.67	+2.73	14.75	+4.69
		0.49	18.45	18.70	19.25	+2.94	19.35	+4.88
		0.75	24.25	24.44	25.48	+4.25	25.55	+5.36
		1.00	33.21	--	--	--	--	--
$Ne-CO_2$ (12)	0	0	3.39	--	--	--	--	--
		0.26	4.47	4.47	4.72	+5.59	4.617	+3.28
		0.47	5.88	5.88	6.03	+2.55	5.87	-0.17
		0.60	6.79	6.79	6.98	+2.80	6.69	-1.47
		0.69	7.31	7.31	7.73	+5.42	7.518	+2.84
		1.00	10.82	--	--	--	--	--
N_2-CO_2 (12)	0	0	3.39	--	--	--	--	--
		0.48	4.55	4.55	4.36	-4.36	4.412	-3.03
		0.75	5.12	5.12	5.03	-1.76	5.084	-0.70
		1.00	5.77	--	--	--	--	--
$He-N_2$ (12)	0	0	5.77	--	--	--	--	--
		0.26	8.64	8.76	8.97	+2.40	9.22	+6.29
		0.55	14.23	14.38	14.42	+0.28	14.91	+4.77
		0.76	19.77	19.88	20.71	+4.17	21.27	+7.58
		1.00	33.21	--	--	--	--	--
C_2H_2-Air (20)	20	0	6.00	--	--	--	--	--
		0.141	5.958	5.958	5.89	-1.11	5.91	-0.83
		0.320	5.832	5.832	5.725	-1.77	5.775	-1.06
		0.536	5.658	5.658	5.56	-1.90	5.595	-1.02
		0.630	5.550	5.550	5.49	-1.04	5.53	-0.30
		0.900	5.298	5.298	5.29	-0.16	5.31	+0.16
		1.000	5.20	--	--	--	--	--
C_2H_2-Air (20)	65	0	6.70	--	--	--	--	--
		0.211	6.76	6.76	6.69	-1.04	6.65	-1.59
		0.464	6.653	6.653	6.61	-0.68	6.55	-1.49
		0.646	6.573	6.573	6.44	-1.95	6.47	-1.51
		0.821	6.325	6.325	6.36	-0.90	6.38	-0.58
		1.000	6.284	--	--	--	--	--
CH_4-Air (20)	22	0	6.03	--	--	--	--	--
		0.076	6.120	6.120	6.125	+0.07	6.129	+0.14
		0.390	6.495	6.495	6.510	+0.38	6.512	+0.45
		0.700	6.868	6.868	6.890	+0.42	6.870	+0.18
		0.880	7.08	7.08	7.075	+0.18	7.210	+2.04
		1.000	7.22	--	--	--	--	--

Table VI (cont'd.)

System and ref.	Temp. (°C)	x_1	$\lambda_m \times 10^5$ $\frac{cal}{sec\ ^oC\ cm}$	$\lambda_c \times 10^5$ $\frac{cal}{sec\ ^oC\ cm}$	$\lambda_{calc'd.}$ (Eq. 49)	Deviation (%)	$\lambda_{calc'd.}$ (Lindsay-Bromley)	Deviation (%)
CO-Air (20)	18	0	5.97	--	--	--	--	--
		0.108	5.946	5.946	5.940	-0.14	5.936	-0.21
		0.321	5.886	5.886	5.873	-0.35	5.873	-0.35
		0.562	5.821	5.821	5.800	-0.35	5.796	-0.42
		0.978	5.626	5.703	5.688	-0.07	5.684	0
		1.000	5.626	--	--	--	--	--
Ne-A (48)	38	0	4.38	--	--	--	--	--
		0.1340	5.03	5.03	5.038	+0.16	5.08	+0.99
		0.1619	5.16	5.16	5.182	+0.43	5.23	+1.36
		0.1714	5.15	5.15	5.227	+1.50	5.288	+2.68
		0.3312	6.07	6.07	6.125	+0.90	6.23	+2.63
		0.5785	7.68	7.68	7.805	+1.63	7.94	+3.38
		0.6528	8.30	8.30	8.395	+1.14	8.52	+2.65
		0.6876	8.39	8.39	8.67	+3.33	8.80	+4.89
		0.8630	10.25	10.25	10.30	+0.49	10.38	+1.27
		0.8817	10.47	10.47	10.47	0	10.56	+0.86
		1.000	11.80	--	--	--	--	--
Ne-Kr (48)	38	0	2.33	--	--	--	--	--
		0.1444	3.07	3.10	3.041	-1.90	3.105	+1.14
		0.3293	3.98	4.03	4.143	+2.80	4.29	+7.78
		0.4930	5.16	5.21	5.358	+2.84	5.55	+7.55
		0.5723	5.91	5.96	6.062	+1.71	6.26	+5.92
		0.6908	6.96	7.01	7.262	+2.16	7.33	+5.31
		0.7924	8.31	8.34	8.491	+1.81	8.65	+3.93
		0.9288	10.35	10.36	10.53	+1.76	10.60	+2.41
		1.000	11.80	--	--	--	--	--
A-Kr (48)	38	0	2.33	--	--	--	--	--
		0.1885	2.56	2.56	2.638	+3.04	2.639	+3.08
		0.3317	2.77	2.77	2.896	+4.55	2.892	+4.40
		0.5160	3.17	3.17	3.255	+2.68	3.25	+2.52
		0.6205	3.34	3.34	3.47	+3.89	3.465	+3.74
		0.7662	3.66	3.66	3.80	+3.82	3.80	+3.82
		0.9134	3.98	3.98	4.15	+4.27	4.15	+4.27
		1.000	4.38	--	--	--	--	--
N_2-CO_2 (36)	50	0	4.34	--	--	--	--	--
		0.3406	4.99	4.99	4.96	-0.60	5.02	+0.60
		0.5288	5.37	5.37	5.33	-0.74	5.42	+0.91
		0.6650	5.67	5.67	5.67	0	5.76	+1.59
		1.000	6.64	--	--	--	--	--

Table VI (cont'd.)

System and ref.	Temp. (°C)	x_1	$\lambda_m \times 10^5$ $\frac{cal}{sec\ ^oC\ cm}$	$\lambda_c \times 10^5$ $\frac{cal}{sec\ ^oC\ cm}$	$\lambda_{calc'd.}$ (Eq. 49)	Deviation (%)	$\lambda_{calc'd.}$ (Lindsay-Bromley)	Deviation (%)
N_2-CO_2 (36)	150	0	6.27	--	--	--	--	--
		0.3406	7.02	7.02	6.84	-2.56	6.88	-1.99
		0.5288	7.38	7.38	7.15	-3.12	7.26	-1.63
		0.6650	7.64	7.64	7.47	-2.22	7.58	-0.79
		1.000	8.31	--	--	--	--	--
N_2-CO_2 (36)	250	0	8.36	--	--	--	--	--
		0.3406	8.91	8.91	8.74	-1.91	7.88	-0.34
		0.5288	9.21	9.21	8.97	-2.60	9.10	-1.19
		0.6650	9.36	9.36	9.24	-1.28	9.34	-0.21
		1.000	9.83	--	--	--	--	--
N_2-CO_2 (36)	350	0	10.58	--	--	--	--	--
		0.3406	11.04	11.04	10.73	-2.80	10.78	-2.35
		0.5288	11.27	11.27	10.76	-4.62	10.82	-3.99
		0.6650	11.30	11.30	10.91	-3.45	10.96	-3.01
		1.000	11.22	--	--	--	--	--
N_2-CO_2 (44)	369	0	10.40	--	--	--	--	--
		0.50	10.45	10.45	10.69	-2.37	10.85	-0.90
		0.53	10.91	10.91	10.73	-1.65	10.86	-0.46
		0.75	11.02	11.02	10.91	-1.00	11.02	0
		1.00	11.15	--	--	--	--	--
N_2-CO_2 (44)	372	0	11.06	--	--	--	--	--
		0.33	11.36	11.36	11.25	-0.97	11.49	+1.14
		0.50	11.61	11.61	11.38	-1.98	11.53	-0.69
		0.67	11.82	11.82	11.53	-2.45	11.66	-1.35
		0.83	11.91	11.91	11.68	-1.93	11.78	-1.09
		1.00	11.87	--	--	--	--	--
N_2-CO_2 (44)	375	0	11.19	--	--	--	--	--
		0.33	11.53	11.53	11.35	-1.56	11.49	-0.35
		0.50	11.78	11.78	11.46	-2.71	11.61	-1.44
		0.67	12.00	12.00	11.58	-3.50	11.71	-2.42
		0.83	12.08	12.08	11.71	-3.06	11.80	-2.32
		1.00	11.87	--	--	--	--	--
N_2-CO_2 (44)	472	0	12.15	--	--	--	--	--
		0.56	12.56	12.56	12.17	-3.10	12.33	-1.83
		1.00	12.32	--	--	--	--	--
N_2-CO_2 (44)	569	0	13.62	--	--	--	--	--
		0.33	13.78	13.78	13.42	-2.61	13.54	-1.73
		0.50	13.88	13.88	13.34	-3.89	13.46	-3.02

Table VI (cont'd.)

System and ref.	Temp. (°C)	x_1	$\lambda_m \times 10^5$ cal / sec °C cm	$\lambda_c \times 10^5$ cal / sec °C cm	$\lambda_{calc'd.}$ (Eq. 49)	Deviation (%)	$\lambda_{calc'd.}$ (Lindsay-Bromley)	Deviation (%)
		0.67	13.94	13.94	13.25	-4.95	13.43	-3.66
		1.00	13.12	--	--	--	--	--
N_2-CO_2 (44)	573	0	13.87	--	--	--	--	--
		0.33	14.03	14.03	13.69	-2.42	13.81	-1.57
		0.50	14.17	14.17	13.59	-4.09	13.74	-3.04
		0.67	14.19	14.19	13.52	-4.72	13.71	-3.38
		1.00	13.39	--	--	--	--	--
N_2-CO_2 (44)	677	0	16.10	--	--	--	--	--
		0.50	16.27	16.27	15.60	-4.12	15.74	-3.26
		1.00	15.12	--	--	--	--	--
N_2-CO_2 (44)	688	0	16.21	--	--	--	--	--
		0.25	16.44	16.44	16.08	-2.19	16.08	-2.19
		0.50	16.51	16.51	15.93	-3.51	15.93	-3.51
		0.75	16.29	16.29	15.68	-3.74	15.68	-3.74
		1.00	15.34	--	--	--	--	--
N_2-CO_2 (44)	774	0	18.29	--	--	--	--	--
		0.50	18.28	18.28	17.46	-3.83	17.79	-2.68
		1.00	16.99	--	--	--	--	--
He-N_2*	104	0	7.45	--	--	--	--	--
		0.219	10.71	10.88	10.77	+1.01	10.89	+1.68
		0.409	14.45	14.70	14.63	-0.48	14.88	+2.97
		0.837	30.58	30.73	30.41	-1.04	30.75	+0.56
		1.00	42.23	--	--	--	--	--
He-N_2*	316	0	10.64	--	--	--	--	--
		0.305	16.21	16.63	17.03	+2.40	17.54	+8.20
		0.637	28.24	28.78	27.80	-3.40	29.60	+4.81
		0.739	33.47	33.99	33.94	-0.15	34.96	+4.45
		1.000	55.6	--	--	--	--	--
He-A*	100	0	5.058	--	--	--	--	--
		0.276	9.439	9.711	9.67	-0.42	9.90	+4.88
		0.525	15.88	16.43	15.92	-3.16	16.14	+1.64
		0.780	25.24	25.49	26.19	+2.74	26.34	+3.34
		1.000	41.94	--	--	--	--	--

*Data of this work.

Table VI (cont'd.)

System and ref.	Temp. (°C)	x_1	$\lambda_m \times 10^5$ $\frac{cal}{sec\ ^oC\ cm}$	$\lambda_c \times 10^5$ $\frac{cal}{sec\ ^oC\ cm}$	$\lambda_{calc'd.}$ (Eq. 49)	Deviation (%)	$\lambda_{calc'd.}$ (Lindsay-Bromley)	Deviation (%)
He-A*	316	0	7.255	--	--	--	--	--
		0.306	13.31	13.89	14.20	+2.23	14.71	+10.52
		0.573	23.00	23.76	23.57	-0.80	24.52	+6.60
		0.774	33.23	33.84	34.65	+2.39	35.69	+7.40
		1.000	55.6	--	--	--	--	--
He-CH_4*	316	0	20.29	--	--	--	--	--
		0.299	24.53	24.86	25.02	+0.64	26.01	+6.04
		0.550	30.54	30.96	31.12	+0.52	32.85	+7.56
		0.746	40.63	40.94	39.43	-3.68	40.41	-0.54
		1.000	55.6	--	--	--	--	--
He-CO_2*	316	0	9.580	--	--	--	--	--
		0.610	23.65	24.29	25.58	+5.30	26.09	+10.31
		1.000	55.6	--	--	--	--	--
CH_4-C_3H_8*	95	0	6.344	--	--	--	--	--
		0.313	7.083	7.083	7.031	-0.73	7.18	+1.37
		0.486	7.636	7.636	7.522	-1.49	7.81	+2.28
		0.779	8.841	8.841	9.140	+3.38	9.54	+7.90
		1.00	10.49	--	--	--	--	--
CO_2-C_3H_8*	95	0	6.344	--	--	--	--	--
		0.291	6.083	6.083	6.023	-0.82	6.082	-0.02
		0.449	5.884	5.884	5.853	-0.53	5.928	+0.75
		0.635	5.715	5.715	5.615	-1.75	5.715	0
		1.000	5.181	--	--	--	--	--
O_2-CO_2*	97	0	5.218	--	--	--	--	--
		0.270	5.777	5.777	5.655	-2.11	5.738	-0.67
		0.315	5.883	5.883	5.779	-1.77	5.788	-1.61
		0.536	6.383	6.383	6.274	-1.71	6.336	-0.74
		0.778	7.027	7.027	6.916	-1.58	6.967	-0.85
		1.000	7.660	--	--	--	--	--
A-C_3H_8*	318	0	14.65	--	--	--	--	--
		0.471	11.86	11.86	11.90	+0.34	11.88	+0.17
		1.000	7.18					
A-C_3H_8*	538	0	25.13	--	--	--	--	--
		0.471	19.80	19.80	19.21	-2.98	18.83	-4.90
		1.000	9.00	--	--	--	--	--

Table VI (cont'd.)

System and ref.	Temp. (°C)	x_1	$\lambda_m \times 10^5$ $\frac{cal}{sec\ ^oC\ cm}$	$\lambda_c \times 10^5$ $\frac{cal}{sec\ ^oC\ cm}$	$\lambda_{calc'd.}$ (Eq. 49)	Deviation (%)	$\lambda_{calc'd.}$ (Lindsay-Bromley)	Deviation (%)
N_2-	318	0	14.65	--	--	--	--	--
C_3H_8*		0.525	13.06	13.06	12.92	-1.07	13.02	-0.31
		1.000	10.68	--	--	--	--	--
N_2-	538	0	25.13	--	--	--	--	--
C_3H_8*		0.476	20.99	20.99	20.74	-1.19	20.53	-2.19
		1.000	13.42	--	--	--	--	--
N_2-A*	320	0	7.291	--	--	--	--	--
		0.497	8.788	8.788	9.03	+2.76	8.96	+1.96
		1.000	16.71	--	--	--	--	--
A-CO_2*	320	0	9.655	--	--	--	--	--
		0.494	8.700	8.700	8.58	-1.38	8.64	-0.69
		1.000	7.291	--	--	--	--	--
C_2H_4-	318	0	9.617	--	--	--	--	--
		0.512	12.69	12.69	12.38	-2.44	12.75	+0.49
CO_2*		1.000	15.30	--	--	--	--	--
CH_4-	317	0	15.26	--	--	--	--	--
C_2H_4*		0.489	16.73	16.73	17.45	+4.30	17.49	+4.54
		1.000	20.34	--	--	--	--	--
N_2-O_2*	319	0	11.62	--	--	--	--	--
		0.3902	11.19	11.19	11.16	-0.27	11.25	+0.54
		1.000	10.70	--	--	--	--	--
N_2-	318	0	15.30	--	--	--	--	--
C_2H_4*		0.498	13.22	13.22	13.36	+1.06	13.16	-0.45
		0.756	12.03	12.03	12.09	+0.50	12.01	-0.17
		1.000	10.68	--	--	--	--	--
CH_4-A*	538	0	9.00	--	--	--	--	--
		0.4767	17.03	17.03	16.58	-2.65	17.59	+3.28
		1.000	25.30	--	--	--	--	--
Average Deviation (177 points)						2.08		2.56
Maximum Deviation						10.47		10.52

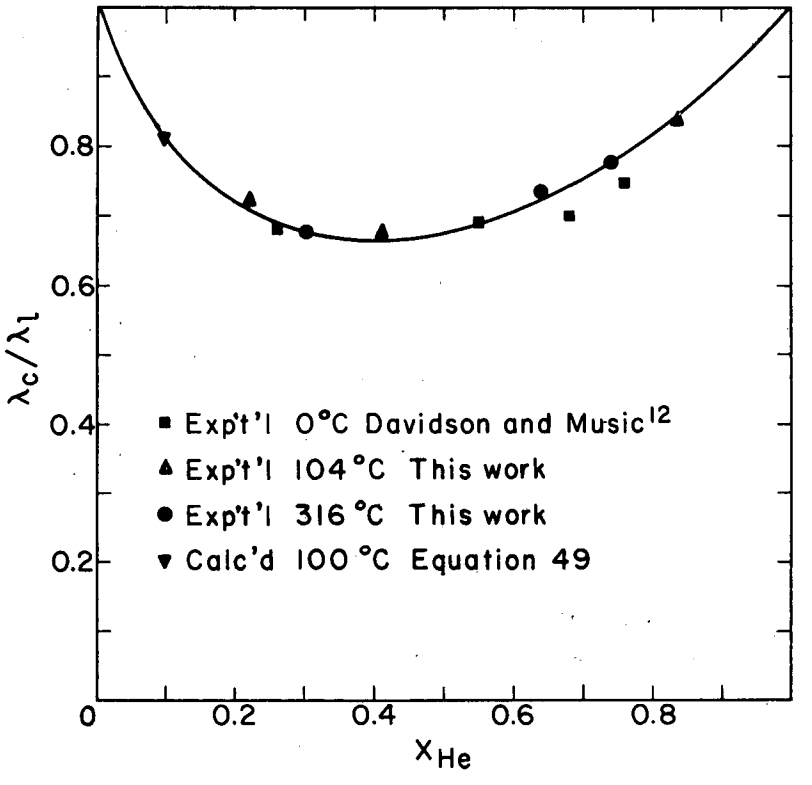

Fig. 17. Temperature effect on λ_c/λ_ℓ of He–N_2 mixtures.

points of seven binary systems of molecules of both Type I and Type II and of only Type II in temperatures from 0 to 320°C. The average deviation is 1.0%. Experimental and calculated conductivities for the He–N_2 system at various temperatures are shown in Fig. .

c. Mixtures containing molecules of Type III. Among molecules of this type, the H_2 molecule is of special interest in two respects. First, its lightness gives rise to mixtures having very high molecular-weight ratios. Second, its rotational energy and translation kinetic energy are transferred by different processes, diffusion and collision, respectively.[29] Thus, mixtures containing H_2 serve to test Eq. 49 not only for the correctness of its account of the relation between molecular-weight differences and conductivity but also for the assumption that molecular energy may be separated into collisional and diffusional parts. A comparison of the experimental and calculated values of the conductivity of mixtures of H_2 and A is shown in Fig. 18. These are the simplest mixtures in which energy transport by diffusion occurs, as the only other form of energy possessed by the molecules is translational kinetic energy. Further, the effect of molecular-weight difference upon the conductivity of these mixtures should be very pronounced. The agreement between Eq. 49 and the data is seen to be good; the average deviation is 1.5%. When, however, the rotational energy of H_2 is considered to be transferred by collision, as in the case of N_2 discussed above, the agreement is poorer; the average deviation becomes 3.3%. The procedure of separating the rotational and translational energies of H_2 appears to be justified.

As another example in support of this procedure, mixtures of H_2 and CO_2 were considered. Here the molecular-weight ratio is 22, and both components have a considerable portion of their energy transported by diffusion (see Table VII). There exists also a large difference between the rates of self-diffusion of H_2 and of CO_2 and their rates of diffusion in the mixture. For a 1 : 1 mixture at 0°C, H_2 diffuses only one-half as rapidly in the mixture as in itself, and CO_2 diffuses about 50% faster in the mixture. Three sets of experimental data with a total of fifteen points for this system are given in Table VI. Calculations based on

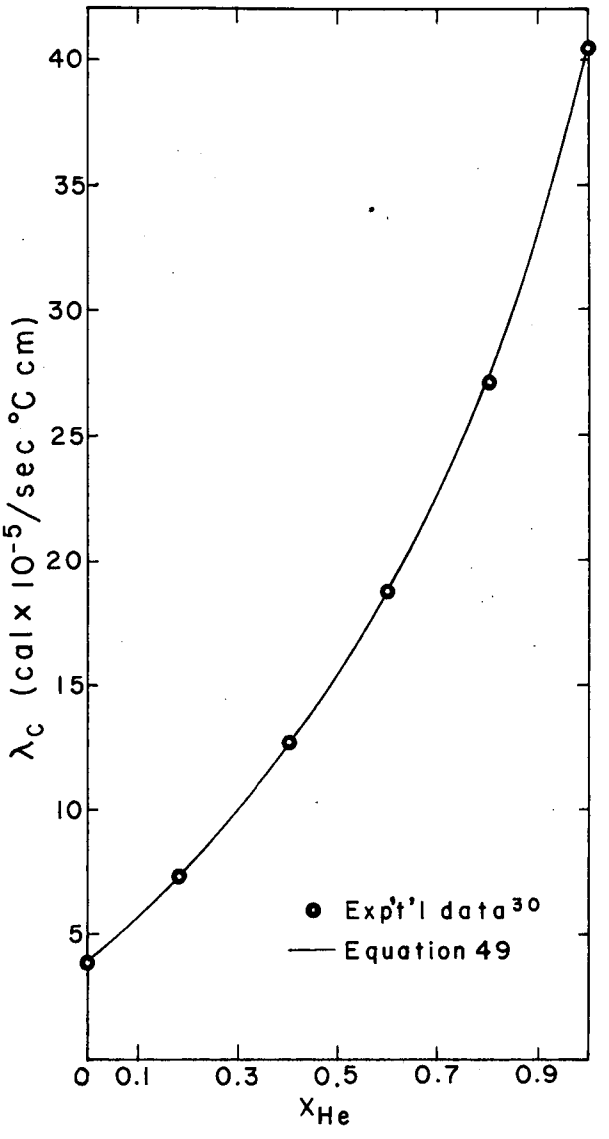

Fig. 18. Experimental and calculated conductivity of H_2–A mixtures.

Table VII

Proportion of energy transferred by diffusion						
Temp. (°C)	CH_4	C_2H_2	C_3H_4	C_3H_8	H_2	CO_2
0	0.22	0.42	0.34	0.57	0.17	0.34
200	0.37	0.53	0.53	0.72	0.18	0.43
400	0.48	0.57	0.61	0.78	0.18	0.49
600	0.55	0.60	0.66	0.81	0.18	0.52
800	0.59	0.62	0.69	0.82	0.20	0.53

splitting molecular energy into two parts show an average deviation of 2.2% from these data, but on the basis of all energy taken as transferred by collision, the deviation rises to 2.85%. Similarly, for the 43 data points of the nine different sets of mixtures containing H_2, the average deviations are 2.6% and 3.5%. For these mixtures, Eq. 49 may be considered as satisfactory in accounting for differences in molecular weights and rates of diffusion.

In theory, the result of splitting the energy into two parts can be best demonstrated in mixtures of molecules of Type III, other than H_2, because these molecules may have more than half of their energy distributed in the vibrational degrees of freedom at temperatures conveniently attainable experimentally. The fraction of conductivity from transport by diffusion for a number of vibrators and H_2 at various temperatures are given in Table VII.

In comparing Eq. 49 with the available data on mixtures of these Type III molecules, it is difficult to justify the procedure of splitting the energy transport into collisional and diffusional portions. According to Eq. 49, the difference in the contributions of the two kinds of energy of a molecule to the conductivity of a mixture depends upon the empirical factor $(M_{ij}/M_i)^{1/8}$. Unless the molecular weights of the components of the mixture were widely different, this factor is near unity, in which case the effective contribution of the two types of energy transport are equal. Of the data available on mixtures of this group, the system He-CH_4 has the highest molecular weight ratio. At 316°C, 35% of the energy transported by CH_4 occurs through diffusion. Nevertheless, values calculated by splitting the energy of CH_4 and those computed by considering its energy to be transferred wholly by collision show the same average deviation from the experimental data. The failure of the two procedures to yield distinctly different results lies in the fact that the contribution of He to the conductivity of the mixture is several times greater than the diffusional contribution of CH_4, except at high CH_4 concentrations; consequently, the small change in calculated values for the diffusional contribution of CH_4 has little effect on the total calculated conductivity. At high concentrations of CH_4, however, the effect upon conductivity of the

difference between the rates of diffusion of CH_4 in the mixture and in itself becomes small. Appreciable differences between the values calculated by the two procedures would appear only in cases where not only the molecular-weight ratio is high, but also the diffusional contribution is a significant portion of the mixture conductivity. In view of these requirements, it appears profitable to consider the system A–CH_4 at 538°C. For a 1 : 1 mixture, roughly one-third of the total energy transported is accounted for by diffusion of CH_4. Although the molecular-wieght ratio has a relatively low value of 2.5, splitting the energy affords a value that is in better agreement with the single experimental point available. For 76 points of 16 binary systems of mixtures of this group over the temperature range of 0 to 774°C, the average deviation of Eq. 49 is 2.2%. If the energy were not split, then the deviation would be 2.1%. It is difficult to determine the advantage of one procedure over the other from the available data.

d. Percentage deviation from data. A comparison of Eq. 49 with data from the literature and those of this work is given in Table VI. The data cover 177 points from 30 different nonpolar binary systems in temperatures ranging from 0 to 774°C. The average deviation of Eq. 49 from the data is 2.1%. Of the many empirical equations found in the literature, that of Lindsay and Bromley[40] is in best agreement with experiment. Table VI also contains values calculated from their relation. The average deviation in this case is 2.6%. Comparison of the two correlations in another way is presented in Table VIII, in which the average and maximum deviations from the data according to source are given. Data for 16 ternary mixtures at temperatures from 0 to 317°C are given in Table IX. The average deviations of Eq. 49 and of the Lindsay-Bromley equation from these data are 2.2% and 3.9% respectively. It appears that for the data presented, Eq. 49 is somewhat more consistent with experiment than the Lindsay-Bromley relation. It should be noted that for some of the systems listed in Table VI, values calculated by Eq. 49 are not directly comparable with those from the Lindsay-Bromley equation, because the latter correlation is based on the measured conductivity while the former is based on the

Table VIII

Comparison of experimental and calculated conductivities according to data source

Data Source	Number of Points	Equation 49 % Deviation		Lindsay-Bromley % Deviation	
		Average	Maximum	Average	Maximum
Collected by Lindsay and Bromley[40]	68	1.97	10.47	2.16	10.28
This work	37	1.59	5.30	2.84	10.52
Rothman[44] N_2-CO_2	23	2.88	4.95	2.03	3.74
Keyes[36] N_2-CO_2	12	2.14	4.62	1.55	3.99
Srivastava and Saxena[48]	22	1.90	4.55	3.48	7.78
Davidson and Music[12]	15	2.80	5.59	3.98	7.58
Total	177	2.08	10.47	2.56	10.52

Table IX

Comparison of experimental and calculated conductivities of ternary mixtures

System and Data source	Temp. (°C)	x_1	x_2	λ_1	λ_2	λ_3	λ_m	λ_c	$\lambda_{calc'd.}$ Eq. 49	Deviation (%)	$\lambda_{calc'd.}$ Lindsay-Bromley	Deviation (%)
				(cal x 10^{-5}/sec °C cm)								
He-CH_4-O_2 (5)	0	0.743	0.060	33.86	7.20	5.77	20.0	20.15	20.93	+3.87	21.1	+5.50
		0.712	0.100				19.5	19.66	19.88	+1.12	20.1	+3.08
		0.684	0.135				18.6	18.77	19.00	+1.22	19.2	+3.23
A-CH_4-O_2 (5)	0	0.751	0.050	3.89	7.20	5.77	4.59	4.59	4.423	-3.64	4.41	-3.92
		0.712	0.100				4.71	4.71	4.568	-3.01	4.56	-3.18
		0.677	0.144				4.91	4.91	4.703	-4.21	4.69	-4.49
Ne-A-Kr (48)	38	0.1387	0.717	11.80	4.38	2.23	4.50	4.506	4.628	+2.71	4.691	+4.26
		0.1861	0.145				3.47	3.484	3.504	+0.57	3.598	+3.69
		0.3019	0.385				4.80	4.816	4.948	+2.74	5.016	+4.09
		0.4537	0.157				5.45	54.71	5.471	0	5.542	+1.69
		0.4984	0.130				6.58	6.60	6.782	+2.75	6.879	+4.54
		0.1279	0.157				3.24	3.251	3.251	0	3.269	+0.90
		0.7919	0.142				8.45	8.46	8.971	+6.03	9.142	+8.19
N_2-O_2-CO_2 (this work)	97	0.3231	0.3729	7.331	7.660	5.218	6.729	6.729	6.760	+0.46	6.792	+0.48
He-N_2-A (this work)	99.5	0.415	0.468	41.90	7.374	5.052	13.95	14.17	14.21	+0.28	14.64	+4.95
He-CH_4-N_2 (this work)	317	0.159	0.365	55.6	20.33	10.67	16.74	16.94	17.51	+3.36	17.76	+6.09
Average Deviation (16 points)										2.2		3.9
Maximum Deviation										6.0		8.2

measured values corrected for conductivity from thermal diffusion. However, the percentage deviations may be compared.

e. The effect of temperature upon mixtures containing vibrators. It is well established experimentally that the conductivity of mixtures of N_2 and CO_2 shows a positive deviation from the simple mixing rule at temperatures above 150°C, and a negative deviation at lower temperatures.[36,44] The data of this work show that the deviation is also positive for the following systems: A–CO_2, N_2–C_3H_8, A–C_3H_8, C_2H_4–CO_2, and N_2–C_2H_4 in the neighborhood of 320°C; CH_4–A, N_2–C_3H_8, and A–C_3H_8 at 538°C; and CO_2–C_3H_8 at 95°C. A similar trend is also seen in the data for the C_2H_4–air mixtures at 20 and 65°C.[47]

That mixtures of nonpolar molecules should behave in this manner has not been heretofore satisfactorily explained. However, these experimental facts appear to be consistent with predictions based upon Eq. 49. It was shown in Paragraphs a and b above that for molecules having only translational and rotational energy, the percentage deviation from a linear relation is nearly independent of temperature. Furthermore, the contribution of the lighter components, which have higher conductivity, is reduced by the lowered persistence of velocity in their collisions with heavier molecules; and similarly the contribution of the heavier molecules is increased. The net result is a negative deviation from the linear relation. Now if the heavier molecule has a diffusional contribution to energy transport, this contribution would be greater in a mixture with a lighter molecule than in itslef, because its rate of diffusion would be raised. This diffusional contribution then tends to offset the negative deviation caused by collisional transfer, provided the lighter molecule possesses little or no energy that is transported by diffusion. With increasing temperature, the diffusional contribution rises and the conductivity of the mixture shifts from a negative to a positive deviation. The data cited at the beginning of this paragraph and other data in Table VI appear to support this argument, because in every case involved, the composition is such that the component having the higher diffusional contribution also has a higher diffusion rate in the mixture than in itself.

f. Conductivity of polar-nonpolar mixtures. In the application of Eq. 49 to nonpolar mixtures, the method of Hirschfelder et al. was used to calculate the ratio D_{ii}/D_{ij}.[27] As pointed out in Chapter II, such a procedure cannot be used for polar-nonpolar mixtures; therefore it was suggested that a modification of Arnold's method might be suitable in this instance.[4] Accordingly, D_{ii}/D_{ij} for these mixtures was computed by the following expression:

$$\frac{D_{ii}}{D_{ij}} = \left(\frac{M_i}{M_{ij}}\right)^{\frac{1}{2}} \left\{\frac{1}{2}\left[1 + \left(\frac{V_j}{V_i}\right)^{\frac{1}{3}}\right]\right\}^2 \frac{T + 0.733\ F\ 1.5\ (\sqrt{T_{B_i} T_{B_j}})}{T + 1.5\ T_{B_i}} \qquad (51)$$

The conductivity of mixtures of NH_3 and air at 20° and 80°C was calculated with D_{ii}/D_{ij} from this equation and from Arnold's original equation. The results of these calculations and the experimental data are shown in Fig. 19. It is seen that modification of Arnold's equation in unquestionably desirable for this system.

It will be shown subsequently that Eq. 51 is applicable to mixtures containing a number of strongly polar molecules. Because it is expected that this equation cannot be applied with equal success to weakly polar molecules, it is desirable at this point, to put an arbitrary limitation on the term "polar". A criterion for measuring the polar character of a substance is the dimensionless quantity introduced by Hirschfelder et al.[28a]

$$\delta^* = \frac{1}{2} \frac{\mu^2}{\epsilon \sigma^3} \qquad (52)$$

This quantity is a measure of the extent to which a polar molecule deviates from nonpolar behavior. On the basis of the δ^* values of the substances to which Eq. 51 will be applied, a polar molecule is defined in this work as one having a value of δ^* greater than 0.27.

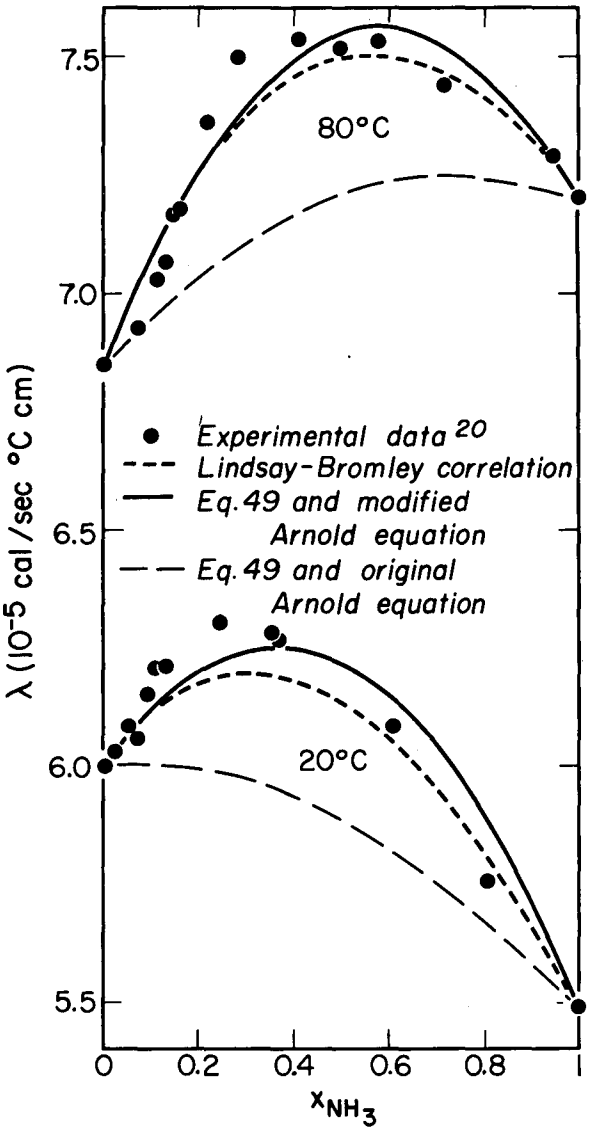

Fig. 19. Experimental and calculated conductivity of NH_3–air mixtures.

Examination of the conductivity data of mixtures of this type reveals that in all cases there is a positive deviation from the simple mixing rule. Vine and Bennett pointed out that when polar molecules are mixed with nonpolar ones, the former should have an effective conductivity larger than in the pure state.[62] This is because in polar-nonpolar collisions, the polar characteristic of the molecules should have little effect; therefore, in polar-nonpolar interactions, the polar molecules should behave effectively as a nonpolar molecule. That the conductivity of all such binary mixtures exhibits positive deviation from a linear relation is the experimental confirmation of this argument. Calculations show that Eqs. 49 and 51 are consistent with this qualitative aspect of the conductivity-vs-composition curves for mixtures of this type. Comparison of calculated values and experimental data is given in Table X. For the 49 points of 9 different binary systems in temperatures from 0 to 121°C, the average deviation of Eq. 49 from the data is 2.2%. Also shown thereon are values calculated with the equation of Lindsay and Bromley.[40] The deviation in this case is 2.1%. Although the two methods show about the same accuracy, the distribution of the deviations of the latter is better. In eight cases out of ten, the values computed by Eq. 49 are higher than the experimental data; whereas, by the method of Lindsay and Bromley, roughly half of the calculated values are higher.

3. Viscosity

a. Viscosity of nonpolar mixtures. It was shown in Paragraph 2a and 2b that for those molecules whose conductivities are proportional to T^n over an extended range of temperature, the ratio of the actual conductivity of a mixture to that calculated by the simple mixing rule is nearly independent of temperature. In the case of conductivity, the change with temperature may be affected by the presence of internal degrees of freedom; consequently, one finds that for many gases the proportionality between viscosity and a power of absolute temperature is valid over wider temperature limits than in the case of conductivity. Further, even in those instances of molecules having no internal degrees of freedom, the

Table X

Comparison of experimental and calculated conductivities of polar-nonpolar binary mixtures

System and data source	Temp. (°C)	x_1	$\lambda_{exp't.}$ $\frac{cal \times 10^{-5}}{sec\ ^\circ C\ cm}$	$\lambda_{calc'd.}$ (Eq. 36)	Deviation (%)	$\lambda_{calc'd.}$ (Lindsay-Bromley)	Deviation (%)
NH_3-Air (20)	20	0.	6.00	--	--	--	--
		0.246	6.306	6.24	-1.24	6.20	-1.70
		0.366	6.270	6.27	-0.39	6.20	-1.20
		0.608	6.084	6.14	+0.68	6.05	-0.60
		0.805	5.754	5.90	+2.32	5.81	+1.0
		1.000	5.490	--	--	--	--
CH_3OH-C_6H_{14} (61)	78	0	4.23	--	--	--	--
		0.25	4.57	4.49	-1.75	4.52	-1.09
		0.50	4.80	4.74	-1.25	4.73	-1.46
		0.75	4.83	4.90	+1.45	4.81	-0.41
		1.00	4.67	--	--	--	--
CH_3OH-C_6H_{14} (61)	98.4	0	4.75	--	--	--	--
		0.25	5.06	5.034	-0.51	5.05	-0.20
		0.50	5.28	5.293	+0.25	5.26	-0.38
		0.75	5.38	5.455	+1.39	5.33	-0.93
		1.00	5.18	--	--	--	--
CH_3OH-C_6H_{14} (61)	121.4	0	5.37	--	--	--	--
		0.25	5.73	5.672	-1.01	5.68	-0.87
		0.50	5.90	5.975	+1.27	5.70	-3.40
		0.75	5.97	6.105	+2.26	5.97	0
		1.00	5.77	--	--	--	--
C_3H_6O-C_6H_6 (61)	76.7	0	3.40	--	--	--	--
		0.25	3.54	3.664	+3.50	3.66	+3.39
		0.50	3.68	3.823	+3.89	3.82	+3.80
		0.75	3.725	3.845	+3.22	3.84	+3.09
		1.00	3.67	--	--	--	--
C_3H_6O-C_6H_6 (61)	102.8	0	4.00	--	--	--	--
		0.25	4.16	4.282	+2.93	4.277	+2.81
		0.50	4.26	4.446	+4.36	4.435	+3.95
		0.75	4.28	4.447	+3.90	4.532	+5.89
		1.00	4.22	--	--	--	--
C_3H_6O-C_6H_6 (61)	125.1	0	4.525	--	--	--	--
		0.25	4.70	4.842	+3.02	4.827	+2.70
		0.50	4.78	5.012	+4.95	4.993	+4.47
		0.75	4.83	5.003	+3.58	4.983	+3.17
		1.00	4.745	--	--	--	--

Table X (cont'd.)

System and data source	Temp. (°C)	x_1	$\lambda_{exp't.}$ $\frac{cal \times 10^{-5}}{sec\ °C\ cm}$	$\lambda_{calc'd.}$ (Eq. 36)	Deviation (%)	$\lambda_{calc'd.}$ (Lindsay-Bromley)	Deviation (%)
H_2O-N_2 (60)	65	0	6.90	--	--	--	--
		0.25	6.90	6.84	-0.87	6.792	-1.56
		0.50	6.40	6.50	+1.56	6.405	+0.08
		0.75	5.70	5.87	+2.98	5.778	+1.37
		1.00	4.95	--	--	--	--
H_2O-CO_2 (60)	65	0	4.62	--	--	--	--
		0.25	5.14	4.99	-2.92	4.997	-2.78
		0.50	5.20	5.23	+0.58	5.17	-0.58
		0.75	5.11	5.27	+3.13	5.16	+0.98
		1.00	4.95	--	--	--	--
CH_3OH-A (61)	78	0	4.85	--	--	--	--
		0.25	4.98	5.19	+4.22	4.737	-4.88
		0.50	4.93	5.195	+5.37	4.640	-5.88
		0.75	4.82	5.003	+3.79	4.575	-5.36
		1.00	4.67	--	--	--	--
CH_3OH-A (61)	100	0	5.10	--	--	--	--
		0.25	5.32	5.507	+3.51	5.024	-5.56
		0.50	5.35	5.598	+4.63	4.982	-6.87
		0.75	5.30	5.475	+3.30	4.990	-5.85
		1.00	5.22	--	--	--	--
NH_3-C_2H_4 (38)	25	0	5.27	--	--	--	--
		0.264	5.76	5.80	+0.79	5.84	+1.4
		0.5879	6.12	6.25	+2.02	6.26	+2.2
		0.7732	6.26	6.365	+1.65	6.35	+1.5
		1.000	6.30	--	--	--	--
NH_3-Air	80	0	6.90	--	--	--	--
		0.216	7.362	7.27	-1.29	7.28	-1.2
		0.410	7.535	7.49	-0.60	7.47	-0.9
		0.576	7.528	7.56	+0.33	7.50	-0.3
		0.715	7.438	7.52	+1.11	7.48	+0.5
		1.000	7.197	--	--	--	--
NH_3-CO (20)	22	0	5.746	--	--	--	--
		0.220	5.97	5.99	+0.21	6.01	+0.7
		0.338	6.03	6.04	+0.21	6.07	+0.7
		0.620	5.947	6.01	+1.04	6.00	+1.0
		0.790	5.825	5.86	+0.57	5.845	+0.4
		1.000	5.559	--	--	--	--

Table X (cont'd.)

System and data source	Temp. (°C)	x_1	$\lambda_{exp't.}$ $\frac{cal \times 10^{-5}}{sec\ ^\circ C\ cm}$	$\lambda_{calc'd.}$ (Eq. 36)	Deviation (%)	$\lambda_{calc'd.}$ (Lindsay-Bromley)	Deviation (%)
H_2O-Air (20)	80	0	6.90	--	--	--	--
		0.197	7.148	6.905	-3.41	7.058	-1.3
		0.306	7.08	6.855	-3.09	7.012	-0.9
		0.444	6.893	6.711	-2.64	6.831	-0.9
		0.519	6.735	6.591	-1.97	6.690	-0.5
		1.000	5.231	--	--	--	--
Average Deviation (49 points)					2.2		2.1
Maximum Deviation					5.4		6.9

rate of change of the functional relationship with temperature is slower in the case of viscosity, because an important effect of rising temperature is an increase in the persistence of velocity, and viscosity is less sensitive to the persistence of velocity than is conductivity. This is particularly true of very soft molecules. As a result of the fact that the viscosities of many gases are proportional to a power of the absolute temperature somewhat greater than 0.5, the hard-sphere value, the ratio η_m/η_ℓ for nonpolar mixtures is found to be independent of temperature over temperature ranges of two to three hundred degrees or more, in accordance with the argument set forth in Paragraph 2a above for conductivity. To test the constancy of η_m/η_ℓ, the data for several binary systems, whose viscosity-vs-concentration relations are highly irregular and dissimilar, have been selected. The room-temperature data for these systems are shown in Fig. 20. Values of η_m/η_ℓ for different temperatures are given in Table XI. With the exception of H_2–C_3H_8 mixtures, the ratio is constant to within 2% through a temperature range of 250°C. For some of the H_2–C_3H_8 mixtures, this ratio increased 3.5% with a temperature rise of 250°C. The excellent agreement between experiment and prediction shows that A_{ij} is essentially independent of temperature (see Appendix V), as would be expected on the basis of Eq. 50, since D_{ii}/D_{ij} should not be very sensitive to temperature.

Equation 50 was compared with 69 selected data points from 19 binary systems. Table XII shows the experimental and calculated values. The numerical average deviation, the algebraic average deviation, and the maximum deviation of Eq. 50 from these data are 1.33%, + 0.15%, and 6.32% respectively. Comparison against data of ternary and quarternary mixtures is given in Table XIII. The numerical average deviation for the nine mixtures tabulated is 2.38%.

The correlation established by Buddenburg and Wilke[7] and the equation proposed by Wilke[67] appear to be in better agreement with the experimental data than other correlations found in the literature. Calculated values based on Wilke's equation are given in Table XII to show a comparison between it and Eq. 50. The numerical average, algebraic average, and maximum deviation in this case are 2.07%, + 1.30%, and 10.8%. The

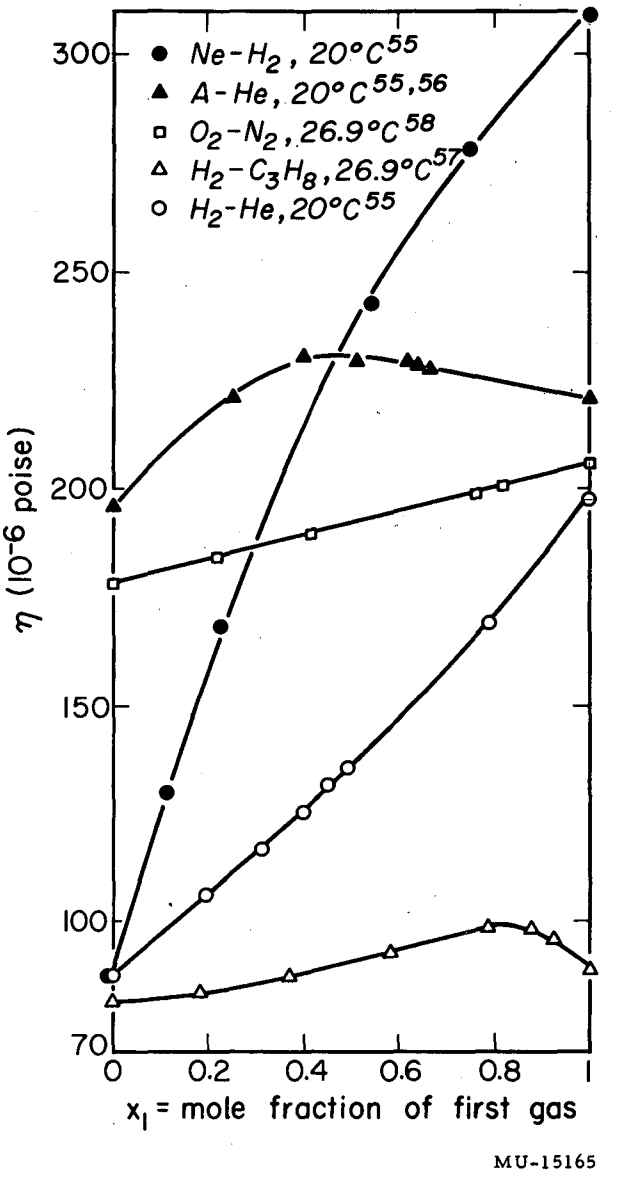

Fig. 20. Viscosity of some nonpolar binary mixtures.

Table XI

The constancy of the ratio η_m/η_ℓ

System and data source	x_1	η_m/η_ℓ 20°C	100°C	200°C	250°C
H_2-Ne (55)	0.8895	1.1616	1.1610	1.1625	1.1619
	0.7715	1.2195	1.2202	1.2209	1.2207
	0.4609	1.1723	1.1756	1.1744	1.1713
	0.2520	1.0972	1.1008	1.0986	1.0978
He-A (53,56)	0.3405	1.0690	1.0691	--	--
	0.3660	1.0719	1.0776	1.0769	--
	0.3820	1.0806	1.0790	1.0762	1.0759
	0.4906	1.0963	1.0977	--	--
	0.5966	1.1134	1.1305	1.1278	--
	0.7565	1.1165	1.1149	1.1126	--
H_2-He (55)	0.2163	0.9751	0.9742	0.9746	--
	0.5130	0.9581	0.9608	0.9609	--
	0.5520	0.9593	0.9652	0.9639	0.9623
	0.6069	0.9579	0.9622	0.9589	0.9606
	0.6918	0.9605	0.9692	0.9672	0.9665
	0.8040	0.9725	0.9751	0.9754	--
		26.9 °C	126.9 °C	226.9 °C	276.9 °C
H_2-C_3H_8 (57)	0.1821	1.0072	1.0168	1.0181	1.0220
	0.3704	1.0338	1.0511	1.0589	1.0602
	0.5818	1.0744	1.0882	1.1078	1.1095
	0.7882	1.1258	1.1443	1.1507	1.1490
	0.8750	1.1202	1.1304	1.1355	1.1328
	0.9225	1.0961	1.1055	1.1064	1.0983
N_2-O_2 (58)	0.1864	1.0005	0.9960	0.9957	--
	0.2408	1.0020	1.0008	1.0007	1.0021
	0.5893	1.0005	1.0000	0.9975	1.0000
	0.7822	1.0016	1.0009	0.9992	1.0014

Table XII

Comparison of experimental and calculated viscosities of nonpolar binary mixtures

System and data source	Temp. (°C)	x_1	$\eta_{exp't.}$ (poise x 10^6)	$\eta_{calc'd.}$ (Eq. 50)	Deviation (%)	$\eta_{calc'd.}$ (Wilke)	Deviation (%)
CO_2-Freon 12 (7)	25	0	124	--	--	--	--
		0.25	130.1	129.8	-0.23	128.8	-1.00
		0.50	135.3	135.7	+0.30	134.4	-0.66
		0.75	142	141.9	-0.07	141.0	-0.70
		1.00	147.8	--	--	--	--
H_2-Freon 12 (7)	25	0	124	--	--	--	--
		0.25	128.1	128.5	+0.31	127.2	-0.70
		0.50	131.9	132.6	+0.53	131.4	-0.38
		0.75	135.1	131.4	-2.74	135.4	+0.22
		1.00	88.4	--	--	--	--
N_2-Freon 12 (7)	25	0	124	--	--	--	--
		0.25	130.7	135.8	+3.90	131.9	+0.92
		0.50	144.1	149.0	+3.40	142.2	-1.32
		0.75	158.4	163.3	+3.09	156.6	+1.14
		1.00	176.8	--	--	--	--
H_2-C_3H_8 (57)	26.9	0	81.7	--	--	--	--
		0.182	83.6	85.6	+2.39	84.1	+0.60
		0.370	87.4	90.0	+2.98	87.3	-0.14
		0.586	92.4	95.0	+2.81	91.6	-0.87
		0.788	98.5	98.1	-0.41	96.7	-1.83
		0.875	98.7	97.3	-0.61	97.8	-0.91
		0.922	97.0	95.5	-1.55	96.9	-0.10
		1.000	89.1	--	--	--	--
N_2-O_2 (58)	26.9	0	205.7	--	--	--	--
		0.1864	200.8	199.8	-0.20	200.0	-0.40
		0.241	199.5	198.2	-0.65	198.6	-0.45
		0.589	189.4	188.3	-0.58	187.8	-0.84
		0.592	189.3	188.2	-0.58	188.6	-0.37
		0.782	184.3	183.7	-0.33	183.6	-0.38
		1.000	178.1	--	--	--	--
He-A (53,56)	20	0	221.1	--	--	--	--
		0.340	227.8	229.6	+0.79	228.3	+0.22
		0.366	228.6	229.8	+0.52	229.3	+0.31
		0.382	229.1	230.1	+0.44	229.6	+0.22
		0.491	229.6	231.4	+0.78	231.3	+0.74
		0.597	230.4	231.1	+0.30	232.9	+1.08
		0.756	227.0	226.7	-0.13	230.8	+1.67
		1.000	197.3	--	--	--	--

Table XII (cont'd.)

System and data source	Temp. (°C)	x_1	$\eta_{exp't.}$ (poise x 10^{-6})	$\eta_{calc'd.}$ (Eq. 50)	Deviation (%)	$\eta_{calc'd.}$ (Wilke)	Deviation (%)
H_2-CO (54)	25	0	174.5	--	--	--	--
		0.193	171.7	170.4	-0.76	173.4	+0.99
		0.410	165.1	162.6	-1.52	169.8	+2.85
		0.476	161.0	159.3	-1.06	167.8	+4.22
		0.695	144.9	142.0	-2.00	155.0	+6.96
		1.000	87.4	--	--	--	--
C_2H_6-C_3H_8 (51)	20	0	80.1	--	--	--	--
		0.153	81.5	81.6	+0.12	81.4	-0.12
		0.256	82.8	82.5	-0.36	82.5	-0.36
		0.433	84.1	84.4	+0.36	84.3	+0.24
		1.000	90.9	--	--	--	--
CH_4-C_3H_8 (51)	20	0	80.1	--	--	--	--
		0.166	83.1	83.9	+0.96	85.5	+2.89
		0.362	87.8	89.1	+1.48	92.2	+4.41
		0.632	94.8	96.9	+2.21	102.6	+8.23
		1.000	108.7	--	--	--	--
H_2-O_2 (51)	26.9	0	205.7	--	--	--	--
		0.394	192.5	189.6	-1.51	198.5	+3.12
		0.603	178.4	172.2	-3.48	185.8	+4.15
		0.863	131.4	129.7	-1.29	145.6	+10.80
		1.000	88.9	--	--	--	--
H_2-He (51)	100	0	234.1	--	--	--	--
		0.039	229.1	229.0	+0.04	228.9	-0.09
		0.403	178.4	182.2	+2.13	181.6	+1.79
		0.812	126.5	129.2	+2.13	128.0	+1.18
		1.000	104.6	--	--	--	--
H_2-He (51)	20	0	197.3	--	--	--	--
		0.552	131.7	136.7	+3.80	136.0	+3.26
		0.607	125.2	130.8	+4.46	130.0	+3.84
		0.692	116.6	121.5	+4.20	120.8	+3.60
		1.000	87.5	--	--	--	--
Ne-A (51)	20	0	221.1	--	--	--	--
		0.258	240.1	241.3	+0.50	236.2	-1.62
		0.391	250.4	252.4	+0.80	245.4	-2.00
		0.732	280.8	282.8	+0.71	275.5	-1.89
		1.000	309.2	--	--	--	--
H_2-A (51)	20	0	221.1	--	--	--	--
		0.294	214.0	210.6	-1.59	217.0	+1.40
		0.446	205.6	201.2	-2.14	211.9	+3.06
		0.626	189.5	182.9	-3.48	199.4	+5.22
		0.652	185.7	179.4	-3.39	196.6	+5.87
		1.000	87.5	--	--	--	--

Table XII (cont'd.)

System and data source	Temp. (°C)	x_1	$\eta_{exp't.}$ (poise$\times 10^{-6}$)	$\eta_{calc'd.}$ (Eq.50)	Deviation (%)	$\eta_{calc'd.}$ (Wilke)	Deviation (%)
H_2-Ne (51)	20	0	309.2	--	--	--	--
		0.252	278.2	278.0	-0.07	285.1	+2.39
		0.461	242.7	243.3	+0.25	257.5	+6.09
		0.772	168.4	169.1	+0.42	184.6	+9.61
		1.000	87.5	--	--	--	--
He-Ne (51)	20	0	309.2	--	--	--	--
		0.266	297.1	295.3	-0.60	300.3	+1.08
		0.562	270.2	270.1	-0.04	279.4	+3.40
		0.763	242.9	243.9	+0.41	254.8	+4.89
		1.000	197.3	--	--	--	--
H_2-CO_2 (51)	26.9	0	149.3	--	--	--	--
		0.190	150.1	149.8	-0.20	148.9	-0.80
		0.595	147.8	143.6	-2.84	143.3	-3.04
		0.889	123.2	115.4	-6.32	118.5	-3.81
		1.000	87.5	--	--	--	--
H_2-CH_4 (51)	20	0	108.7	--	--	--	--
		0.281	109.9	110.5	+0.55	110.4	+0.45
		0.486	109.8	110.1	+0.27	110.1	+0.27
		0.602	108.6	108.8	+0.18	110.0	+1.29
		1.000	87.6	--	--	--	--
CO_2-N_2 (51)	20	0	178.1	--	--	--	--
		0.229	178.1	179.0	+0.51	178.3	+0.11
		0.657	177.5	179.0	+0.84	178.1	+0.34
		0.837	177.4	178.3	+0.51	177.7	+0.17
		1.000	177.6	--	--	--	--
C_2H_6-C_3H_8 (59)	250	0	136.2	--	--	--	--
		0.4327	142.5	142.9	+0.28	142.6	-0.07
		0.2563	140.1	140.0	-0.07	139.4	-0.50
		0.1526	138.2	138.5	+0.22	138.0	-0.14
		1.000	152.6	--	--	--	--
Average deviation (69 points)					1.33		2.07
Maximum deviation					6.32		10.8

Table XIII

Comparison of experimental and calculated viscosities of multicomponent mixtures

System and data source	x_1	x_2	x_3	Temp. (°C)	$\eta_{exp't.}$ poise$\times 10^{-6}$	$\eta_{calc'd.}$ Eq. 50 poise$\times 10^{-6}$	Deviation (%)	$\eta_{calc'd.}$ Wilke Eq. 23-24 (poise$\times 10^{-6}$)	Deviation (%)
Ne-A-He (56)	0.5576	0.2670	0.1754	20	274.0	273.2	-0.29	270.3	-1.35
	0.2166	0.5851	0.1983	100	288.6	288.8	+0.07	290.0	+0.49
	0.3193	0.3213	0.3594	200	357.4	356.1	-0.36	360.0	+0.72
Ne-H_2-CO_2 (7a)	0.3353	0.3333	0.3333	25	185.7	200.5	+7.96	190.2	+2.42
H_2-N_2-CCl_2F_2 (7a)	0.3333	0.3333	0.3333	25	146.9	150.2	+2.24	145.7	-0.82
N_2-CO_2-CCl_2F_{12} (7a)	0.3333	0.3333	0.3333	25	145.8	150.0	+2.88	144.6	-0.82
CO_2-O_2-N_2 (21a)	0.062	0.107	0.831	20	179.3	176.7	-1.45	176.0	-1.84
Ne-H_2-CO_2-CCl_2F_2(7a)	0.2500	0.2500	0.2500	25	168.1	175.9	+4.64	159.3	-5.24
H_2-CO_2-N_2-CCl_2F_2(7a)	0.2500	0.2500	0.2500	25	147.1	150.8	+2.51	146.7	-0.27
Average deviation (9 points)							2.49		1.55
Maximum deviation							7.96		5.24

data presented in Table XIII include all of the systems shown in Fig. 1 of Ref. 67. In the case of the data of the nine multicomponent mixtures of Table XII, however, Wilke's equation is in somewhat better agreement with experiment than Eq. 50. The average and maximum deviation of the former equation from the data are 1.55 and 5.24% respectively. The corresponding deviations of Eq. 50 are 2.49 and 7.96%. An approximate comparison of Eq. 50 with the correlation of Buddenburg and Wilke was also made on the basis of the 30 data points for the 7 binary systems listed in Table II of Ref. 7. The average deviation of Eq. 50 and of the Buddenburg-Wilke correlation from these data are 1.2% and 2.18% respectively. The corresponding maximum deviations are 3.9% and 6.0%. Because the number of points and systems taken are limited, these comparative percentage deviations should be considered with reservation. However, a further qualitative comparison between these correlations may be made. The data in Table XII represents 12 of the 21 systems listed in Table I of Ref. 7. For the 21 systems the average deviation of the Buddenburg-Wilke relation is 3.02%, and that of Eq. 50 for the 12 systems is 1.33%.

b. Viscosity of polar-nonpolar mixtures. Thirty-four data points from seven selected binary systems were used to test the applicability of Eq. 50 to polar-nonpolar mixtures. As in the case of the conductivity of such mixtures, the modified Arnold's equation was used to compute the diffusivity ratios. The calculated and experimental values are shown in Table XIV. For these data the numerical average, algebraic average, and maximum deviations of Eq. 50 are 1.12%, -0.03%, and 4.26% respectively. These deviations are of the same order as those for nonpolar mixtures. The close agreement between correlation and experiment appears to justify the application of Eq. 50 to polar-nonpolar mixtures as well as of the modified Arnold's equation for calculating the diffusivity ratio.

Wilke's equation was also used to calculate the viscosities for these mixtures.[67] The average deviation from the data in this case is 4.36%, and the calculated value is lower than the experimental value in every case (See Table XIV). It has been shown (Appendix I) that for nonpolar systems the function ϕ_{ij} (Eq. 24) is equivalent to D_{ii}/D_{ij}; hence,

Table XIV

Comparison of experimental and calculated viscosities of polar-nonpolar binary mixtures

System and data source	Temp. (°C)	x_1	$\eta_{exp't.}$ ($poise \times 10^{-6}$)	$\eta_{calc'd.}$ (Eq.50)	Deviation (%)	$\eta_{calc'd.}$ (Wilke Eqs.23,24)	Deviation (%)	$\eta_{calc'd.}$ (modified Wilke Eqs.23,53)	Deviation (%)
H_2-NH_3 (51)	20	0	98.2	--	--	--	--	--	--
		0.2913	104.7	103.6	-1.05	100.6	-3.92	102.8	-1.81
		0.4823	108.0	105.9	-1.94	101.0	-6.49	105.5	-2.31
		0.7761	107.2	103.2	-3.73	100.9	-5.88	105.3	-1.77
		1.000	87.5	--	--	--	--	--	--
N_2-NH_3 (51)	20	0	98.2	--	--	--	--	--	--
		0.1117	109.2	108.5	-0.65	105.6	-3.30	108.2	-0.91
		0.4362	138.3	139.0	+0.50	128.8	-6.86	136.3	-1.44
		0.8889	169.0	171.5	+1.48	166.6	-1.42	170.5	+0.89
		1.000	177.6	--	--	--	--	--	--
CO_2-HCl (51)	18	0	142.6	--	--	--	--	--	--
		0.20	145.3	147.8	+1.72	144.4	-0.62	149.5	+2.88
		0.50	148.0	151.3	+2.23	143.7	-2.90	153.8	+3.92
		0.80	148.1	149.9	+1.22	135.2	-8.71	151.4	+2.23
		1.00	146.4	--	--	--	--	--	--
SO_2-CO_2 (51)	15.8	0	145.8	--	--	--	--	--	--
		0.20	142.8	148.4	+3.92	142.2	-0.42	150.0	+5.04
		0.50	136.7	141.7	+4.26	136.4	-0.22	149.0	+9.72
		0.80	129.9	132.5	+2.00	129.4	-0.38	137.8	+6.08
		1.00	124.3	--	--	--	--	--	--
NH_3-CH_4 (51)	14.5	0	107.7	--	--	--	--	--	--
		0.20	109.1	108.6	-0.46	105.3	-3.48	109.2	+0.09
		0.50	107.7	106.7	-0.93	101.8	-5.48	108.4	+0.65
		0.80	102.5	101.5	-0.98	98.6	-3.80	102.6	+0.10
		1.00	96.6	--	--	--	--	--	--
Air-HCl (51)	16.5	0	140.7	--	--	--	--	--	--
		0.10	147.0	146.5	-0.34	143.7	-2.44	146.2	-0.68
		0.30	157.0	157.0	0	152.2	-3.06	156.7	-0.19

Table XIV (cont'd.)

System and data source	Temp. (°C)	x_1	$\eta_{exp't.}$ (poise x 10^6)	$\eta_{calc'd.}$ (Eq. 50)	Deviation (%)	$\eta_{calc'd.}$ (Wilke Eqs. 23,24)	Deviation (%)	$\eta_{calc'd.}$ (modified Wilke Eqs. 23,53)	Deviation (%)
		0.50	165.6	165.8	+0.12	157.3	-5.01	165.8	+0.12
		0.70	173.0	173.0	0	165.5	-4.33	173.1	+0.06
		0.90	177.0	178.0	+0.56	174.5	-1.41	178.3	+0.73
		1.00	179.4	--	--	--	--	--	--
Air-H_2S (51)	17.2	0	124.3	--	--	--	--	--	--
		0.10	131.	131.4	+0.31	127.2	-2.90	130.8	-0.15
		0.30	145	145.1	+0.07	137.2	-5.38	143.5	-1.03
		0.50	158.2	157.1	-0.70	147.1	-7.02	155.3	-1.83
		0.70	169	168.1	-0.53	158.7	-6.10	166.5	-1.48
		0.90	177	177.0	0	172.4	-2.60	176.2	-0.45
		1.00	180.2	--	--	--	--	--	--
Air-NH_3 (51)	15.5	0	97.5	--	--	--	--	--	--
		0.10	109	108.1	-0.83	105.0	-2.67	108.8	-0.18
		0.20	118.8	118.2	-0.50	113.7	-4.29	119.5	+0.59
		0.30	129	127.6	-1.08	121.9	-5.51	129.3	+0.23
		0.40	138	136.6	-1.01	130.1	-5.72	138.5	+0.36
		0.50	147.3	145.2	-1.43	138.2	-6.18	147.0	-0.20
		0.60	156	153.1	-1.86	146.4	-6.16	154.7	-0.83
		0.70	160	160.4	+0.25	154.4	-3.50	161.8	+1.12
		0.80	169.1	167.2	-1.12	162.6	-3.85	168.0	-0.65
		0.90	174	173.3	-0.40	170.5	-2.01	173.7	+0.17
		1.00	178.7	--	--	--	--	--	--
Average deviation (34 points)					1.12		4.36		1.50
Maximum deviation					4.26		8.72		9.72

it appears reasonable to assume that the agreement between Wilke's equation and the experimental data might also be improved by modifying ϕ_{ij} as defined by Eq. 24 in the same way as Arnold's equation was modified. With this assumption, ϕ_{ij} should be multiplied by a correction factor as follows:

$$\phi'_{ij} = \phi_{ij} \frac{T + 0.733\ F\ S_{12}}{T + F\ S_{12}} \qquad (53)$$

The significant improvement of this procedure over Wilke's original equation is shown by the calculated values given in Table XII. The average deviation is reduced from 4.36% to 1.50%. Empirical justification for introducing the numerical factor, 0.733, in the calculation of D_{ii}/D_{ij} of polar-nonpolar mixtures is thereby again established.

CONCLUSIONS

From the kinetic theory and a number of empirical assumptions, equations have been developed to relate the thermal conductivity and the viscosity to the diffusion coefficient in gas mixtures. These equations have been found to be in qualitative agreement with the experimental facts. The relation between conductivity and diffusion coefficient, Eq. 32, and that between viscosity and diffusion coefficient, Eq. 37, are identical in form. With slight empirical modifications they have been made to conform with experimental data as shown in Chapter V, although the formal identity of the equations are no longer preserved.

The proposed correlations for thermal conductivity, Eq. 49, and viscosity, Eq. 50, appear to be in better agreement, in general, with experimental data than correlations found in the literature. According to the proposed relations the ratio λ_c/λ_ℓ for very simple molecules and the ratio η_m/η_ℓ for most molecules should be approximately constant within rather wide temperature limits. It has been shown that experimental data support this prediction. In the case of the thermal conductivity of mixtures of polyatomic molecules, it has been pointed out that λ_c/λ_ℓ should be more dependent upon temperature and that the positive deviation of the thermal conductivity from the simple mixing rule in such cases may be due primarily to high vibrational and internal rotational heat capacities, which increase their diffusional contribution to heat conduction. Equations 49 and 50 are applicable to both nonpolar and polar-nonpolar mixtures. In the former case calculation of the diffusivity ratio according to the method of Hirschfelder et al. appears to be satisfactory in spite of the fact that the diffusivities calculated this way deviate, on the average, 6% from the experimental values.[27] For polar-nonpolar mixtures, the suitability of the modified Arnold's equation, Eq. 51, for calculating these ratios has been demonstrated.[4]

It should be noted that the proposed correlations have been tested against data of mixtures of rather simple molecules. Very long or complex molecules that may intercoil or stick during collision have not been considered. Also, systems involving chemical reactions have been excluded.

Furthermore, all the data for comparison were taken at pressures less than those having an effect upon conductivity or viscosity.

SYMBOLS

English Symbols

a	accommodation coefficient, dimensionless
A	area for heat transfer
A_{12}, A_{21}	constants in Eq. 10
c	heat capacity (cal/gm-^{o}C)
c_i	internal heat capacity
c_{ir}	internal rotational heat capacity
c_r	rotational heat capacity
c_{vt}	translational heat capacity at constant volume
c_v	vibrational heat capacity at constant volume
C	proportionality constant
C'	cell constant (watt-sec-cm/cal)
C_p	heat capacity at constant pressure
C_v	heat capacity at constant volume
D	diffusion coefficient (cm^2/sec)
D_{12}=D_{ij}	binary diffusion coefficients
D_{lm}	diffusion coefficient given by Eq. 29
e	base of natural logarithms
E=emf	electromotive force
f	constant in Eq. 9, dimensionless
F	function defined by Eqs. 10-III and 10a-III
g	gravitational constant
g'	temperature-jump distance (cm)
h	heat transfer coefficient (BTU/hr-ft^2)
h_c	heat transfer coefficient by conduction
h_r	heat transfer coefficient by radiation
k	thermal conductivity (BTU/hr-ft-^{o}F)
l	distance of thermocouple junction from bottom of guard (in. or ft)
l'	characteristic length in Grashof Number
L	length of thermal conductivity cell
L'	length of connecting tube in "two bulb" thermal-diffusion apparatus (cm)
ln	natural logarithm

m	mass of molecule
M	molecular weight
n	number density of molecules
N'	number of molecules in the hot bulb of a "two-bulb" thermal-diffusion apparatus
N''	number of molecules in the cold bulb of a "two-bulb" thermal-diffusion apparatus
p	pressure, (atmospheres or mm of Hg)
q	heat flow (cal/sec, watt, or BTU/hr)
r_1	radius of emitter (in. or cm)
r_2	inner radius of receiver (in. or cm)
R	universal gas constant
R_i through R_8, and R'	radii in thermocouple assembly, (in. or ft) (see Fig. 3-III in Appendix III)
S_1	Sutherland's constant for component 1 ($^\circ$K)
S_{12}	$\sqrt{S_1 S_2}$
T	temperature ($^\circ$C, $^\circ$F, $^\circ$K)
T_{bi}	normal boiling temperature of component "i" ($^\circ$K)
T_e	temperature of emitter ($^\circ$C or $^\circ$K)
T_r	temperature of receiver ($^\circ$C or $^\circ$K)
T_w	temperature at any point along the thermocouple well ($^\circ$C)
T'	temperature of hot bulb of "two-bulb" thermal-diffusion apparatus ($^\circ$K)
T''	temperature of cold bulb of "two-bulb" thermal-diffusion apparatus ($^\circ$K)
ΔT	temperature difference ($^\circ$C)
v	root mean square velocity of molecules
V''	volume of cold bulb in "two-bulb" thermal diffusion apparatus (cm^3)
V'	volume of hot bulb in "two-bulb" thermal-diffusion apparatus (cm^3)
V_i	molecular volume of the ith component in the liquid state at the boiling point
x	clearance at bottom of cell (in. or cm)
x'	mole fraction of a gas in the hot bulb in "two-bulb" thermal diffusion apparatus.

x'' mole fraction of a gas in the cold bulb in "two-bulb" thermal-diffusion apparatus

x_1 mole fraction of component 1

x_f steady-state mole fraction in cell

x_o initial mole fraction in cell

Z distance from bottom of guard (in. or ft)

Greek Symbols

α thermal-diffusion factor (dimensionless)

α' value of empirical function given by Brokaw,[5] (See Eq. 16)

β coefficient of cubic expansion ($^{\circ}C^{-1}$)

γ heat-capacity ratio, C_p/C_v (dimensionless)

ϵ intermolecular potential energy

η viscosity, poise

η_1 viscosity of gas 1

η_ℓ viscosity of a mixture calculated by the simple mixing rule; i.e., $\eta_\ell = x_1 \eta_1 + x_2 \eta_2$

η_m viscosity of a mixture

θ $T_w - T_r$ ($^{\circ}C$)

Λ mean free path of molecules (cm)

λ thermal conductivity (cal/cm sec $^{\circ}C$)

λ_1 thermal conductivity of gas 1

λ_a apparent measured thermal conductivity

λ_c conductivity of a gas mixture from conduction only

$\lambda_\ell = \lambda_{sm}$ conductivity of a mixture calculated by the simple mixing rule; i.e., $\lambda_\ell = x_1 \lambda_1 + x_2 \lambda_2$

λ_m apparent measured conductivity of a mixture

λ_{mon} conductivity of a polyatomic gas calculated by assuming it to be monatomic

λ_{rm} conductivity of a mixture calculated by the reciprocal mixing rule; i.e., $1/\lambda_{rm} = (x_1/\lambda_1) + (x_2/\lambda_2)$

λ_{td} conductivity of a mixture from diffusion

λ_{ci} collisional conductivity of the ith component (Eq. 35)

λ_{di} diffusional conductivity of the ith component (Eq. 36)

μ	dipole moment (Debye)
ν	kinematic viscosity (cm^2/sec)
π	numerical factor = 3.1416
ρ	density of a gas (gm/cm^3)
ρ_{lm}	density of gas 1 in a mixture
σ	molecular diameter (angstroms)
σ'	cross section area of connecting tube in "two-bulb" thermal-diffusion apparatus (cm^2)
τ	relaxation time (sec)
ϕ	difference between the temperature of any point along the thermocouple wire in the receiver and the actual temperature of the receiver
Ω	collision integrals (dimensionless)

APPENDIX I. The Equivalence of D_{11}/D_{12} and ϕ_{12}

The expression for the binary diffusion coefficient in terms of the coefficient of self-diffusion in the case of hard spherical molecules is approximately:[67]

$$D_{12} = \frac{\frac{4}{\sqrt{2}}\left(\frac{m_1 + m_2}{m_1 m_2}\right)^{1/2}}{\left[\left(\frac{1}{D_{11}^2 m_1}\right)^{1/4} + \left(\frac{1}{D_{22}^2 m_2}\right)^{1/4}\right]^2} \quad ; \qquad (1\text{-I})$$

therefore we have

$$\frac{D_{11}}{D_{12}} = \frac{\left[\left(\frac{1}{m_1}\right)^{1/4} + \left(\frac{D_{11}}{D_{22}}\right)^{1/2}\left(\frac{1}{m_2}\right)^{1/4}\right]^2}{\frac{4}{\sqrt{2}}\left(\frac{m_1 + m_2}{m_1 m_2}\right)^{1/2}} . \qquad (2\text{-I})$$

Following Wilke,[67] we assume

$$\frac{D_{11}\,\rho_1}{\eta_1} = \frac{D_{22}\,\rho_2}{\eta_2} \qquad (3\text{-I})$$

or

$$\frac{D_{11}}{D_{22}} = \frac{\rho_2\ \eta_1}{\rho_1\ \eta_2} \quad ; \qquad (4\text{-I})$$

hence, we have

$$\frac{D_{11}}{D_{12}} = \frac{\left[\left(\frac{1}{m_1}\right)^{1/4} + \left(\frac{\rho_2 \eta_1}{\rho_1 \eta_2}\right)^{1/2} \left(\frac{1}{m_2}\right)^{1/4}\right]^2}{\frac{4}{\sqrt{2}}\left(\frac{m_1 + m_2}{m_1 m_2}\right)^{1/2}}$$

$$= \frac{\left[\left(\frac{1}{M_1}\right)^{1/4} + \left(\frac{M_2 \eta_1}{M_1 \eta_2}\right)^{1/2} \left(\frac{1}{M_2}\right)^{1/4}\right]^2}{\frac{4}{\sqrt{2}}\left(\frac{1}{M_1} + \frac{1}{M_2}\right)^{1/2}}$$

$$= \frac{\left[1 + \left(\frac{\eta_1}{\eta_2}\right)^{1/2} \left(\frac{M_2}{M_1}\right)^{1/4}\right]^2}{\frac{4}{\sqrt{2}}\left[1 + \frac{M_1}{M_2}\right]^{1/2}} \equiv \phi_{12} \qquad (5\text{-I})$$

Here m is the mass of a single molecule, and M is the molecular weight. The correlation between ϕ_{12} and D_{11}/D_{12} calculated on the basis of the first approximation by the Lennard-Jones 6–12 model is shown in Fig. 1-I. The points fall fairly close to the 45° line. In view of the fact that molecules are not really hard spheres and hence the group $\rho D/\eta$ is not constant, the correlation is about as good as can be expected.

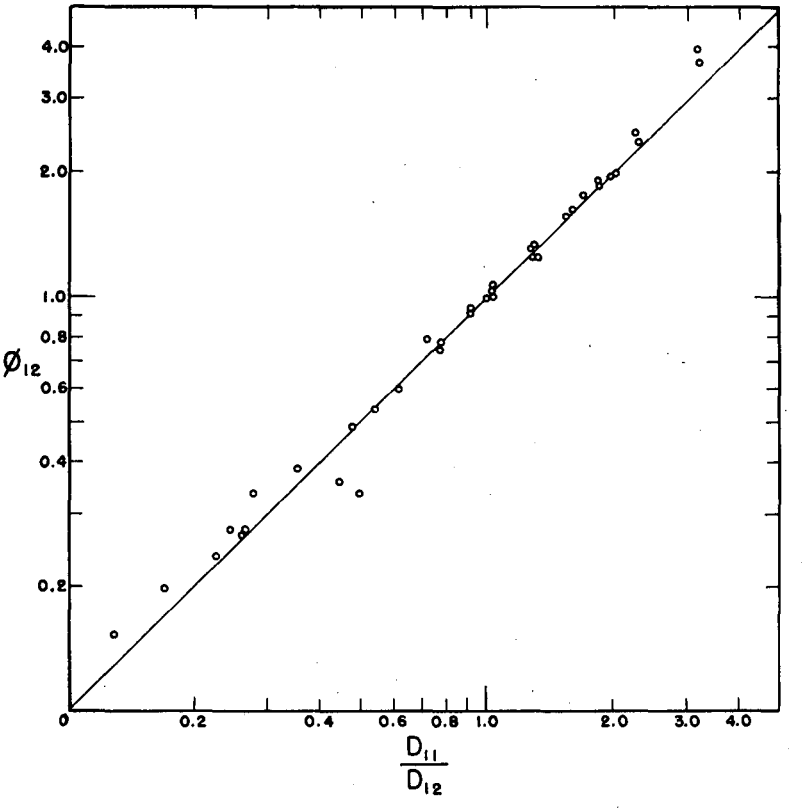

MU-15180

Fig. 1-I. Correlation between ϕ_{12} and D_{11}/D_{12}.

APPENDIX II.

A Method for Estimation of the Self-Diffusion Coefficient

It appeared that Eq. 5-I in Appendix I might be used to estimate self-diffusion coefficients from experimental values of binary coefficients. Accordingly, calculations were carried out for five different gases with 15 different binary diffusion coefficients. The experimental values of the self-diffusion coefficient and the calculated values are given in Table 1-II for comparison. Very good agreement between Eq. 5-I and the experimental data is found for several cases, but for a few other cases, the calculated values are 10% to 30% higher than the data. For the 15 points compared, the average deviation is about 10%. Equation 5-I may be said to be only qualitatively consistent with experiment. When one considers the drastic assumptions made in deriving Eq. 5-I and the difficulty of predicting diffusion coefficients in general, an average of 10% discrepancy is not too surprising.

Also shown in Table 1-II are values computed by the method of Wilke and Lee,[69] and by the method of Hirschfelder et al.[28] The average deviations of these methods are 6.1% and 4.1% respectively. Furthermore, the maximum deviations are in the neighborhood of 10% to 15%. In spite of the limited number of points tested, it appears safe to state that, in general, values obtained by these methods are in better agreement with experimental data than those from Eq. 5-I.

Table 1-II

Experimental and calculated self-diffusion coefficient

Gas	D_{11} exp't. and source[a]	Expt'l. D_{12} used in Eq.5-I[a]	Calc'd. D_{11}, Eq.5-I	Deviation (%)	Calc'd. D_{11} Wilke and Lee[b]	Deviation (%)	Calc'd. D_{11} HBS 28b[b]	Deviation (%)
H_2	1.285 (21)	H_2-A	1.39	+8.2	1.119	-12.9	1.262	-1.8
		H_2-CO_2	1.302	+1.3				
		H_2-C_3H_8	1.572	+22.4				
		H_2-O_2	1.27	-1.2				
		H_2CO	1.195	-7.0				
		H_2-He	1.468	+14.2				
		H_2-C_2H_4	1.273	-0.9				
		H_2-C_2H_4	1.26	-1.9				
A	0.156 (70)	H_2-A	0.1775	+13.8	0.1675	+7.3	0.1534	-1.7
		He-A	0.174	+11.5				
		Ne-A	0.1695	+8.6				
CH_4	0.206 (70)	H_2-CH_4	0.211	+2.4	0.198	-3.9	0.187	-9.2
CO_2	0.0970 (1)	N_2-CO_2	0.112	+15.4	0.1013	+3.3	0.0915	-5.7
		CO_2-H_2	0.1087	+12.0				
Ne	0.452 (70)	He-Ne	0.576	+27.4	0.468	+3.4	0.438	-3.1
		A-Ne	0.531	+17.5				

[a] All data taken or reduced to 0°C.

[b] First approximation values.

APPENDIX III.

Variation of Thermocouple Junction Temperature with Depth of Immersion

Experiments showed that heat conduction along the thermocouple well and wires would cause the thermocouple junction temperature at certain distances below the guard to be different from the actual temperature in the receiver, when the guard was kept at a temperature equal to that of the emitter. This difference between actual and measured temperatures may be estimated on the basis of constant temperatures in the guard and in the receiver from the geometry and thermal properties of the thermocouple assembly.

For mathematical convenience, certain assumptions are made. First, the 0.5-in. space between the guard and the cell is ignored, i.e., the thermocouple assembly is assumed to pass through the constant-temperature region in the guard immediately into another isothermal zone in the receiver. Because the lateral heat transfer from the part of the well within this space is relatively small, the effect of this assumption is a minor error in the axial coordinate. Second, the well is treated as a semi-infinite hollow cylinder, the inside of which is insulated, since, as will be demonstrated subsequently, the axial conduction by the contents within the well is small in comparison to that along the well. Third, for the same reason as in the case of the well, the thermocouple wires are considered as finite cylinders extending from the isothermal zone in the guard into the zone within the well where temperature is a function of distance. Equations expressing temperature as a function of distance from the guard are derived below to describe the assumed conditions, which, incidentally, appear not to have been treated in the literature. These equations are then compared with the experiments referred to in Section B, Chapter IV.

A. Derivations of Temperature-vs-Distance Equations

1. Temperature along the well

Consider the heat balance around a differential length of the well (Fig. 1-III):

$$q_1 + q_4 = q_2 + q_3 \qquad (1\text{-III})$$

and

$$k\,\pi\,(R_7^2 - R_6^2)\,\left(\frac{\Delta T}{\Delta Z}\right)_I + h_6\,2\,\pi\,R_6\,\Delta Z =$$

$$k\,\pi\,(R_7^2 - R_6^2)\,\left(\frac{\Delta T}{\Delta Z}\right)_{II} + h_7\,\pi\,R_7\,\Delta Z\ . \qquad (2\text{-III})$$

As pointed out above, the inner wall of the well may be considered insulated; hence the q_4 term is discarded. The heat balance then yields Eq. 3-III,

$$\frac{d^2 T_w}{d Z^2} = \frac{h_7\,2\,R_7}{k\,(R_7^2 - R_6^2)}\,(T_w - T_r) = 0\ , \qquad (3\text{-III})$$

where T_w is the temperature at any point and Z is measured from the bottom of the guard. If we let

$$\frac{h_7\ 2\ R_7}{k\ (R_7 - R_6)} = b^2$$

and $$\theta = T_w - T_r,$$

then we have $$\frac{d^2\theta}{d Z^2} - b^2\,\theta = 0. \qquad (4\text{-III})$$

This equation is to be solved to satisfy the following boundary conditions:

(a) at $Z = 0$ $\quad \theta = T_w - T_r = T_e - T_r$

(b) at $Z = \infty$ $\quad \theta = T_w - T_r = 0$.

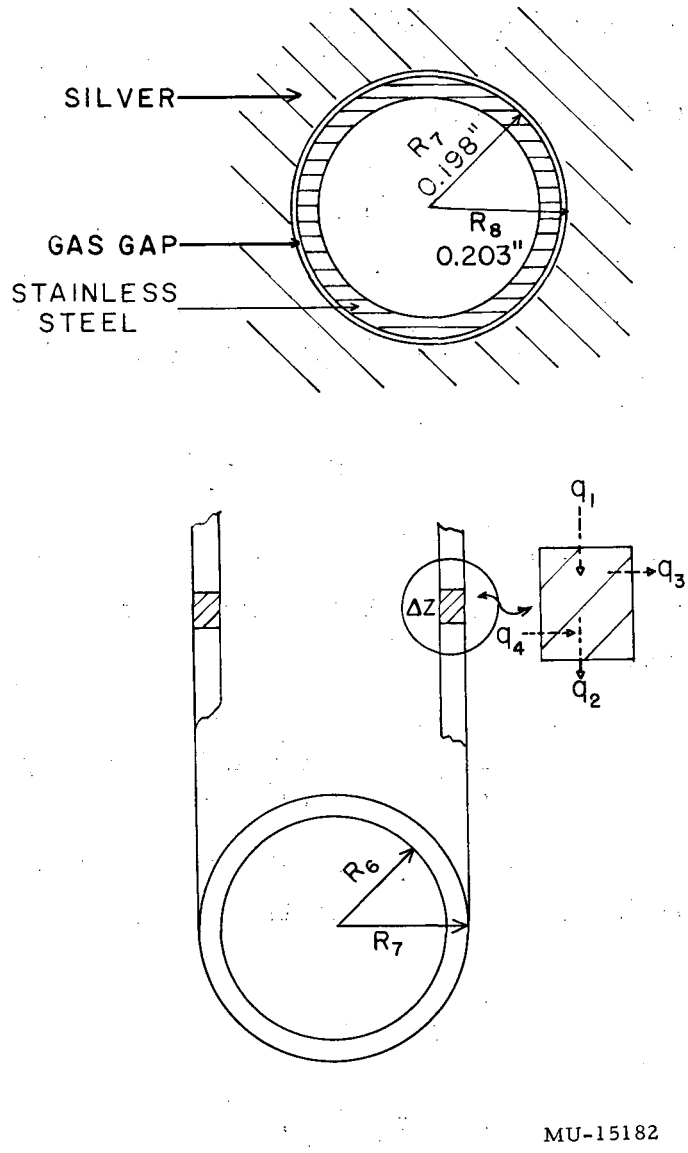

Fig. 1-III. Elementary heat balance along thermocouple well.

Fig. 2-III. Dimensions determining heat transfer from thermocouple well.

The solution is

$$\theta = T_w - T_r = (T_e - T_r)\ (\cosh b Z - \sinh b Z). \qquad (5\text{-III})$$

Equation 5-III represents the temperature distribution along the well.

2. Temperature of the Thermocouple Junction.

For the temperature distribution along the thermocouple wires, an analogous development shows that the differential equation to be solved is

$$\frac{d^2 T}{d Z^2} = \frac{2 h_1}{k R_1} (T - T_w) = a^2 (T - T_w) , \qquad (6\text{-III})$$

where $$a^2 = \frac{2 h_1}{k R_1} .$$

Substituting T_w from Eq. 5-III above, we obtain

$$\frac{d^2 T}{d Z^2} = a^2 [\ T - T_r - (T_e - T_r)(\cosh b Z - \sinh b Z)]. \qquad (7\text{-III})$$

If we let $T - T_r = \phi$

and $T_e - T_r = c$,

then we have $$\frac{d^2 \phi}{d Z^2} - a^2 \phi = - a^2 c\ (\cosh b Z - \sinh b Z). \qquad 8\text{-III})$$

A solution of 8-III is to be obtained to satisfy the following boundary conditions:

(a) at $Z = 0$, $\phi = T - T_r = T_e - T_r = c$

(b) at $Z = 1$, $\phi' = 0$.

The second condition corresponds to the assumption that no heat is transferred in the axial direction at the tip of the thermocouple. The solution of Eq. 8-III is, accordingly,

$$\phi = \alpha \cosh a Z + \beta \sinh a Z + \gamma (\sinh b Z - \cosh b Z), \tag{9-III}$$

where

$$\alpha = \frac{b^2 c}{b^2 - a^2},$$

$$\beta = \frac{a b c (\sinh bl - \cosh bl) - b^2 c \sin al}{(b^2 - a^2) \cosh al},$$

$$\gamma = \frac{a^2 c}{b^2 - a^2}.$$

Equation 9-III gives the temperature at any point of the thermocouple wires as a function of the distance of the point from the guard and the distance of the junction from the guard, l. Writing 9-III for the junction temperature of the thermocouple, one obtains, after simplification,

$$\phi_l = c\left[\left(1 + \frac{a^2}{b^2 - a^2}\right)(\cosh al - \tanh al \sinh al) - \frac{a^2}{b^2 - a^2} e^{-bl}\left(1 + \frac{b}{a} \tanh al\right)\right] \tag{10-III}$$

$$= c F. \tag{10a-III}$$

3. The Ratio $\Delta T_l / \Delta T_\infty$.

In order to find the ratio of the measured ΔT at any length, l, to the true ΔT, i.e., the ΔT as $l \to \infty$, the following transformation is made. By definition we have

$$\phi_l = T_l - T_r = T_l - T_e + T_e - T_r = -\Delta T_l + \Delta T_\infty,$$

and also

$$c = T_e - T_r = \Delta T_\infty.$$

Substituting into 10a-III and rearranging, we obtain

$$\frac{\Delta T_1}{\Delta T_\infty} = 1 - F. \qquad (11\text{-III})$$

B. Evaluation of the Constants a and b

The values of a and b required to calculate F are determined by the dimensions, axial conduction, and lateral resistance to heat transfer. The constant b is related to heat transfer down the well to the receiver by

$$b = \frac{2 h_7 R_7}{k (R_7^2 - R_6^2)} , \qquad (12\text{-III})$$

where k is the thermal conductivity of the well, R_7 is the outer radius of the well, R_6 is the inner radius of the well, and h is the heat transfer coefficient from the well to the receiver. The heat-transfer coefficient is the sum of 3 terms, corresponding to the three modes of heat transfer — radiation, conduction, and convection. Because the gap, $R_8 - R_7$, is small, convection is negligible. The Grashof number, $(g\beta/\nu 2)(1')^3 \Delta T$, based on the well diameter and ΔT of $10^\circ C$ is approximately 100. Hence, we have

$$h = h_c + h_r$$

$$= \frac{\lambda}{R_7 \ln R_7/R_8} + h_r ,$$

where the first term is the transfer coefficient for conduction across the fluid between the well and the receiver. The pertinent dimensions required for computing h are shown in Fig. 2-III.

The radiant heat transfer coefficient, h_r, is estimated from the surface temperature and emissivity of the stainless steel thermocouple well. For $100^\circ C$ and an emissivity of 1.0, h_r is 2 BTU/hr ft^2 according

to McAdams.[42] As a conservative estimate, the emissivity is taken to be 0.5, and so h_r is 1. Because for the cases under consideration, $h_c >>> h_r$ except when the cell is under vacuum, error in the estimate of h_r should not seriously affect the accuracy of the calculations to be performed.

The constant a is related to the parameters determining heat flux in the thermocouple wires by

$$a = \frac{2\,h_1}{k\,R_1} \quad . \tag{14-III}$$

The rate of lateral heat transfer from the thermocouple wires is controlled by the series of resistances consisting of fluid gaps and porcelain insulators. As in the case of heat transfer from the well to the silver, the Grashof numbers are small, and transfer across the fluid gaps takes place by radiation and conduction. In the calculation of h, the effect of axial conduction along the porcelain and fluid gaps may be neglected in comparison to that of the wires, i.e., it may be assumed that only lateral heat flux exists within these parts. As an example, the lateral conductive heat transfer coefficient based on the surface of the thermocouple wires for case III is given by

$$\frac{1}{h_{c1}} = 2\,R_1 \left[\frac{\ln \frac{R_2}{R_3}}{2\,k_f} + \frac{\ln \frac{R_3'}{R_2}}{2\,k_p} + \frac{\ln \frac{R_6}{R_3}}{k_f} \right] . \tag{15-III}$$

The conductivities and dimension of the thermocouple components for this case are shown in Fig. 3-III in which R_3' is a mean radius taken as $\sqrt{R_3^2 - R_2^2}$.

C. Comparison of Calculation and Experiment

Calculations have been made to predict the ratio $\Delta T_1 / \Delta T_\infty$ for the four cases investigated experimentally. The descriptions of the four cases are shown in Figs. 3-III and 4-III. Comparison of the thermal conductivities and dimensions of the component parts of the thermocouple

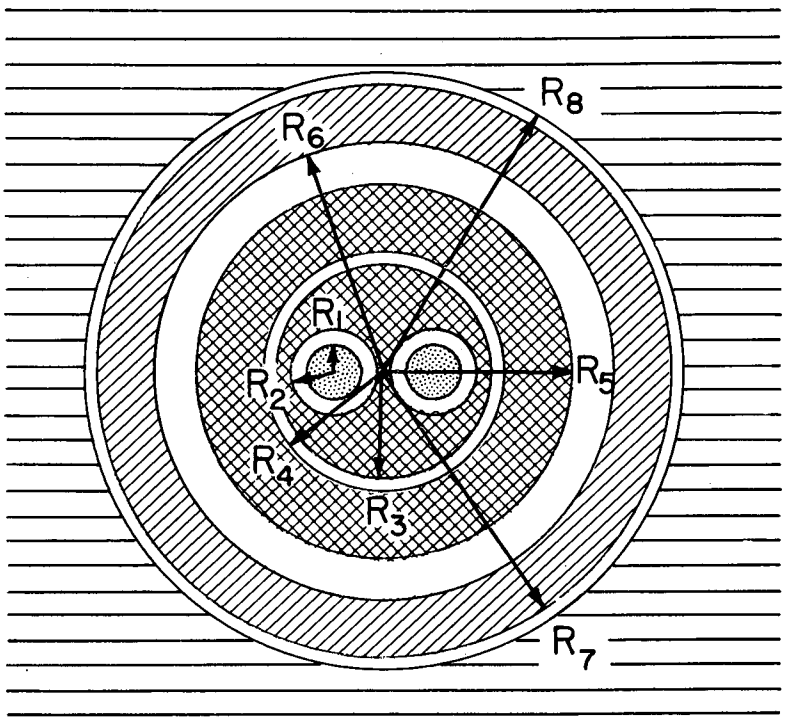

MU-15166

Fig. 3-III. Thermocouple assembly for cases I and III

	k (BTU/hr ft^2 $^\circ$F/ft)
silver	240
thermocouple wire	40
stainless steel	20
ceramic	0.15
Interspace for case I = air	0.018

Interspace for case III = air except vacuum between silver and steel.

Radii are R_1 = 0.010 in., R_2 = 0.014 in., R_3 = 0.035 in., R_4 = 0.039 in., R_5 = 0.062 in., R_6 = 0.076 in., R_7 = 0.099 in., and R_8 = 0.101 in.

$a = 35.2\ ft^{-1}$, $b = 33.5\ ft^{-1}$	case I
$a = 35.2\ ft^{-1}$, $b = 6.11\ ft^{-1}$	case III

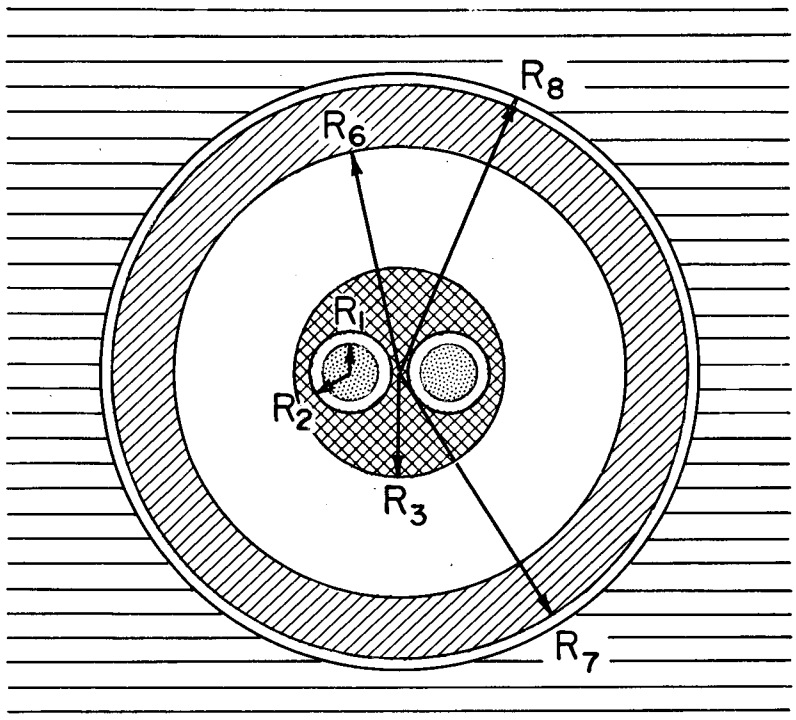

MU-15167

Fig. 4-III. Thermocouple assembly for cases II and IV

k (BTU/hr ft^2 $^\circ$F/ft)

silver.....240

thermocouple wire.....40

stainless steel.....20

ceramic.....0.15

Blank space inside steel well = dimethylformamide.....1.0

Space between silver and steel in case II = air.....0.018

Space between silver and steel in case IV = 40% He - 60% N_2....0.036

Radii are R_1 = 0.010 in., R_2 = 0.014 in., R_3 = 0.035 in.,

R_6 = 0.076 in., R_7 = 0.099 in., and R_8 = 0.101 in.

a = 61 ft^{-1}, b = 33.5 ft^{-1} } case II

a = 61 ft^{-1}, b = 53 ft^{-1} } case IV

assemblys shows that in all cases heat conduction between the guard and receiver takes place primarily by way of the well and wires. Furthermore, conduction by the wire is small in comparison to that by the well. Advantage was taken of these facts in making simplifying assumptions in the derivation of the temperature-vs-distance equations above. The a and b values are also given in these figures. Computed values of $\Delta T_1/\Delta T_\infty$ as a function of distance from the guard are presented in Table I-III. Comparison of these calculations with experiment is shown in Fig. 5-III. Excellent agreement is found in all cases except I for the evacuated cell. As pointed out in Chapter IV, the results derived here may be taken as sufficient proof that the cell temperature is uniform along its axis.

Table 1-III

Computed values of $\Delta T_1/\Delta T_\infty$							
Case I		Case II		Case III		Case IV	
l(in.)	$\Delta T_1/\Delta T_\infty$	l(in.)	$\Delta T_1/\Delta T_\infty$	l(in.)	$\Delta T_1/\Delta T_\infty$	l(in.)	$\Delta T_1/\Delta T_\infty$
0.25	0.104	0.25	0.171	0.50	0.086	0.25	0.427
0.5	0.323	0.50	0.518	1.00	0.274	0.50	0.688
0.75	0.566	0.75	0.732	1.50	0.435	0.75	0.793
1.00	0.83	1.00	0.862	2.00	0.562	1.00	0.907
1.50	0.924	1.50	0.966	3.00	0.737	1.50	0.9904
2.00	0.947	2.00	0.992	4.00	0.842	2.00	0.9989
--	--	3.00	0.995	6.00	0.943	--	--

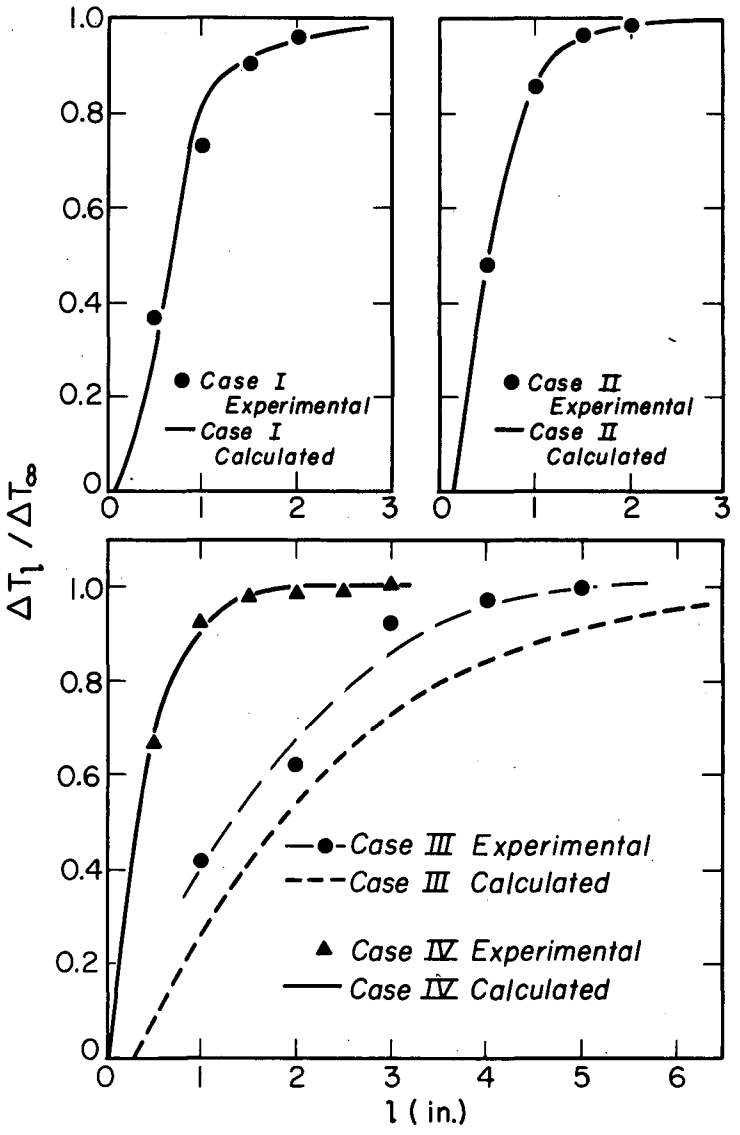

Fig. 5-III. Temperature gradient in thermocouple assembly.

APPENDIX IV

Thermal Diffusion Between Cell and Connecting Pipes

A. Separation

According to the rigorous kinetic theory, a temperature gradient within a gas is accompanied by a corresponding concentration gradient. The relation between the steady-state concentrations in the hot and cold portions of a binary mixture and the temperature difference may be written approximately as[18]

$$x'' - x' = \alpha x_1 x_2 \ln \frac{T'}{T''} , \qquad (1\text{-IV})$$

where α is known as the thermal diffusion factor. This factor depends in a complex way upon intermolecular forces, the ratios of the molecular masses and of the diameters, and relatively insensitively on composition. For the present purpose, it is assumed constant for a given mixture.

That part of the equipment used in this work in which separation by thermal diffusion can occur is shown schematically in Fig. 1-IV. The cell and connecting pipe shown correspond approximately to the two-bulb apparatus usually employed for the determination of thermal-diffusion factors. That part of the cell and of the pipe up to the end of the horizontal section on the top of the copper block may be visualized as the "hot-bulb", and that portion of the pipe at room temperature as the "cold-bulb. The change in composition at steady state is dependent upon temperature difference as well as upon the relative volume of the hot and cold volumes. If the volume of the connecting pipe is small, then the change in composition of the hot volume is[19]

$$x_o - x_f = \frac{x'' - x'}{1 + \frac{V' T''}{V'' T'}} . \qquad (2\text{-IV})$$

Although the hot volume, connecting pipe, and cold volume as given in Fig. 1-IV are 814 cm^3, 147 cm^3 and 313 cm^3, it is assumed that as a first approximation no correction need be made for the volume of the connecting pipe.

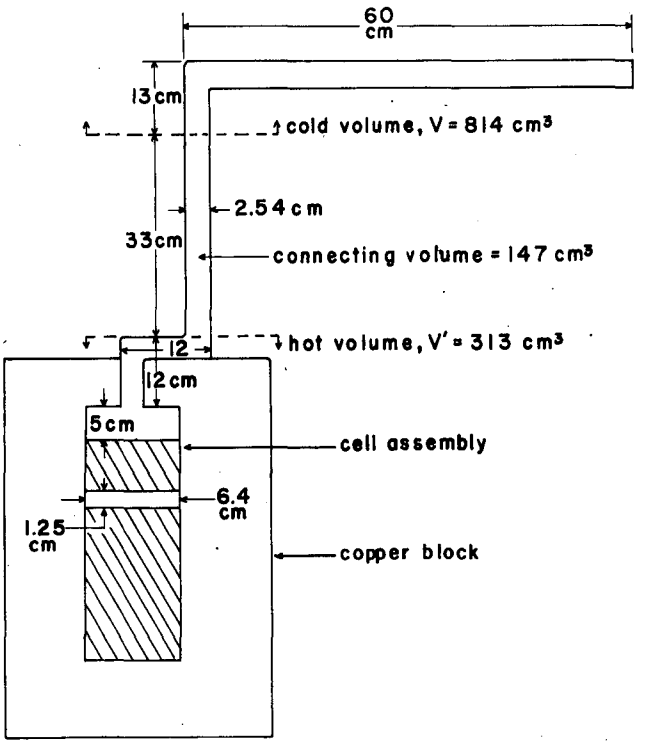

Fig. 1-IV. Conductivity cell as thermal-diffusion apparatus.

By combining Eqs. 1-IV and 2-IV, the expression for computing change of composition in the cell is obtained:

$$x_o - x_f = \frac{\alpha x_1 x_2 \ln \frac{T'}{T''}}{1 + \frac{V' T''}{V'' T'}} \quad . \qquad (3\text{-IV})$$

As an example, for a 1 : 1 He—A mixture at a cell temperature of 320°C, the difference between the steady-state He concentration and initial He concentration is

$$x_o - x_1 \cong \frac{0.40\ (0.5)\ (0.5)\ \ln \frac{593}{293}}{1 + \frac{313\ (293)}{814\ (593)}} = 0.058 \ .$$

This is the maximum separation that may occur in the mixtures investigated experimentally in this work.

B. Relaxation Time

The time required to approach steady state in the usual two-bulb thermal diffusion apparatus has been discussed by Clark Jones and Furry.[11] Their expression for the relaxation time is

$$\tau = \frac{N'' N' T'' L' \ln (T'/T'')}{(N'' + N') n D_{12} \sigma' \Delta T} \quad . \qquad (4\text{-IV})$$

This equation was derived on the assumption that the connecting pipe volume is small. As a first approximation, however, Eq. 4-IV is assumed to be applicable to the system as shown in Fig. 1-IV, and the relaxation time cited in Chapter IV for the various mixtures were so calculated.

APPENDIX V.

Temperature Dependence of λ_c/λ_ℓ and η_m/η_ℓ

From Eq. 34, the conductivity of a binary mixture is

$$\lambda_c = \frac{x_1 \lambda_1}{x_1 + A_{12} x_2} + \frac{x_2 \lambda_2}{x_2 + A_{21} x_1} . \qquad (1\text{-V})$$

The simple-mixing-rule value is

$$\lambda_\ell = x_1 \lambda_1 + x_2 \lambda_2 . \qquad (2\text{-V})$$

Dividing Eq. 1-V by 2-V, we obtain

$$\frac{\lambda_c}{\lambda_\ell} = \frac{\dfrac{x_1 \lambda_1}{x_1 + A_{12} x_2} + \dfrac{x_2 \lambda_2}{x_2 + A_{21} x_1}}{x_1 \lambda_1 + x_2 \lambda_2} \qquad (3\text{-V})$$

If $\lambda_1 = a\, T^{n'}$ and $\lambda_2 = b\, T^{n''}$, then we have

$$\frac{\lambda_c}{\lambda_\ell} = \frac{\dfrac{a\, x_1}{x_1 + A_{12} x_2} + \dfrac{b\, x_2\, T^{n''-n'}}{x_2 + A_{21} x_1}}{a\, x_1 + b\, x_2\, T^{n''-n'}} \qquad (4\text{-V})$$

Now, if n' is equal to n'' and A_{12} and A_{21} are independent of temperature, then λ_c/λ_ℓ is a constant for any given composition.

The expression for η_m/η_ℓ is identical with Eq. 4-V, except for the values of the constants.

ACKNOWLEDGMENT

The author is indebted to Professor LeRoy A. Bromley and to Professor Charles R. Wilke for encouragement and indispensable advice.

This work was performed under the auspices of the United States Atomic Energy Commission.

REFERENCES

1. Amdur, I., Irvine, J. W., Jr., Mason, E. A., and Rosa, J., J. Chem. Phys. 20, 436 (1952).

2. Archer, C. T., Phil. Mag. 19, 901 (1935).

3. Archer, C. T., Proc. Roy. Soc. (London) A165, 474 (1938).

4. Arnold, J. H., Ind. Eng. Chem. 22, 1091 (1930).

5. Brokaw, R. S., Ind. Eng. Chem. 47, 2398 (1955).

6. Bromley, L. A., Thermal Conductivity of Gases at Moderate Pressures, UCRL-1852, June 12, 1952.

7. Buddenburg, J. W., and Wilke, C. R., Ind. Eng. Chem. 41, 1345 (1949).

7a. Buddenburg, J. W., and Wilke, C. R., J. of Phys. and Colloid Chem. 55, 1491 (1951).

8. Chapman, S., Phil. Trans. Roy. Soc. London A216, 279 (1916).

9. Chapman, S., and Cowling, T. G., Mathematical Theory of Nonuniform Gases, (University Press, Cambridge, 1939), p. 167.

10. Chapman, S., and Cowling, T. G., ibid., pp 144-145.

10a. Chapman, S., and Cowling, T. G., ibid., pp 237-240.

11. Clark Jones, R., and Furry, W. H., Rev. Mod. Phys. 18, 151 (1946).

12. Davidson, J. M. and Music, J. F., Experimental Thermal Conductivities of Gases and Gaseous Mixtures at Zero Degrees Centigrade, HW-29021, July 3, 1953.

13. Enskog, D., The Kinetic Theory of Phenomena in Fairly Rare Gases, Ph.D. Dissertation, University of Upsala, 1917.

14. Eucken, A. T., Physik. Z. 14, 324 (1913).

15. Eucken, A. T., Forschung, 11, 6 (1940).

16. Franck, E. U., Z. Elektrochem 55, 636 (1951).

17. Franck, E. U., Z. physik. Chem. 201, 16 (1952).

18. Grew, K. E. and Ibbs, T. L., Thermal Diffusion in Gases, (University Press, Cambridge), 1952, pp 6-7.

19. Grew, K. E., and Ibbs, T. L., ibid., p. 37.

20. Gruss, H., and Schmick, H., Wiss. Veroffentl. Siemens-Konzern. 7, 202 (1928).

21. Harteck, P., and Schmidt, H. W., Z. für Physik. Chem. 21B, 447 (1933).

21a. Herning, F., and Zipperer, L., Gas-u Wasserfach 79, 49 (1936).

22. Hirschfelder, J. O., Heat Conductivity in Polyatomic, Electronically Excited, or Chemically Reacting Mixtures, III, University of Wisconsin Report CM-880, NOrd-15884, Aug. 15, 1956.

23. Hirschfelder, J. O., Curtiss, C. F., and Bird, R. B., Molecular Theory of Gases and Liquids, (Wiley, New York, 1954), pp 536-537.

24. Hirschfelder et al., ibid., pp 534-536, 575-576.

25. Hirschfelder et al., ibid., pp 528-533.

26. Hirschfelder et al., ibid., Tables IA and IM.

27. Hirschfelder et al., ibid., pp 538-540, 580-582.

28. Hirschfelder et al., ibid., pp 50-51, 523-528.

28a. Hirschfelder et al., ibid., pp 597-600.

28b. Hirschfelder, Bird, and Spotz, Chem. Rev. 44, 205 (1949).

29. Huber, P. W., and Kantrowitz, A. J., Chem. Phys. 15, 275 (1947).

30. Ibbs, T. L., and Hirst, A. A., Proc. Roy. Soc. (London) A123, 134 (1929).

31. International Critical Tables, Vol. 5, Edward W. Washborn, Ed., (McGraw-Hill Book Co., New York, 1929).

32. Johnston, H. L., and Grilly, E. R., J. Chem. Phys. 14, 233 (1946).

33. Kannuluik, W. G., and Carmen, E. H., Proc. Phys. Soc. (London) 65B, 601 (1952).

34. Kennard, E. H., Kinetic Theory of Gases, (McGraw-Hill Book Co., New York, 1938), p. 183.

35. Kennard, E. H., ibid., pp 312-315.

36. Keyes, F. G., Trans. Am. Soc. Mech. Engrs. 74, 1303 (1952).

37. Keyes, F. G. Project Squid, Tech. Rep't. 37, Massachusetts Institute of Technology, (U. S. Navy and U. S. Air Force), April 1, 1952.

38. Kornfeld, G., and Hilferding, K., Z. für Physik. Chem., Bodenstein-Festband, 792 (1931).

39. Kuenen, J. P., Konink. Akad. Wetenschap. Amsterdam, 16, 1162 (1914) and 17, 1068 (1915).

40. Lindsay, A. L., and Bromley, L. A., Ind. Eng. Chem. 42, 1508 (1950).

41. Mann, W. B., and Dickens, B. G., Proc. Roy. Soc. (London) A134, 77 (1931).

42. McAdams, W. H., Heat Transmission, Second edition, (McGraw-Hill Book Co., New York, 1942), p. 63.

43. Nuttall, R. L., and Ginnings, D. C., J. Research Nat. Bur. Standards 58, 271 (1957).

44. Rothman, A. J., Thermal Conductivity of Gases at High Temperatures (Thesis), University of California, 1954.

45. Schaefer, K., Z. Physik. Chem. 53, 149 (1943).

46. Schottky, W. F., Z. Elektrochem. 56, 889 (1952).

47. Schudel, W., Schweiz. Ver. Gas-u Wasserfach. Monats-Bull. 22, 112 (1942).

48. Srivastava, B. N., and Saxena, S. C., Proc. Phys. Soc. (London) B70, 369 (1957).

49. Stops, D. W., The Effect of Temperature Upon the Thermal Conductivity of Gases Between 0° and 1000°C (Thesis), London University, 1949.

50. Sutherland, W., Phil. Mag. 40, 421 (1895).

51. Taschenbuch für Chemiker und Physiker, (Springer-Verlag, Berlin, 1949), p. 1110.

52. Thiesen, M., Verhandl. deut. physik. Ges. 4, 348 (1902).

53. Thomas, L. B., and Olmer, F., J. Am. Chem. Soc. 65, 1036 (1943).

54. Trautz, M., and Baumann, P. B., Ann. Physik 2, 733 (1929).

55. Trautz, M., and Binkele, H. E., Ann.Physik. 5, 561 (1930).

56. Trautz, M., and Kipphan, K. F., Ann.Physik. 2, 743 (1929).

57. Trautz, M., and Kurz, F., Ann. Physik. 9, 992 (1931).

58. Trautz, M., and Melster, A., Ann. Physik 7, 409 (1930).

59. Trautz, M., and Sorg, K. G., Ann. Physik 10, 81 (1931).

60. Vergaftig, N. B., and Timroth, D. L., Transcription of the Fourth World Power Conference, III, (Lund-Humphries, London, 1952), p. 1642.

61. Uhlenbeck, G. E., Wang, C. S., and deBowe, J., Physica 23, (1957).

61a. Uyehara, O. A., and Watson, K. M., Nat. Petrol. News 36, R764, (1944).

62. Vine, R. G., and Bennett, L. A., J. Chem. Phys. 23, 1587 (1955).

63. Vine, R. G., and Bennett, L. A., J. Chem. Phys. 22, 360 (1954).

64. Wachsmuth, J., Physik Z. 7, 235 (1908).

65. Wassiljewa, A., Physik Z. 5, 737 (1904).

66. Weber, S. T. H., Ann. Physik 54, 481 (1917).

67. Wilke, C. R., J. Chem. Phys. 18, 517 (1950).

68. Wilke, C. R., Chem. Eng. Progr. 46, 95 (1950).

69. Wilke, C. R., and Lee, C. Y., Ind. Eng. Chem. 47, 1253 (1955).

70. Winn, E. B., Phys. Rev. 80, 1024 (1950).